ผลของขนาดผลึกของนาโนไทเทเนียต่อคุณลักษณะของนาโนคอมโพสิทของพอลิเอทิลีนชนิดความ
หนาแน่นต่ำแบบโซ่ตรงกับไทเทเนียซึ่งสังเคราะห์โดยพอลิเมอร์ไรเซชันแบบอินซิตูด้วยตัวเร่ง
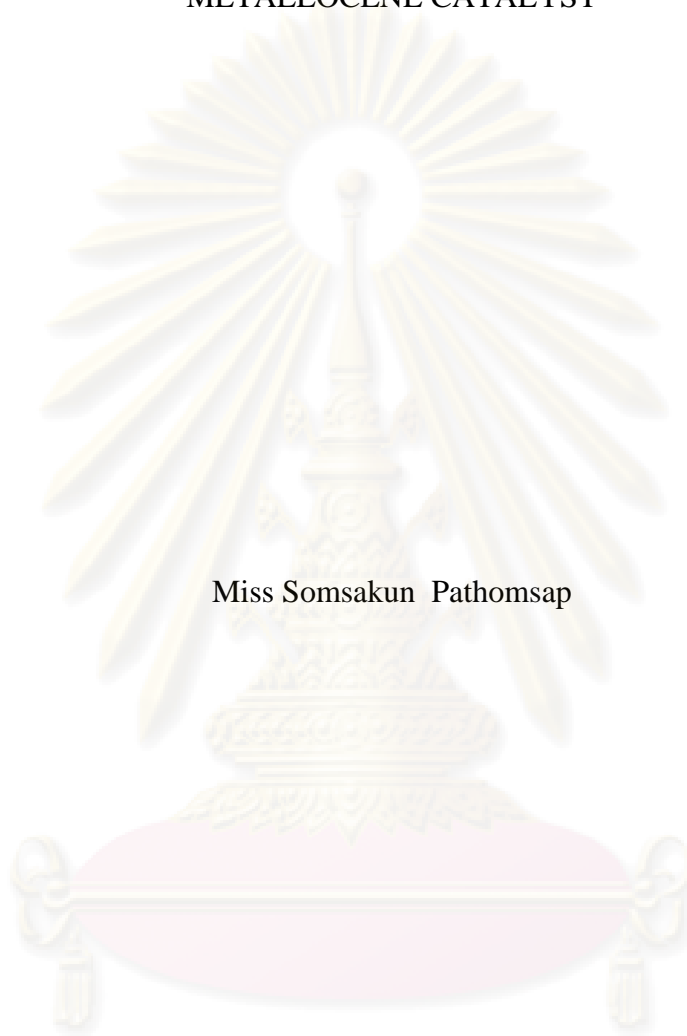ปฏิกิริยาเมทัลโลซีน

นางสาวสมสกุล ปฐมทรัพย์

EFFECT OF THE CRYSTALLITE SIZE OF NANO-TITANIA ON THE
CHARACTERISTICS OF LLDPE/TITANIA NANOCOMPOSITES
SYNTHESIZED BY *IN SITU* POLYMERIZATION USING
METALLOCENE CATALYST

Miss Somsakun Pathomsap

A Thesis Submitted in Partial Fulfillment of the Requirements
for the Degree of Master of Engineering Program in Chemical Engineering
Department of Chemical Engineering
Faculty of Engineering
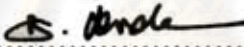Chulalongkorn University
Academic Year 2008

Thesis Title   EFFECT OF THE CRYSTALLITE SIZE OF NANO-TITANIA ON THE CHARACTERISTICS OF LLDPE/TITANIA NANOCOMPOSITES SYNTHESIZED BY *IN SITU* POLYMERIZATION USING METALLOCENE CATALYST

By   Miss Somsakun Pathomsap

Field of Study   Chemical Engineering

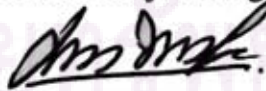Advisor   Assistant Professor Bunjerd Jongsomjit, Ph.D.

Accepted by the Faculty of Engineering, Chulalongkorn University in Partial Fulfillment of the Requirements for the Master's Degree
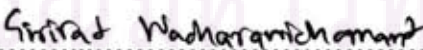
……………………………Dean of the Faculty of Engineering

(Associate Professor Boonsom Lerdhirunwong, Dr. Ing.)

THESIS COMMITTEE

…………………………………. Chairman

(Assistant Professor Montree Wongsri, D.Sc.)

…………………………………. Advisor

(Assistant Professor Bunjerd Jongsomjit, Ph.D.)

………………………………….. Examiner

(Associate Professor ML Supakanok Thongyai, Ph.D.)

…………………………………… External Examiner

(Assistant Professor Sirirat Wacharawichanant, D.Eng.)

สมสกุล ปฐมทรัพย์ : ผลของขนาดผลึกของนาโนไทเทเนียต่อคุณลักษณะของนาโนคอม
โพสิทของพอลิเอทิลีนชนิดความหนาแน่นต่ำแบบโซ่ตรงกับไทเทเนียซึ่งสังเคราะห์โดยพอ
ลิเมอร์ไรเซชันแบบอินซิตูด้วยตัวเร่งปฏิกิริยาเมทัลโลซีน.   (EFFECT OF THE
CRYSTALLITE SIZE OF NANO-TITANIA ON THE CHARACTERISTICS OF
LLDPE/TITANIA NANOCOMPOSITES SYNTHESIZED BY *IN SITU*
POLYMERIZATION USING METALLOCENE CATALYST)
อ.ที่ปรึกษาวิทยานิพนธ์หลัก: ผศ. ดร. บรรเจิด จงสมจิตร, 104 หน้า.

เป็นที่รู้กันว่าพอลิเอทิลีนชนิดความหนาแน่นต่ำแบบโซ่ตรงสามารถสังเคราะห์ได้จากการ
โคพอลิเมอร์เซชันของเอทิลีนกับหนึ่งโอเลฟินด้วยตัวเร่งปฏิกิริยาเมทัลโลซีน ระบบของตัวเร่ง
ปฏิกิริยาเมทัลโลซีนแบ่งเป็นสองระบบได้แก่ ระบบของตัวเร่งปฏิกิริยาเมทัลโลซีนที่ไม่มีตัวรองรับ
และระบบของตัวเร่งปฏิกิริยาเมทัลโลซีนที่มีตัวรองรับ ซึ่งพบว่าระบบของตัวเร่งปฏิกิริยาเมทัล
โลซีนที่ไม่มีตัวรองรับยังคงมีข้อเสียอยู่สองประการ คือไม่สามารถควบคุมโครงสร้างสัณฐานของ
พอลิเมอร์ที่ผลิตได้และเกิดสิ่งสกปรกติดที่เครื่องปฏิกรณ์ ดังนั้นการนำตัวรองรับมาใช้ในระบบของ
ตัวเร่งปฏิกิริยาเมทัลโลซีนจะสามารถช่วยลดปัญหาดังกล่าวได้   พอลิเมอร์เมตริกซ์ที่มีการเติม
สารเติมแต่งในระดับนาโนเมตรเป็นตัวเติมเรียกว่าพอลิเมอร์นาโนคอมพอสิท ซึ่งพอลิเมอร์นาโน
คอมโพสิทนี้ สามารถผลิตได้จากการพอลิเมอร์ไรเซชันแบบอินซิตูด้วยการเติมสารเติมแต่งใน
ระดับนาโนเมตรเป็นตัวเติมในระหว่างการสังเคราะห์โดยใช้เป็นตัวรองรับของตัวเร่งปฏิกิริยา ใน
การศึกษานี้จะสังเคราะห์พอลิเมอร์นาโนคอมโพสิทโดยวิธีอินซิตูพอลิเมอร์ไรเซชัน ด้วยตัวเร่ง
ปฏิกิริยาเซอร์โคโนซีนและใช้โมดิฟายด์เมทิลอะลูมินอกเซนเป็นตัวเร่งปฏิกิริยาร่วม ซึ่งในส่วน
แรกสารเติมแต่งในระดับนาโนเมตรที่นำมาศึกษาคือไทเทเนียที่มีขนาดผลึกแตกต่างกัน พบว่าไท
เทเนียที่มีขนาดผลึกใหญ่มีความสามารถในการเกิดของพอลิเมอร์นาโนคอมพอสิทที่ดีกว่าไทเทเนีย
ที่มีขนาดผลึกเล็ก เนื่องจากไทเทเนียที่มีขนาดผลึกใหญ่จะมีแรงยึดเหนี่ยวระหว่างตัวเร่งปฏิกิริยา
ร่วมน้อย และสำหรับส่วนที่สองสารเติมแต่งในระดับนาโนเมตรที่นำมาศึกษาคือไทเทเนียที่มีการ
ปรับปรุงแตกต่างกัน พบว่าไทเทเนียที่ไม่มีการปรับปรุงมีความสามารถในการเกิดของพอลิเมอร์นา
โนคอมพอสิทที่ดีกว่าไทเทเนียที่มีการปรับปรุง เนื่องจากไทเทเนียที่ไม่มีการปรับปรุงจะมีแรงยึด
เหนี่ยวระหว่างตัวเร่งปฏิกิริยาร่วมน้อย

ภาควิชา_____วิศวกรรมเคมี_____ลายมือชื่อนิสิต_____สมสกุล ปฐมทรัพย์_____
สาขาวิชา_____วิศวกรรมเคมี_____ลายมือชื่ออ.ที่ปรึกษาวิทยานิพนธ์หลัก_____
ปีการศึกษา_____2551_____

5070481021: MAJOR CHEMICAL ENGINEERING

KEYWORDS: ZIRCONOCENE CATALYST/TITANIA/LLDPE

/SUPPORTED CATALYST/POLYMER NANOCOMPOSITE

SOMSAKUN PATHOMSAP: EFFECT OF THE CRYSTALLITE SIZE OF NANO-TITANIA ON THE CHARACTERISTICS OF LLDPE/TITANIA NANOCOMPOSITES SYNTHESIZED BY *IN SITU* POLYMERIZATION USING METALLOCENE CATALYST.
ADVISOR: ASST. PROF. BUNJERD JONGSOMJIT, Ph.D.,104 pp.

It is known that the linear low-density polyethylene (LLDPE) can be produced by copolymerization of ethylene and 1-olefins using metallocene catalysts. Metallocene catalyst system can be divided into two systems; homogeneous metallocene catalyst and heterogeneous metallocene catalyst. It was found that homogeneous metallocene catalyst has two major disadvantages; the lack of morphology control of the polymers produced and reactor fouling. Therefore, heterogeneous metallocene catalyst was brought to solve these problems. Polymers filled with inorganic nanoparticles as nanofillers are so-called polymer nanocomposites. It can be produced by the *in situ* polymerization with the presence of nanofillers added during synthesis by the application of supported metallocene catalysts. In this present study, LLDPE/TiO$_2$ nanocomposites were synthesized by the *in situ* polymerization with modified methylaluminoxane (MMAO)/zirconocene catalyst. In the first part, the TiO$_2$ nanofillers having different crystallite sizes were employed. The polymerization activities obtained from TiO$_2$ having the highest crystallite size exhibited the highest activity due to its exhibited the weakest interaction. In the second part, the TiO$_2$ nanofillers having different modification with metals were employed. The polymerization activities obtained from unmodified TiO$_2$ exhibited the highest activities due to the unmodified TiO$_2$ had weakest interaction.

Department :... Chemical Engineering...   Student's Signature : Somsakun Pathomsap ....
Field of Study :...Chemical Engineering...Advisor's Signature :.... Bunjerd ....
Academic Year :.....2008.....................

ACKNOWLEDGEMENTS

CONTENTS

LIST OF TABLES

LIST OF FIGURES

Page

CHAPTER I

INTRODUCTION

For years, there have been tremendous industrial and academic interests in the development of metallocene catalysts for olefin polymerization [Shi et al., 2007]. Metallocene catalysts have revolutionized olefin polymerization catalysis because of their tailor-made polymer properties. In general, metallocene catalysts provide higher activity and narrower molecular weight distribution (MWD) than the conventional Ziegler-Natta catalysts. Moreover, metallocene catalysts can produce an extremely uniform polymer due to their single site catalytic nature. However, it was found that the homogeneous metallocene catalytic systems still have some drawbacks, such as (1) the lack of morphology control of polymer causing the reactor fouling (2) the limitation of being able to use only in the solution process, whereas the existing technologies are mainly based on the gas phase and slurry processes and (3) they require a lot of cocatalysts, which cost highly. Hence, binding these metallocene catalysts onto suitable inorganic supports can provide a promising way to overcome these drawbacks [Jiamwijitkul et al., 2007; Bunchongturakarn et al., 2007]. It has been known that the copolymerization of ethylene with higher 1-olefins is a commercial importance for production of elastomer and linear low-density polyethylene (LLDPE). LLDPE is one of the most widely used polyolefins in many applications because of its specific properties that can be obtained by varying comonomer content and condition for polymerization.

As known, polymer composites filled with nanofillers are so-called polymer nanocomposites. The most commonly used inorganic nanofillers are SiO_2, Al_2O_3, ZrO_2 and TiO_2. Basically, polymer nanocomposites can be prepared by three methods: (1) melt mixing [Nawang et al., 2001; Verbeek, 2002a,b] (2) solution blending [Rossi et al., 2002] and (3) *in situ* polymerization [Cheng et al., 2007; Jongsomjit et al., 2005,2007] . Due to the direct synthesis by polymerization along with the presence of nanofillers, the *in situ* polymerization is perhaps considered the most promising technique to produce polymer nanocomposites with homogeneous dispersion of nanofillers inside the polymer matrix [Jongsomjit et al., 2005;

Chaichana et al., 2006]. Although LLDPE composites have been studied by many authors [Danjaji et al., 2002; Nawang et al., 2001; Verbeek, 2002a,b] , those polymer samples were only synthesized by the melt mixing and solution blending. But there are only few research reported on the synthesizing of LLDPE nanocomposites by *in situ* polymerization using metallocene catalysts.

In the present study, LLDPE/TiO$_2$ nanocomposites synthesized by *in situ* polymerization of ethylene/1-hexene using a zirconocene/MMAO catalyst, which prepared by *in situ* impregnation method were investigated and compared with the homogeneous system. In the first part, the crystallite sizes of nano-TiO$_2$ fillers was varied. In order to obtained different crystallite sizes of nano-TiO$_2$ fillers, the nano-TiO$_2$ fillers were prepared by the sol-gel method using different water:alkoxide ratios in the range of 4 to 80. The reason for chosen the sol-gel method is due to its inexpensive method. It can be prepared at low temperature and being suitable for scale up to commercial process. In the second part, the modification of nano-TiO$_2$ fillers was varied. In order to obtain Ga-modified TiO$_2$ fillers and Zr-modified TiO$_2$ fillers, the modification of nano-TiO$_2$ fillers was prepared by the incipient wetness impregnation method. Polymerization yield, catalytic activity and properties of polymer nanocomposites were further investigated and discussed in more details.

1.1 The objectives of this thesis

1.1.1 To investigate the effect of the crystallite size of nano-TiO_2 fillers on the characteristics of LLDPE/TiO_2 nanocomposites synthesized by *in situ* polymerization of ethylene/1-hexene using a zirconocene/MMAO catalyst, which prepared by *in situ* impregnation method.

1.1.2 To investigate the effect of the modification of nano-TiO_2 fillers on the characteristics of LLDPE/TiO_2 nanocomposites synthesized by *in situ* polymerization of ethylene/1-hexene using a zirconocene/MMAO catalyst, which prepared by *in situ* impregnation method.

1.2 The scopes of this thesis

1.2.1 Preparation of nano-TiO_2 fillers by the sol-gel method using different water:alkoxide ratios in the range of 4 to 80 in order to obtain different crystallite sizes of TiO_2.

1.2.2 Preparation of Ga-modified TiO_2 fillers and Zr-modified TiO_2 fillers by the incipient wetness impregnation method.

1.2.3 Characterization of nano-TiO_2 fillers using scanning electron microscopy (SEM), transmission electron microscopy (TEM), X-ray diffraction (XRD) and single point BET surface area.

1.2.4 Synthesize LLDPE/TiO_2 nanocomposites by *in situ* polymerization of ethylene/1-hexene using a zirconocene/MMAO catalyst.

1.2.5 Characterize LLDPE/TiO_2 nanocomposites with scanning electron microscopy (SEM), energy dispersive X-ray spectroscopy (EDX), transmission electron microscopy (TEM), differential scanning calorimetry (DSC) and ^{13}C nuclear magnetic resonance spectrometer (^{13}C NMR).

CHAPTER II

LITERATURE REVIEW

2.1 Polymerization of olefins

Until 1953, processes for olefin polymerization were bases on a radical process at high pressure and high temperature. Polymerization of ethylene under this condition (2000-3000 bars; 423-503 K) yields low-density polyethylene, a low melting, highly branched polyethylene, containing both long and short chain branches [Smedberg et al., 2003]. With propylene only atactic, low molecular weight material can be obtained. Ziegler found that ethylene could also be polymerized using $TiCl_4$ and alkylaluminium. The process yields linear polyethylene with a high molecular weight. Natta proved that the same type of catalysts also polymerized propylene . The resulting polymer mixture is predominantly isotactic with addition polymer fractions that are of a lower stereoregularity or atactic. Copolymerization of ethylene with 1-hexene/1-octene with the titanium ziegler catalysts result in copolymers in which the degree of incorporation of the alpha-olefin varies over molecular weight distribution. Upon reaction of a vanadium compound, e.g. $V(acac)_3$ (acac = acetylacetonato) or VCl_4, with and alkylaluminium cocatalysts a catalyst for the production of EP (copolymerization of ethylene and propylene) and EPDM (ethylene-propylene-diene elastomer) are obtained [Gambarotta , 2003]. The homogeneous system shows high (initial) activity, but is deactivated rapidly [Milione et al., 2002]. An important advantage is that the comonomers are randomly incorperated in the polymer over the full range of the molecular weight distribution.

The heterogeneity of Ziegler Natta system and Phillip/Union Carbide type catalysts make them very attractive for industrial application, and most polyolefin materials are still produced by means of heterogeneous catalysts [Kashiwa, 2004]. These heterogeneous systems combine high activity with an easy processability of the resulting product mixture and good polymer particle morphology. The catalyst system contain various type of active sites with different geometries and activities, which often leads to polymers with broad or polymodal molecular weight distribution or to

mixtures of different type of polymers (e.g. mixture of atactic and isoatactic propylene [Kissin , 2003]. Many improvement on the classical Ziegler Natta type catalysts have been made over the last 30 years, and modern Ziegler Natta system allow a much better control of polymer properties. Most of these improvement were achieved by empirical method .

In 1957, the first article on homogeneous titanium-based olefin polymerization were published by Brselow and Newburg, (1957) and by Natta and Pino (1957). When reacting Cp_2TiCl_2 with Et_2AlCl (DEAC) under conditions similar to those used with Ziegler Natta system, a catalyst that polymerizes ethylene is obtained. The first homogeneous system showed a low activity, when compared to classical Ziegler Natta system and was also not active in polymerization of higher olefin. In contrast to heterogeneous system, homogeneous catalysts have a single type of well-defined active sites. Although heterogeneous catalysts are in general industrially more practical, a higher control of properties of the catalyst, and more detailed kinetic and mechanistic studies are possible with well-defined molecular catalysts ("single site" catalysts) [Krentsel et al., 1990].
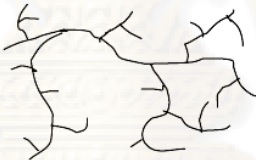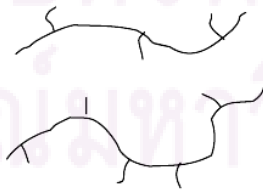
2.2 Classification of polyethylene

Polyethylene (PE) is the most important material in plastic and polymer type. Normally, polyethylene is classified to three type according to its density and structure, high density polyethylene (HDPE), low density polyethylene (LDPE) and linear low density polyethylene (LLDPE). The numerous studies show that the global market of LLDPE was increased in very interesting rate about 10 % per annum [Richards, 1998].

Table 2.1 summarized the characteristic of three type of polyethylene. The different in structure of polymer affects to the physical properties of polymer i.e. density of polymer and hence the application of polymer. HDPE is the polymer that has very less or does not have any branch in the polyethylene backbone. From this microstructure HDPE has very high crystalline phase in polymer morphology and highest density about 0.96 g/cm^3. Polyethylenes which have many long and short

chains branching formed by radical process is LDPE. The amount of long chain branching (LCB) and short chain branching (SCB) also affect the crystalline and others physical properties too.

Table 2.1 Density range, molecular structure, synthesis, and applications of various type polyethylenes [Richards, 1998].

Type of PE	Density (g/cm³)	Molecular structure	Synthesis	Common uses
HPDE	0.945-0.965		Polymerization of ethylene on Philips, Ziegler-Natta and metallocene catalyst	Gas pipe, car gas tanks, bottles rope and fertilizer bag
LDPE	0.890-0.940		Free radical polymerization of ethylene at high temperature and high pressure	Packing film, bags, wire, sheathing, pipes, waterproof of membrane
LLDPE (VLDPE,ULDPE)*	0.910-0.925		Copolymerization of ethylene with α-olefins on Ziegler-Natta and metallocene catalysts	Shopping bag, stretch wrap, greenhouse film

* A family of LLDPE with density of 0.87-0.915 g/cm³

Normally, long chain branching has the main effect on the polymer viscosity and melt rheology due to the molecular size and shape. On the other hands, short chain branching has the influence to polymer morphology and solid state properties of polyethylene. LLDPE was produced by the copolymerization of ethylene and α-olefins such as propylene, 1-butene, 1-hexene and 1-octene. Mostly, side chain in LLDPE distributed in short chain branching type by non-uniformly with linear microstructure of backbone polyethylene chain. The properties of LLDPE such as, thermal, physical and mechanical properties depend on the distribution of short chain in the copolymer and polymer microstructure (triad and dyad distribution). Thus, the several LLDPE grades are classified by the primarily result via microstructure of polymer and molecular weight of polymer.

2.3 Evolution of polyolefin catalysts

In 1953 Karl Ziegler, who succeeded in polymerizing ethylene into HDPE at standard pressure and room temperature, discovered of catalysts based on titanium trichloride and diethylaluminum chloride as cocatalyst, at the Max-Planck-Institute in Mulheim. A little later, Natta, at the Polytechnical Institute of Milan, was able to indicate that an appropriate catalyst system was capable of polymerizing propene into semi-crystalline polypropene. Ziegler and Natta shared a Nobel Prize for Chemistry in 1963 for their work [Kaminsky and Laban , 2001]. With this so-called Ziegler-Natta catalyst.

Ziegler-Natta catalyst has been widely used in olefin polymerization; the coordination polymerization allows the catalyst geometry around the metal center to control the polymer structure. In homogeneous polymerization, the ligand of catalyst largely controls the geometry of an active metal center on which the polymerization reaction occurs. However, the conventional Ziegler-Natta catalysts the molecular structure of the polymers cannot be controlled well the molecular structure of the polymers because these catalysts have different nature types of catalytic sites.

In the last two decade Kaminsky and Sinn discovered the metallocene and other transition metal complexes activated by methylaluminoxane are highly active

catalysts for the polymerization of olefin, diene, and styrene; they have proven to be a major breakthrough for the polyolefin industry. Contrast to Phillips and Ziegler-Natta catalysts that have been used already commercially to produce polyolefins, the metallocene catalysts are single site catalysts. Therefore, these catalysts produce a very uniform polymer, having a narrow molecular weight distribution (Mw/Mn = 2). Since the defined ligand sphere greatly influences the properties of the catalysts and that way the polymer, it is possible to tailor the ligand environment according to need (their structure can be easily changed) [Kaminsky , 2004] . The metallocence catalysts allow control of molecular weight, incorporation of comonomer, and in the case of polypropylene, the isotaticity and the amount of misinsertions [Kristen , 1999]. Furthermore, they are soluble in hydrocarbons or liquid propene. In addition, their catalytic activity is 10-100 times higher than that of the classical Ziegler-Natta catalysts.

The evolution of the metallocene catalysts structures for olefin polymerization is shown in **Table 2.2**. [Mashima et al., 1997]

Table 2.2 Timetable and historical development of metallocene research

1952	Development of the structure of metallocenes (ferrocene) by Fischer and Wilkinson
1955	Metallocene as component of Ziegler-Natta catalysts, low activity with common aluminum alkyls.
1973	Addition of small amount of water to increase the activity (Al:H_2O = 1:0.05 up to 1:0.3) (Reichert, Meyer and Breslow)
1975	Unusual increase in activity by adding water at the ratio Al:H_2O = 1:2 (Kaminsky, Sinn and Motweiler)
1977	Using separately prepared methylaluminoxane (MAO) as Cocatalyst for olefin polymerization. (Kaminsky and Sinn)
1982	Synthesis of *ansa* metalocenes with C_2 symmetry (Brintzinger)
1984	Polymerization of propylene using a *rac/meso* mixture of *ansa* titanocenes lead to partially isotactic polypropylene. (Ewen)
1984	Chiral ansa zirconocenes produce highly isotactic polypropylene (Kaminsky and Brintzinger)

Initially, it was found that using simple group 4 metallocenes like bis(cyclopentadienyl)titanium dichloride together with a cocatalyst like diethylaluminium chloride for the polymerization of ethylene lead to a catalyst system that showed initial fair activity which then rapidly decreased, due to factors like alkyl exchange reactions, hydrogen transfer and reduction of the transition metal species. Reichart and Meyer found a remarkable increase in activity (20-100 times better) by adding small amounts of water to the system $Cp_2TiCl_2/C_2H_5AlCl_2$ [Reichert and Meyer , 1973]. An enormous increase in activity was found in 1975 (up to 1 million times better) when water was added in a far greater amount, and, in 1977, when MAO was used with titanocenes and zirconocenes [Andesen et al., 1976 ; Sinn and Kaminsky, 1980]. Thereafter the next important step was using *ansa* metallocenes synthesized by Brintzinger *et al* in 1982 . This allowed stereospecific polymerization of propylene. Ewen synthesized a C_s symmetric zirconocene ([$Me_2C(Flu)(Cp)$]$ZrCl_2$) in 1988 which allowed for the production of syndiotactic polypropylene in high

quantities [Ewen et al., 1988]. Since 1985, a rapid world-wide industrial and academic development began in the field of metallocene catalysts which continues today.

2.4 Metallocene catalysts

Metallocene catalysts are organometallic coordination compounds in which one or two π-carbocylic ligands such as cyclopentadienyl ring, substituted cyclopentadienyl ring, or derivative of cyclopentadienyl ring (such as fluorenyl, indenyl etc.) are chained to a metal central transition atom. The typical chemical structure of a metallocene catalyst is represented by **Figure 2.1**.
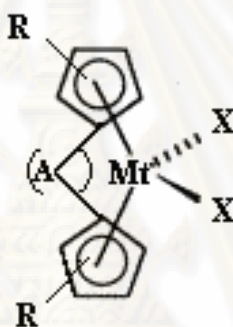
Figure 2.1 Typical chemical structure of a metallocene catalyst [Alt, 1999]
where Mt = Group 4, 5, or 6 transition metal (e.g. Zr, Ti or Hf)

A = an optional bridging unit consisting of 1-3 atoms in the backbone

R = hydrocarbyl substituents or fused ring systems (indenyl, fluorenyl and substituted derivatives)

X = chlorine or other halogens from group 7 or an alkyl group

Single site catalysts can be separated into five main symmetry group, which influence on the polymer architectures as shown in **Figure 2.2**. It is assumed that the polymer rapidly equilibrates with the available coordination site for the purposes of assigning symmetry. Catalysts exhibiting C_{2v} symmetry typically produce atactic polymers or moderately stereoregular polymers by chain-end control mechanisms. C_s-symmetric catalysts that have mirror planes containing the two-diastereotopic coordination sites behave similarly. However, C_s-symmetric catalysts that have a mirror plane reflecting two enantiotopic coordination sites frequently produce

syndiotactic polymers. C_2-symmetric complexes, both racemic mixtures and enantiomerically pure ones, typically produce isotactic polymers via a site-control mechanism. Stereoselectivities of asymmetric (C_1) complexes are unpredictable and have been reported to produce polymer architectures ranging from highly isotactic, to atactic, including isotactic-atactic stereoblock and hemiisotactic. Polymer architectures relevant to this modification of ligands are shown in **Figure 2.3**.
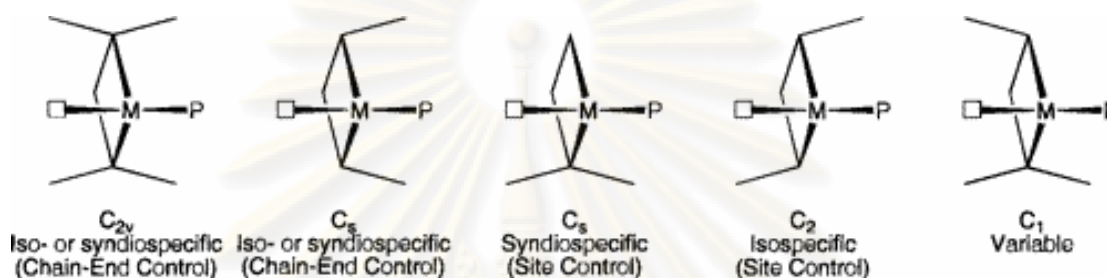
Figure 2.2 General symmetry classifications, based on ligand geometries, of catalysts and their stereoselectivities for polyolefin synthesis [Coates, 2000]
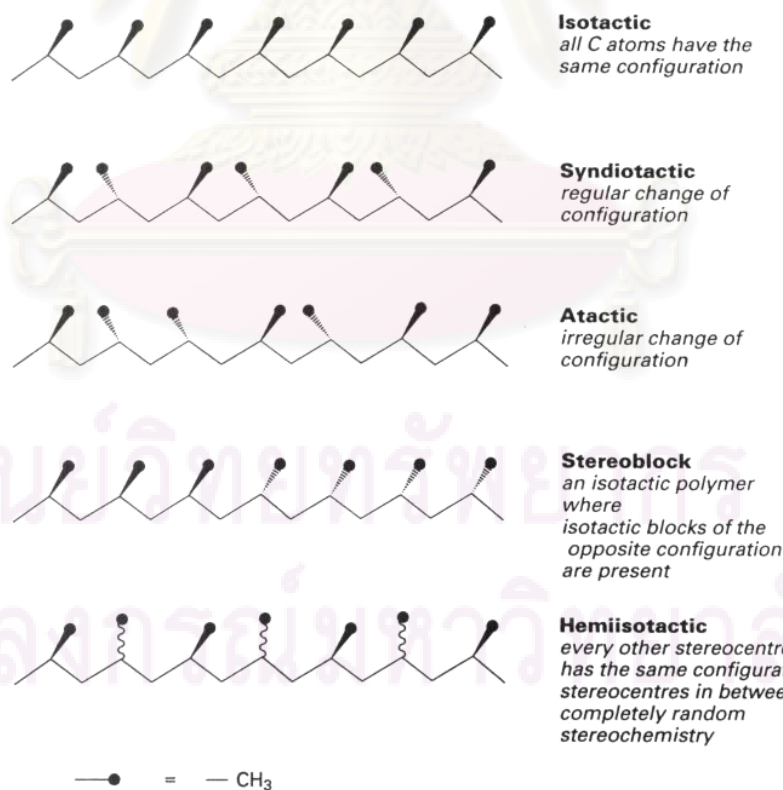
Figure 2.3 Different types of polymer tacticity [Long, 1998]

Representative examples of each category of metallocenes and some of zirconocene catalysts are shown in **Table 2.3** and **Figure 2.4**, respectively.

Table 2.3 Representative examples of metallocenes [Gupta et al., 1994]

Category of Metallocenes	Metallocene Catalysts
[A] Nonstereorigid metallocenes	1) Cp_2MCl_2 (M = Ti, Zr, Hf) 2) Cp_2ZrR_2 (M = Me, Ph, CH_2Ph, CH_2SiMe_3) 3) $(Ind)_2ZrMe_2$
[B] Nonstereorigid ring-substituted metallocenes	1) $(Me_5C_5)_2MCl_2$ (M = Ti, Zr, Hf) 2) $(Me_3SiCp)_2ZrCl_2$
[C] Stereorigid metallocenes	1) $Et(Ind)_2ZrCl_2$ 2) $Et(Ind)_2ZrMe_2$ 3) $Et(IndH4)_2ZrCl_2$
[D] Cationic metallocenes	1) $Cp_2MR(L)+[BPh_4]^-$ (M = Ti, Zr) 2) $[Et(Ind)_2ZrMe]+[B(C_6F_5)4]^-$ 3) $[Cp_2ZrMe]+[(C_2B_9H_{11})_2M]^-$ (M = Co)
[E] Supported metallocenes	1) Al_2O_3-$Et(IndH_4)_2ZrCl_2$ 2) $MgCl_2$-Cp_2ZrCl_2 3) SiO_2-$Et(Ind)_2ZrCl_2$
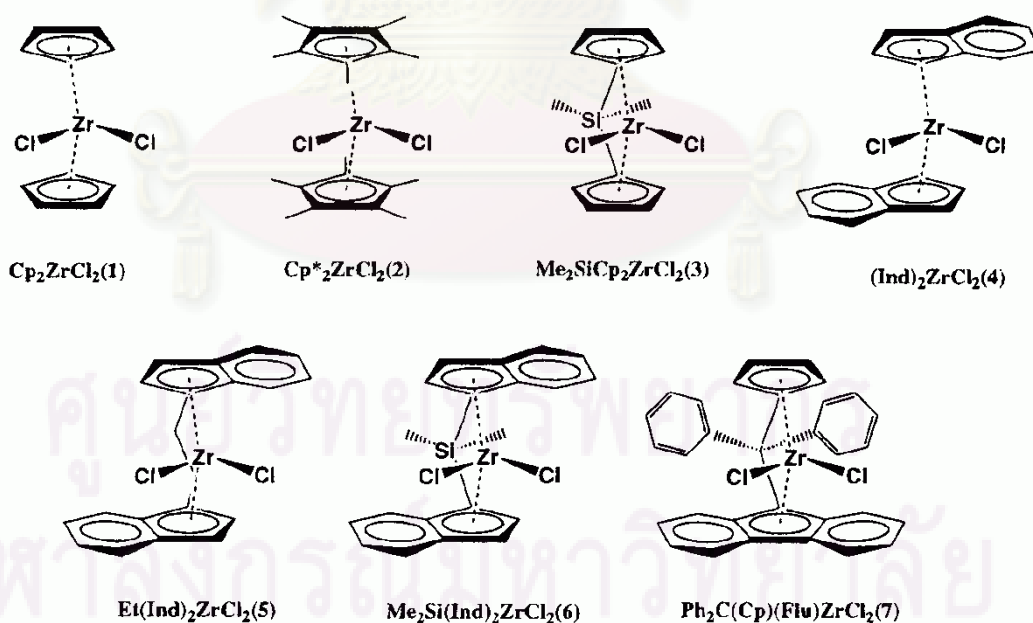
Figure 2.4 Some of zirconocene catalysts structure [Naga and Imanishi, 2001]

2.5 Cocatalyst

Aluminoxane, especially methylaluminoxane (MAO) plays the very important role to activate metallocene catalyst. Before the MAO was discovered, in Ziegler-Natta catalyst alkylaluminumchloride was used to activate Cp_2TiCl_2 but it exhibited the very poor activity. Using of MAO as cocatalyst can promote the productivity of polymerization by several order of magnitude. Otherwise using of MAO, the other aluminoxanes such as, ethylaluminoxane (EAO) or iso-buthylaluminoxane (iBAO) or modified methylaluminoxane was employed to use as cocatalyst too. (Structure of MAO, EAO, iBAO and MMAO was shown in **Figure 2.5**)
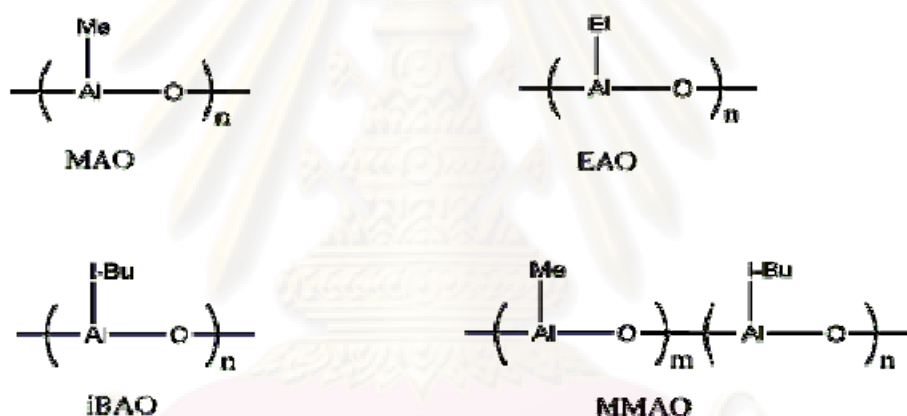
Figure 2.5 Several kinds of MAO [Pasynkiewicz, 1990; Chien, 1976]

A metallocene catalyst precursor can be activated with organoalumoxanes, especially methylaluminoxane (MAO), which affords highly active catalysts for polymerization ethylene, propylene, and higher α-olefins when combined with group 4 metallocene. MAO is a compound in which aluminum and oxygen atoms are arranged alternately and free valances are saturated by methyl substitutions. It is prepared by carefully controlled partial hydrolysis of trimethylaluminum (TMA) and according to investigations [Koide et al., 1996; Sinn, 1995; Ystenes, 2000]. The hydrolysis of AlR_3 (R = Me, Et, iBu) has been shown to proceed via the formation of an alkylaluminum water complex shown in **Equation 1** [Mason, 1993], which subsequently eliminates an alkane to form a dialkylaluminum hydroxide complex as

shown in **Equation 2**. This result rapidly associates to give dimers or larger oligomers in solution.

$$AlR_3 + H_2O \longrightarrow AlR_3(H_2O) \tag{1}$$

$$AlR_3(H_2O) \longrightarrow 1/n[R_2Al(OH)]_n + RH \tag{2}$$
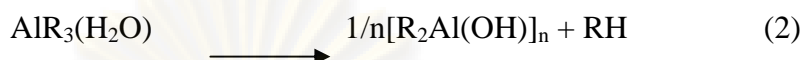
The structure of MAO consists mainly of units of the basic structure $[Al_4O_3Me_6]_4$, which contains four aluminum, three oxygen atoms and six methyl groups. Although very extensive research has been carried out in both academia and industry, the exact composition and structure of MAO are still not entirely clear or well understood. The proposed structures for MAO in the open literature [Chen and Marks, 2000] shown in **Figure 2.6** include: (1) one-dimensional linear chains, (2) cyclic rings, which contain three-coordinate Al centers, (3) two-dimensional structures, and (4) three-dimensional clusters is based on structural similarities with *tert*-butylaluminoxanes, which form isolable and X-ray crystallographically characterizable cage structures (5) [Sinn, 1995].
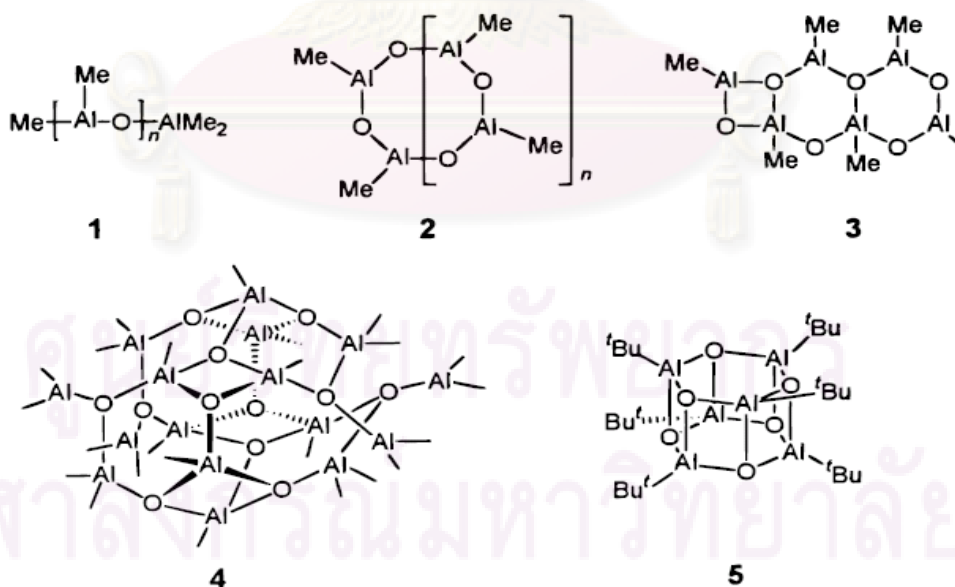
Figure 2.6 The general proposed structure of MAO [Sinn, 1995]

Depending on the nature of the hydrated salt (the H_2O source) used for the MAO synthesis and the exact MAO synthetic reaction conditions; MAO activated metallocenes may exhibit widely differing activities in olefin polymerization. The MAO structure can hardly be elucidated directly because of the multiple equilibria present in MAO solutions, and residual trimethylaluminum in MAO solutions appears to participate in equilibria that interconvert various MAO oligomers [Giannetti et al., 1985]. There are two types of TMA present in typical MAO solutions: "free" TMA and "associated" TMA shown in **Equation 3**.

$$\{Al(Me)O\}_n \cdot xAlMe_3 \rightleftharpoons \{Al(Me)O\}_n \cdot (x-y)AlMe_3 + yAlMe_3 \qquad (3)$$

$$\text{" associated" "free"}$$
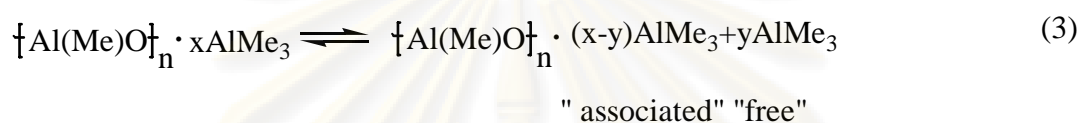
Cryoscopy MAO molecular weight decrease after $AlMe_3$ addition according to a linear relationship, which is caused by disproportionate reactions [Tritto, 1997]. However, recent in-situ FTIR spectroscopy investigations do not indicate any obvious reaction between TMA and MAO. Nevertheless, in light of its complicated, unresolved structural features, MAO is usually represented for the sake of simplicity as having linear chain or cyclic ring structures $[-Al(Me)-O-]_n$, containing threecoordinate aluminum centers [Chen and Marks, 2000]. However, conventional MAO has very low solubility in aliphatic solvents as well as poor storage stability in solution. To solve these limits, MAO can be modified. Commercial modified methylaluminoxanes (MMAO), which prepared by controlled hydrolysis of mixture of trimethylaluminum and triisobutylaluminum, exhibit improved solution storage stability and improved solubility in aliphatic solvents and can be produced at lower cost while providing good polymerization efficiency (Chen and Marks, 2000). Recently, the modification by evacuated MAO was studied. Dried methylaluminoxane (dried MAO) which was free of Me_3Al, was more active than the standard MAO system, resulting in a steady polymerization rate and giving higher Mw polypropylenes. Additive effects of trialkylaluminum on the dried MAO system showed that the polymer yield was increased by the addition of i-Bu_3Al and Oct_3Al and decrease by Me_3Al and Et_3Al [Ioku et al., 2002].

Cam and Giannini (1992) investigated the role of TMA present in MAO by a direct analysis of Cp_2ZrCl_2/MAO solution in toluene-d8 using 1H-NMR. Their observation indicated that TMA might be the major alkylating agent and that MAO acted mainly as a polarization agent. However, in general it is believed that MAO is the key cocatalyst in polymerizations involving metallocene catalysts. The role of MAO included 1) alkylation of misallocate, thus forming catalyst active species, 2) scavenging impurities, 3) stabilizing the cationic center by ion-pair interaction and 4) preventing bimetallic deactivation of the active species. Ethylene/α-olefins copolymers with bimodal CCD were produced with homogeneous Cp_2ZrCl_2 with different co catalysts such as MAO and mixture of TEA/borate or TIBA/borate. It seemed that the active species generated with different co catalysts have different activities and produce polymers with different molecular weights [Cam and Giannini, 1992].

Shiono, T. et al., (2000) have studied on the effect of trialkylaluminum type to the characteristic of polymerization. For example, the addition of Oct_3Al and Et_3Al increased the propagation rate of living polymerization with [t-BuNSiMe$_2$Flu]TiMe$_2$ / B(C_6F_5)$_3$ system at 223 K [Shiono et al., 2000].

On the one hand, not only the aluminoxane has effect to the polymerization behavior but the trialkylaluminum has the influence too. Lui et al. (2006) have studied on the effect of trialkylaluminum type to the characteristic of polymerization, are investigated for ethylene polymerization without MAO or Ph_3CB (C_6F_5)$_4$. The effects of alkylaluminums, Al/Zr molar ratio, polymerization temperature and time as well as the comonomer 1-hexene on polymerization performance are examined. In appropriate range of Al/Zr molar ratio, the catalyst system bis(phenoxy-imine)Zr complex/trialkylaluminum shows high activity for ethylene polymerization, which approximates to bis(phenoxy-imine)Zr complex/MAO system. Their catalytic activities depend on not only the nature, but also the amount, of the trialkylaluminum. Both the molecular weights and the polydispersities (Mw/Mn) of polyethylene produced by bis(phenoxy-imine)Zr complex with Et_3Al, He_3Al, or Me_3Al are higher than those with MAO. The nature, rather than the amount, of alkylaluminum determines the Mw and the polydispersity of polymer in polymerization with the same

complex. Unexpectedly, Mw of the polyethylenes produced with bis(phenoxy-imine)Zr complex/triethylaluminum increases with polymerization time. The catalyst system bis(phenoxy-imine)Zr complex/trialkylaluminum has low capacity of copolymerization [Lui et al., 2006].

2.6 Classification of metallocene catalyst systems

Polymerization with metallocene catalyst can be arranged to 2 major types, the supported system and non-supported system. For the non-supported system, the cocatalyst was a mobile phase in the polymerization medium. On the other hands, the supported metallocene catalyst system, the co-catalyst mostly was immobilized on the organic or inorganic support. In the early category, the activity was very high and easy to control the molecular weight. These systems still can divide to 2 sub-categories, aluminoxane system and cationic metallocene system. To study the metallocene catalyst behavior by changing the substitute bridge or effect of activator are very famous to pick the homogenous metallocene catalyst system to study, because it did not have effect of interaction between inorganic support (silica or alumina) and metallocene catalyst systems.

2.6.1 Homogeneous metallocene catalyst with aluminoxane systems

At the first generation of this system, metallocene catalyst was a simple model which assembled from the cyclopentadienyl or substituted cyclopentadienyl ligands were π-bonded to the central metal atom. The development of metallocene catalyst was going on the synthesis of metallocene compounds. Breslow and Newbreg were the first researchers who apply the metallocene catalyst for polymerization [Newburg, 1957]. They used the soluble bis(cyclopentadienyl)titanium derivative and alkylaluminum for ethylene polymerization. However, it was found that the productivity of these catalyst system was very low and the low molecular weight of polymer too. Moreover, these catalysts systems did not show activity when propylene was chosen to be a monomer for olefin polymerization. The breakthrough step of this typical metallocene occurred when Kaminsky and co-workers observed that the addition of water to trialkylaluminum in

molar ratio 1:1 during the polymerization of ethylene could improve the productivity rate in significance [Sinn, 1980]. It was known that the improved activity in the event above came from the reaction between water and trialkylaluminum to produce alkylaluminoxane in the system. Thus, Kaminsky and his group decided to use the alkylaluminoxane as the cocatalyst coupling with the metallocene compound. From this combination, the next generation of metallocene catalyst was born.

It brought to the development in olefins polymerization because metallocene/aluminoxane system showed the activity higher than conventional Ziegler-Natta catalyst. In addition, the produced polymer from metallocene system gave the narrower polymer distribution than the traditional system.

2.6.2 Homogeneous metallocene catalyst with Lewis base activators systems

In this decade, not only the aluminoxane can activate the metallocene catalysts. Lewis bases can be used to produce the activator for metallocene catalyst system too. Naturally, metallocene catalyst will be active when the positive ion charged to the metal central atom. And to stabilize the cation of metal complex, the anion must be introduced to the system. Now we have enough experimental evidence to prove the hypothesis that all active center types operative with metallocenes are cation that stabilized with the counter anion derived from the cocatalyst. Cationic metallocene are prepared by combination of at least 2 compounds. The first one is the metallocene and the other is an activator that exchanges to charge the metallocene complex from neutral state to cationic state and forms a counter anion. The later component is the new step of development in polymerization from the aluminum activators. This compound must be capable of stabilizing the cationic metallocene complex and must be labile enough to displace with monomer the insertion step of polymerization too. Non-aluminum activators such as $B(C_6F_5)_3$ (Borane), $Ph_3CB(C_6F_5)_4$ (Borate) and $PhMe_2NHB(C_6F_5)_4$, may be replace the disadvantage of MAO as an activator for metallocene complexes. Several cations (metallocene) have been developed for the $[B(C_6F_5)_4]$- anion. Recently the silysium salts prepared by methathesis of $Li[B(C_6F_5)_4]$ with R_3SiCl [Devore, 1997] can be used as an activator

for polymerization. In addition, tris(pentafluorophynyl)boron is a widely used activator for converting metallocene dihydrides and dialkyls to cationic catalyst. It has been prepared by the reaction of C_6F_5MgBr (from C_6F_5Br and alkylmagnesium halides) with BF_3 etherate [Yamamoto, 1996]. These systems are very interesting in development to replace the disadvantage of MAO since it produced the near productivity. Unfortunately the active species of metallocene catalyst with these counter anions is very sensitive to air and any impurities during the polymerization.

2.6.3 Supported metallocene catalyst

Metallocene catalysts in dissolved form are in most cases unsuitable for the application in an industrial scale. In order to use them in existing technical processes (drop-in technology) by exchanging the conventional Ziegler-Natta catalysts, metallocenes have to be supported. Different methods are possible by using MAO as cocatalyst [Kaminsky and Laban, 2001].

(1) In the method of direct heterogenization, the metallocene or a mixture of the metallocene and MAO is anchored via physisorption or chemisorption onto the support. In the first case, the metallocene must be activated by external MAO.

(2) The metallocene can be supported by covalent bonding of its ligand environment to the support followed by activation with external MAO. The metallocene can be synthesized gradually as a covalent bonded species direct on the supporting material.

(3) Initial impregnation of MAO onto the support followed by adsorption and simultaneous activation of the metallocene (indirect heterogenization). In analogy to the homogeneous metallocene catalysis, the bonding between the active species $[Cp_2ZrCH_3]^+$ and the supported MAO is ionic. When performing the method of indirect heterogenization, no further MAO has to be added.
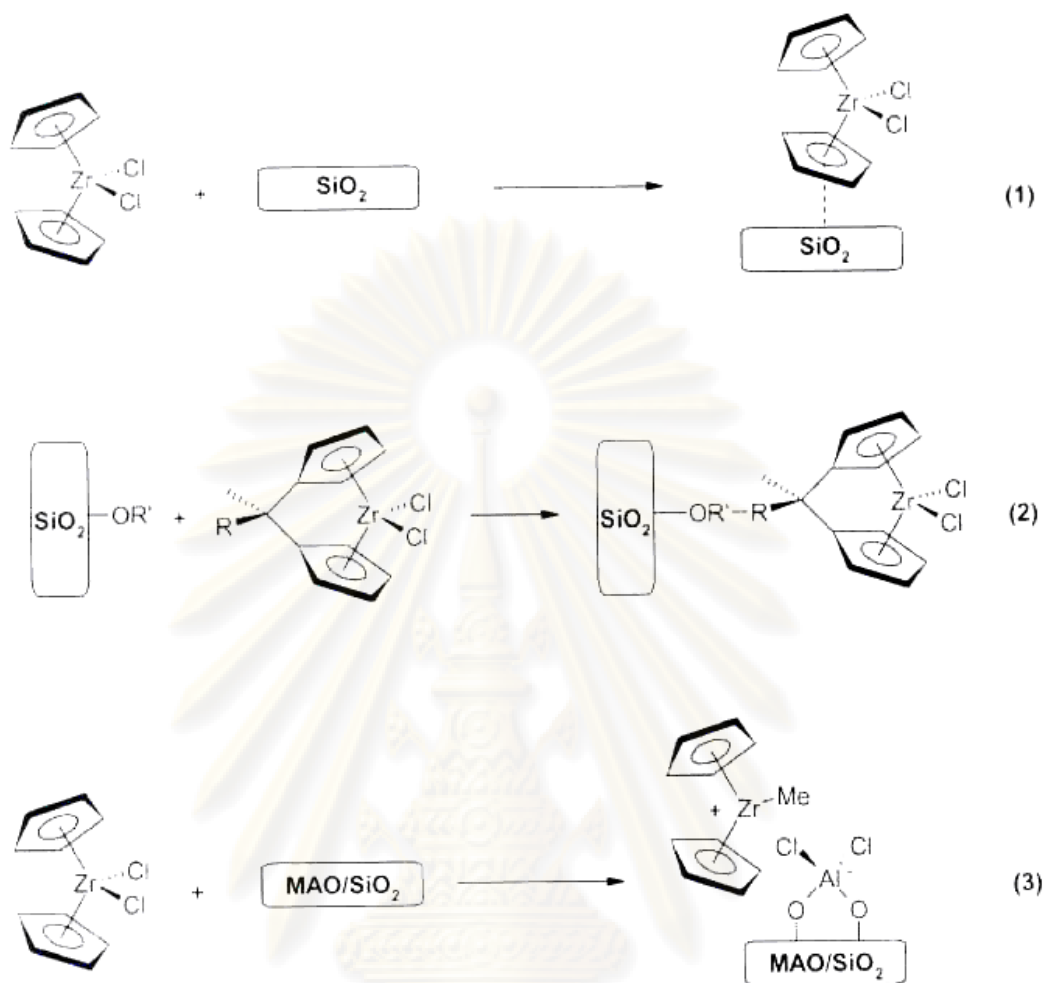
Figure 2.7 Supporting methods of metallocenes: (1) direct heterogenization, (2)
covalent bonding on the support, (3) indirect heterogenization [Kaminsky
and Laban, 2001]

Metallocenes supported according to the method of direct
heterogenization have been known to produce polymers with higher molecular weight
than those afforded by the homogeneous catalysts. However, direct heterogenization
has also been known to change the polymerization characteristics of the metallocene,
possibly by the interaction with surface hydroxyl groups. Sacchi et al. (1995) carried
out propylene polymerization in the presence of the isospecific Et[Ind]$_2$ZrCl$_2$ and the
aspecific [Ind]$_2$ZrCl$_2$ complexes in solution and anchored to SiO$_2$ and SiO$_2$/MAO
supports. From the stereochemical analysis of the polypropylene samples obtained it
can be deduced that the same active species is formed when a metallocene is in
solution and when it is anchored to the SiO$_2$/MAO support and a completely different

active species is formed when the metallocene is anchored to the silica [Sacchi et al., 1995]. Difficulties can also be encountered in the covalent bonding of metallocene complexes. If they are successively synthesized on the support, chemically non-uniform anchor groups, such as vicinal and geminal silanol group, can lead to a mixture of different active species. The most promising method of supporting is indirect heterogenization as the chemical nature of the metallocene is changed, if at all, only to a small degree. The polymers obtained by the method of indirect heterogenization are very similar to those obtained by the homogeneous system. Each metallocene on the support forms an active center and the starting point for the growth of a polymer chain. The improvements a supported catalyst needs to achieve in order to be accepted in existing manufacturing facilities are the following [Chien, 1999]:

(a) The supported catalyst system should have activity approaching those of the homogeneous catalysts.

(b) The supported system needs to be more stable.

(c) The amount of methylaluminoxane has to be greatly reduced for economic viability of the supported catalysts.

(d) The supported catalyst should produce higher Mw polymers at high temperature of polymerization compared to those produced by homogeneous system.

(e) Polyolefins obtained in homogeneous processes have a very low particle size, as well as a broad size distribution and low bulk density. Supported catalysts must be able to control the polymer morphology.

(f) The supported systems should have the capability of producing polymers having desired broad or bimodal MWD for good rheological and physical properties.

(g) Some supported metallocenes catalysts have been reported to cause fouling of gas-phase reactors. Corrective measures must be found.

(h) The steric control of metallocene catalysts is determined by molecular structure. It would be advantageous if this can be controlled or even altered by the support.

2.7 Copolymerization

By adding a small amount of comonomer to the polymerization reactor, the final polymer characteristics can be dramatically changed. For example, the Unipol

process for linear low density polyethylene (LLDPE) uses hexene and the British Petroleum process (BP) uses 4-methylpentene to produce high-performance copolymers. The comonomer can be affected the overall crystallinity, melting point, softening range, transparency and also structural, thermochemical, and rheological properties of the formed polymer. Copolymers can also be used to enhance mechanical properties by improving the miscibility in polymer blending [Albano et al., 1998].

Ethylene is copolymerized with α-olefin to produce polymers with lower densities. It is commonly observed that the addition of a comonomer generally increases the polymerization rate significantly. This comonomer effect is sometimes linked to the reduction of diffusion limitations by producing a lower crystallinity polymer or to the activation of catalytic sites by the comonomer. The polymer molecular weight often decreases with comonomer addition, possibly because of a transfer to comonomer reactions. Heterogeneous polymerization tends to be less sensitive to changes in the aluminum/transition metal ratio. Chain transfer to aluminum is also favored at high aluminum concentrations. This increase in chain transfer would presumably produce a lower molecular weight polymer. In addition, some researchers observed the decrease, and some observed no change in the molecular weight with increasing aluminum concentration [Shan et al., 2002].

The effect of polymerization conditions and molecular structure of the catalyst on ethylene/α-olefin copolymerization have been investigated extensively. Pietikainen and Seppala investigated the effect of polymerization temperature on catalyst activity and viscosity average molecular weights for low molecular weight ethylene/propylene copolymers produced with homogeneous Cp_2ZrCl_2 [Pietikainen and Seppala, 1994]. Soga and Kaminaka compared copolymerizations (ethylene/propylene, ethylene/1-hexene, and propylene/l-hexene) with $Et(H_4Ind)_2ZrC1_2$ supported on SiO_2, Al_2O_3 or $MgCl_2$. Broadness of MWD was found to be related to the combination of support types and types of monomers[Soga and Kaminaka, 1992].

Copolymer based on ethylene with different incorporation of 1-hexene, 1-octene, and 1-decene were investigated by Quijada et al.(1996). The type and the

concentration of the comonomer in the feed do not have a strong influence on the catalytic activity of the system, but the presence of the comonomer increases the activity compared with that in the absence of it. From ^{13}C-NMR it was found that the size of the lateral chain influences the percentage of comonomer incorporated, 1-hexene being the highest one incorporated. The molecular weight of the copolymers obtained was found to be dependent on the comonomer concentration in the feed, showing that there is a transfer reaction with the comonomer. The polydispersity (Mw/Mn) of the copolymers is rather narrow and dependent on the concentration of the comonomer incorporation [Quijada et al., 1996].

The effect of different catalyst support treatments in the 1-hexene/ethylene copolymerization with supported metallocene catalyst was investigated by Soares et al. The catalysts in the study were supported catalysts containing SiO_2, commercial MAO supported on silica (SMAO) and MAO pretreated silica(MAO/silica) with Cp_2HfCl_2, $Et(Ind)_2HfCl_2$, Cp_2ZrCl_2 and $Et(Ind)_2ZrCl_2$. All the investigated supported catalysts showed good activities for the ethylene polymerization (400-3000 kgpolymer/mol metal.h). Non-bridged catalysts tend to produce polymers with higher molecular weight when supported on to SMAO and narrow polydispersity. The polymer produced with Cp_2HfCl_2 supported on silica has only a single low crystallinity peak. On the other hand, Cp_2HfCl_2 supported on SMAO and MAO/silica produced ethylene/1-hexene copolymers having bimodal CCDs. For the case of Cp_2ZrCl_2 and $Et(Ind)_2ZrCl_2$, only unimodal CCDs were obtained. It seems that silica-MAO-metallocene and silicametallocene site differ slightly in their ability to incorporate comonomer into the growing polymer chain, but not enough to form bimodals CCDs [Kim and Soares, 1999].

Soares et al. (2000) investigated copolymerization of ethylene and 1-hexene with different catalysts: homogeneous $Et(Ind)_2ZrCl_2$, Cp_2HfCl_2 an $[(C_5Me_4)SiMe_2N(tert\text{-}Bu)]TiCl_2$, the corresponding in-situ supported metallocene and combined in-situ supported metallocene catalyst (mixture of $Et(Ind)_2ZrCl_2$ and Cp_2HfCl_2 and mixture of $[(C_5Me_4)SiMe_2N(tert\text{-}Bu)]TiCl_2$. They studied properties of copolymers by using ^{13}C NMR, gel permeation chromatography (GPC) and crystallization analysis fractionation (CRYSTAF) and compared with the

corresponding homogeneous metallocene. The in-situ supported metallocene produced polymers having different 1-hexene fractions, SCBD and MDW. It was also demonstrated that polymers with broader MWD and SCBD can be produced by combining two different in-situ supported metallocenes [Chu et al., 2000].

In addition, Soares et al. studied copolymerization of ethylene and 1-hexene with an in situ supported metallocene catalysts. Copolymer was produced with alkylaluminum activator and effect on MWD and SCBD was examined. They found that TMA exhibited the highest activity while TEA and TIBA had significantly lower activities. Molecular weight distributions of copolymers produced by using the different activator types were unimodal and narrow, however, short chain branching distributions were very different. Each activator exhibited unique comonomer incorporation characteristics that can produce bimodal SCBD with the use of a single activator. They used individual and mixed activator system for controlling the SCBDs of the resulting copolymers while maintaining narrow MWDs [Shan et al., 2000].

2.8 Polymer/inorganic or/and organic nanocomposites

From the many previous study results, they reported that different composite systems can lead to very different results. One important observation is that composites with nano-sized inclusions generally have different properties than composites with larger scale inclusions [Jordan et al., 2005]. The specific reasons why the polymer matrix composites with nano-sized reinforcement have different properties than composites with micron-sized reinforcement are not fully understood, but several theories have been introduced to explain some of the changes in material morphology and behavior that are seen at the nano-scale. It is important to point out, however, that most of these theories were developed to explain particular results and, therefore, are not necessarily applicable to a large number of polymer nanocomposites.

Kontou and Niaounakis studied thermo-mechanical properties of LLDPE/SiO$_2$ nanocomposites. Linear low-density polyethylene (LLDPE)/SiO$_2$ nanocomposites were prepared by two types of catalysts, one prepared by metallocene (mLLDPE) and the other by traditional Ziegler–Natta (zLLDPE) catalysts, and silica

nanoparticles surface treated with dimethyldichlorosilane. The silica nanonparticles used have an average diameter of 16 nm., and their weight fraction varied from 2 up to 10%. The structure and thermal-mechanical features of the nanocomposites were characterized by scanning electron microscopy (SEM), differential scanning calorimetry (DSC), dynamic mechanical spectroscopy (DMA) as well as tensile tests. The effect of nanoparticles on crystallinity, and hence to the morphology of the materials was studied. The secondary transitions were also affected by the filler presence, while the tensile properties were reinforced with varying the nanoparticle weight fraction. The addition of the nanofillers brought up an increase in the elastic modulus and the tensile strength of mLLDPE accompanied by an unusual dramatic increase in the elongation at break. The same trend, although to a lesser extent, was observed for the zLLDPE/SiO$_2$ composites. The increment of the elastic modulus of the composites with increasing filler content was simulated with three micromechanical models developed in previous works. The model which assumes an effective interface between the matrix and the nanoparticles provided the best fitting with the experimental data of mLLDPE/SiO$_2$ [Kontou and Niaounakis , 2006].

Li et al. investigated nano-sized and micro-sized silica particles. The particles were used to support Cp$_2$ZrCl$_2$/MAO catalyst for ethylene polymerization. Nano-sized catalyst exhibited much better ethylene polymerization activity than micro-sized catalyst. At the optimum temperature of 60 ^{o}C, nano-sized catalyst's activity was 4.35 times the micro-sized catalyst's activity, which was attributed to the large specific external surface area, the absence of internal diffusion resistance, and the better active site dispersion for the nano-sized catalyst. Polymers produced were characterized with SEM, XRD, DSC, and densimeter. SEM indicated that the resulting polymer morphology contained discrete tiny particles and thin long fiberous interlamellar links [Li et al., 2007].

Kuo et al. studied the poly(ether-ether-ketone) (PEEK) polymer filled with nano-sized silica or alumina measuring 15-30 nm to 2.5-10 wt.% are fabricated by vacuum hot press molding at 400 ^{o}C. The resulting nanocomposites with 5-7.5 wt% SiO$_2$ or Al$_2$O$_3$ nanoparticles exhibit the optimum improvement of hardness, elastic modulus, and tensile strength by 20-50%, with the sacrifice of tensile ductility. With

no surface modification for the inorganic nanoparticles, the spatial distribution of the nanoparticles appears to be reasonably uniform. There seems no apparent chemical reaction or new phase formation between the nanoparticle and matrix interface. The crystallinity degree and thermal stability of the PEEK resin with the addition of nanoparticles are examined by X-ray diffraction, differential scanning calorimetry, and thermogravity analyzer, and it is found that a higher crystallinity fraction and degradation temperature would result in the composites as compared with the unfilled PEEK [Kuo et al., 2005] .

2.9 Polymer/Titania (TiO_2) nanocomposites

Although the high amount of nanocomposite researches have done, there still have the low amount of them dealing with the nano-sized titania were used as fillers. The adequately experimental made by some researches include here.

Wang et al. (2005) studied dispersion behavior of TiO_2 nanoparticles in LLDPE/LDPE/TiO_2 nanocomposites where TiO_2 was pre-dispersed in LDPE by melt compounding. The dispersion behavior of TiO_2 nanoparticles was investigated by field-emission scanning electron microscopy (FE-SEM). The rheology results show that the viscosity of LDPE/TiO_2 master batch is lower than that of LLDPE/LDPE composites. Energy dispersive x-ray spectrometer (EDS) composition distribution map indicates that TiO_2 nanoparticles were dispersed randomly in the master batch. Scanning electron microscopy (SEM) images show that LDPE/TiO_2 master batch is crushed into micron scale dispersed phases due to the shear stress during the blow-forming process. Subsequently, TiO_2 nanoparticles in the dispersed phases are released into the ambient matrix and form a wide ring composed of monodispersed particles. The sizes of spherical crystals decrease due to the presence of TiO_2 nanoparticles in LLDPE/LDPE/TiO_2 nanocomposites. The transparency of LLDPE/LDPE/TiO_2 composite films decreases little compared to that of LLDPE/LDPE composite films [Wang et al., 2005].

Ma et al. (2005) studied effect of titania nanoparticles on the morphology of LDPE. The role of TiO_2 nanoparticle surfaces in affecting the crystalline structure of

LDPE has been investigated by varying the nanoparticle surface from hydrophilic (as-received) to less hydrophilic (dried) or more hydrophilic (polar silane treated). Differential scanning calorimetry (DSC) and wide-angle X-ray diffraction (WXRD) were used to determine the degree of crystallinity and crystalline structure. The impact of nanoparticle aggregates on the nanometer to micrometer organization of LDPE crystals was studied with atomic force microscopy (AFM) and small-angle light scattering (SALS). This characterization showed that the presence of the TiO_2 nanoparticles, with the various different surface conditions investigated, did not alter the degree of LDPE crystallinity, the unit cell dimensions, the average lamellar thickness, or the average spherulite size. However, the nanoparticles did affect the internal arrangement of intraspherulitic crystalline aggregates by decreasing the relative optic axis orientation of these crystals, usually referred to as internal spherulite disorder. The LDPE filled with the nanoparticles treated with a polar silane (N-(2-aminoethyl) 3-aminopropyl-trimethoxysilane (AEAPS)) showed the highest internal spherulitic disorder and exhibited the most poorly developed spherulite structure. The combination of SALS with AFM has allowed a detailed characterization of the morphology of the semicrystalline polymer nanocomposites. Information on the internal organization of the spherulites, the size of the nanoparticle aggregates, and the location of the nanoparticle aggregates can be uniquely obtained when both techniques are used [Ma et al., 2005].

Liu et al. investigated effect of nanoscale SiO_2 and TiO_2 as the fillers on the mechanical properties and aging behavior of LLDPE/LDPE blends. LLDPE was blended with LDPE at a fixed ratio (80 wt LLDPE and 20 wt %LDPE) and filled with nanoparticles of SiO_2 and TiO_2 at a ratio up to wt 5%, so as to develop the polymeric composites suitable to preparing the agricultural micro-irrigation pipes having good environmental adaptability. These compounds were blended using calcium stearate, polyethylene wax, and titanate coupling agent as the auxiliary dispersants, and ethylene-vinyl acetate copolymer (EVA) as the toughness improver. The LLDPE/LDPE composites filled with the nanoparticles were extruded and injected to prepare the composites specimens for the performance evaluations and micro-irrigation pipe field test. The mechanical properties, thermostability, and processibility of the injected composites were investigated. The effect of heating in an

oven and irradiating by ultraviolet on the mechanical properties of the composites was explored. The environmental adaptability of the micro-irrigation pipes made of the filled LLDPE/LDPE composites was evaluated making use of long-term outdoor field test in northwest China where the arid and harsh natural conditions are of great concerns. It was found that the LLDPE/LDPE blend with the LLDPE mass fraction fixed as 80% showed balanced mechanical and thermal properties and flexibility, and was suitable to be used as the basic resin matrix. The incorporation of nano-TiO_2 contributed to effectively improving the resistance to heating and ultraviolet irradiation of the composites. The composite made from 91% basic resin matrix, 6% EVA, and 3% mixed nano-SiO_2 and TiO_2, showed balanced comprehensive properties. The micro-irrigation pipes made of this filled LLDPE/LDPE composite had good environmental adaptability and service behavior in a three-year field test and were suitable to be used in arid area [Liu et al., 2005].

Chau et al. prepared acetic acid-modified TiO_2 nanoparticles by sol–gel synthesis method. The nanoparticles can be incorporated directly into the polymer matrix to form transparent high refractive index nanocomposite thin films. The result shows that increasing the titania content in the hybrid nanocomposite thin films can significantly increase the refractive index. Hybrid nanocomposite thin film with refractive index value of 2.38 had been prepared. All prepared films also exhibit excellent optical transparency in the visible region [Chau et al., 2007].

Nakayama et al. studied novel of nanocomposite films of TiO_2 nanoparticles and hydrophobic polymers having polar groups, poly(bisphenol-A and epicholohydrin) or copolymer of styrene and maleic anhydride, with high refractive indices, high transparency, no color, solvent-resistance, good thermal stability, mechanical properties were prepared by incorporating surface-modified TiO_2 nanoparticles into polymer matrices. In the process of preparing colloidal solution of TiO_2 nanoparticles, severe aggregation of particles can be reduced by surface modification using carboxylic acids and long chain alkyl amines. These TiO_2 nanoparticles dispersed in solvent were found not to aggregate after mixing with polymer solutions. Transparent colorless free-standing films were obtained by drying a mixture of TiO_2 nanoparticles colloidal solution and polymer solution in vacuum.

Transmission electronic microscopic studied of the films suggest that the TiO$_2$ nanoparticles of 3-6 nm in diameter were dispersed in polymer matrices while maintaining their original size. Thermogravimetric analysis results indicate that the nanocomposite film has good thermal stability and the weight fraction of observed TiO$_2$ nanoparticles in the film is in good accordance with that of theoretical calculations. The refractive index of nanocomposite films of TiO$_2$ and poly(bisphenol-A and epichlorohydrin) was in the range of 1.58-1.81 at 589 nm, which linearly increased with the content of TiO$_2$ nanoparticles from 0 to 80 wt% [Nakayama and Hayashi, 2007].

CHAPTER III

EXPERIMENTAL

Research Methodology

This thesis was divided into two parts :

Part 1 : Investigation of the effect of the crystallite size of nano-TiO$_2$ fillers on the characteristics of LLDPE/TiO$_2$ nanocomposites synthesized by *in situ* polymerization of ethylene/1-hexene using a zirconocene/MMAO catalyst which prepared by *in situ* impregnation method. (Research Methodology of flow diagram is shown in **Figure 3.1**)

Part 2 : Investigation of the effect of the modification of nano-TiO$_2$ fillers on the characteristics of LLDPE/TiO$_2$ nanocomposites synthesized by *in situ* polymerization of ethylene/1-hexene using a zirconocene/MMAO catalyst which prepared by *in situ* impregnation method. (Research Methodology of flow diagram is shown in **Figure 3.2**)

All reactions were conducted under argon atmosphere using Schlenk techniques and glove box.

```
┌─────────────────────────────────────────────────┐
│   Preparation of different crystallite size of    │
│      nano-TiO₂ fillers by the sol-gel method      │
└─────────────────────────────────────────────────┘
                        │
                        ▼
┌─────────────────────────────────────────────────┐
│        Characterization of nano-TiO₂ fillers       │
│     using XRD, SEM, TEM and BET surface area       │
└─────────────────────────────────────────────────┘
                        │
                        ▼
┌─────────────────────────────────────────────────┐
│               In situ impregnation                 │
└─────────────────────────────────────────────────┘
                        │
                        ▼
┌─────────────────────────────────────────────────┐
│ Copolymerization of ethylene with 1-hexene reaction at 70˚C │
│  [initiated copolymerization by introducing ethylene gas   │
│       (at 6 psi consumption and total pressure 50 psi)]     │
└─────────────────────────────────────────────────┘
                        │
                        ▼
┌─────────────────────────────────────────────────┐
│            LLDPE /TiO₂ nanocomposites              │
└─────────────────────────────────────────────────┘
                        │
                        ▼
┌─────────────────────────────────────────────────┐
│         Characterization of LLDPE/TiO₂             │
│    nanocomposites using  SEM/EDX, TEM,             │
│            DSC and ¹³C-NMR                          │
└─────────────────────────────────────────────────┘
                        │
                        ▼
┌─────────────────────────────────────────────────┐
│            Discussion and conclusion               │
└─────────────────────────────────────────────────┘
```

Figure 3.1 Flow diagram of research methodology in Part 1

```
┌─────────────────────────────────────────┐
│ Preparation of different modification (Ga,Zr) of │
│        nano-TiO₂ fillers by the incipient wetness │
│              impregnation method          │
└─────────────────────────────────────────┘
                    │
                    ▼
┌─────────────────────────────────────────┐
│      Characterization of nano-TiO₂ fillers │
│    using XRD, SEM, TEM and BET surface area │
└─────────────────────────────────────────┘
                    │
                    ▼
┌─────────────────────────────────────────┐
│            In situ impregnation           │
└─────────────────────────────────────────┘
                    │
                    ▼
┌─────────────────────────────────────────┐
│ Copolymerization of ethylene with 1-hexene reaction at 70°C │
│   [initiated copolymerization by introducing ethylene gas │
│        (at 6 psi consumption and total pressure 50 psi)] │
└─────────────────────────────────────────┘
                    │
                    ▼
┌─────────────────────────────────────────┐
│          LLDPE /TiO₂ nanocomposites       │
└─────────────────────────────────────────┘
                    │
                    ▼
┌─────────────────────────────────────────┐
│       Characterization of LLDPE/TiO₂       │
│      nanocomposites using  SEM/EDX, TEM,  │
│            DSC and ¹³C-NMR                 │
└─────────────────────────────────────────┘
                    │
                    ▼
┌─────────────────────────────────────────┐
│          Discussion and conclusion        │
└─────────────────────────────────────────┘
```

The flow diagram shows the following steps connected by downward arrows:

1. Preparation of different modification (Ga,Zr) of nano-TiO_2 fillers by the incipient wetness impregnation method
2. Characterization of nano-TiO_2 fillers using XRD, SEM, TEM and BET surface area
3. *In situ* impregnation
4. Copolymerization of ethylene with 1-hexene reaction at 70°C [initiated copolymerization by introducing ethylene gas (at 6 psi consumption and total pressure 50 psi)]
5. LLDPE /TiO_2 nanocomposites
6. Characterization of LLDPE/TiO_2 nanocomposites using SEM/EDX, TEM, DSC and ^{13}C-NMR
7. Discussion and conclusion

Figure 3.2 Flow diagram of research methodology in Part 2

Experimental Section

The experimental was divided into four major parts:

(i)   Chemicals and equipments,

(ii)   Preparation of nano-TiO$_2$ fillers,

(iii)   Ethylene and 1-hexene copolymerization procedure,

(iv)   Characterization of nano-TiO$_2$ fillers and polymer nanocomposites.

The details of the experiments are explained as follows :

3.1 Chemicals and equipments

3.1.1 Chemicals

The chemicals used in these experiments are analytical grade, but only major materials are specified as follows:

1.   Ethylene gas (99.96%) was devoted from National Petrochemical Co., Ltd., Thailand and used as received.

2.   1-Hexene (99+%) was purchased from Aldrich Chemical Company, Inc. and purified by distilling over sodium under argon atmosphere before use.

3.   Hexane (95%) was donated from Shell (Public) Company, Inc. and purified by distilling over sodium under argon atmosphere before use.

4.   Heptane ($\geq$ 97%) was purchased from Fluka Chemie A.G. Switzerland and purified by distilling over sodium under argon atmosphere before used.

5.   Toluene was devoted from EXXON Chemical Ltd., Thailand.   This solvent was dried over dehydrated CaCl$_2$ and distilled over sodium/benzophenone under argon atmosphere before use.

6.   Modified Methylaluminoxane (MMAO) 1.86 M in hexane was donated from Tosoh Akso, Japan and used without further purification.

7.   Trimethylaluminum (TMA) 2.0 M in toluene was supplied from Nippon aluminum Alkyls Ltd., Japan and used without further purification.

8. Rac-ethylenebis(indenyl)zirconiumn dichloride (Et(Ind)$_2$ZrCl$_2$) was suppleid from Aldrich Chemical Company, Inc. and used without further purification.

9. Hydrochloric acid (Fuming 36.7%) was supplied from Sigma and used as received.

10. Methanol (Commercial grade) was purchased from SR lab and used as received.

11. Sodium (99%) was purchased from Aldrich Chemical Company, Inc. and used as received.

12. Benzophenone (99%) was purchased from Fluka Chemie A.G. Switzerland and used as received.

13. Calciumhydride (99%) was purchased from Fluka Chemie A.G. Switzerland and used as received.

14. Ultra high purity argon gas (99.999%) was purchased from Thai Industrial Gas Co., Ltd., and further purified by passing through columns packed with molecular sieve 3A, BASF Catalyst R3-11G, sodium hydroxide (NaOH) and phosphorus pentaoxide (P$_2$O$_5$) to remove traces of oxygen and moisture.

15. Titanium isopropoxide (99.999%) was purchased from Aldrich Chemical Company, Inc. and used as received.

16. Ethanol (anhydrous) was purchased from Aldrich Chemical Company, Inc. and used as received.

17. Titanium (IV) oxide nanopowder (100 % anatase, TiO$_2$ (A)) was purchased from Aldrich Chemical Company.

18. Gallium (III) nitrate hydrate (99.9%) was purchased from Aldrich Chemical Company.

19. Zirconium (IV) *n*-propoxide 70wt% solution in 1-propanol was purchased from Aldrich Chemical Company.

3.1.2 Equipments

Because of the metallocene system is extremely sensitive to the oxygen and moisture. Thus, the special equipments are required to handle while the preparation and polymerization process. For example, glove box: equipped with the oxygen and

moisture protection system is used to produce the inert atmosphere. Schlenk techniques (Vacuum and Purge with inert gas) are the others set of the equipment used to handle air-sensitive product.

3.1.2.1 Cooling system

The cooling system was in the solvent distillation in order to condense the freshly evaporated solvent.

3.1.2.2 Inert gas supply

The inert gas (argon) was passed through columns of BASF catalyst R3-11G as oxygen scavenger, molecular sieve 3×10^{-10} m to remove moisture. The BASF catalyst was regenerated by treatment with hydrogen at 300°C overnight before flowing the argon gas through all the above columns. The inert gas supply system can be shown in **Figure 3.3**.
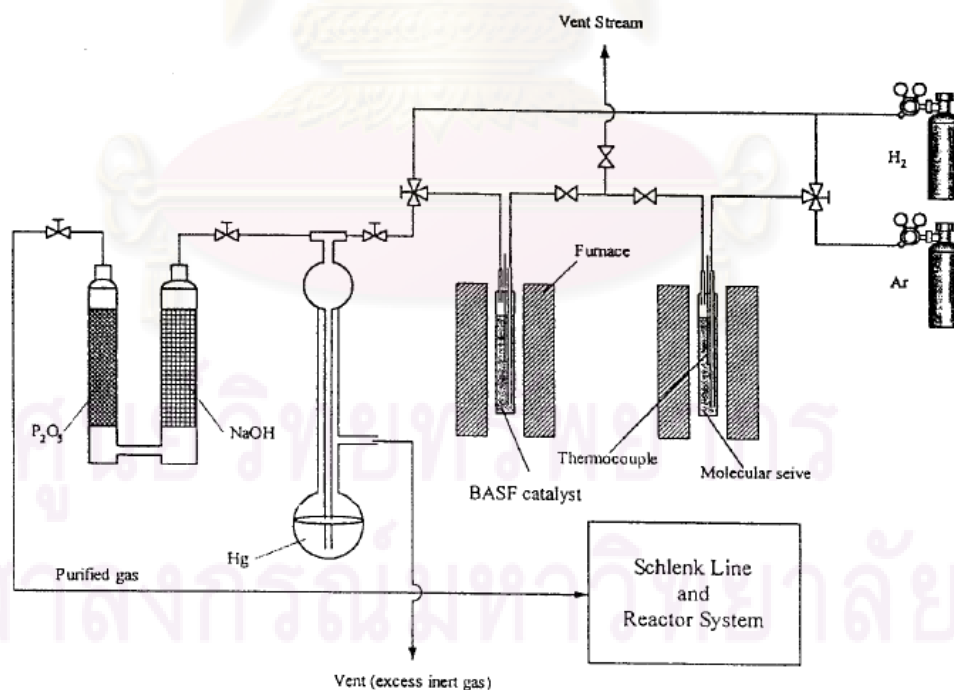
Figure 3.3 Inert gas supply system

3.1.2.3 Magnetic stirrer and heater

The magnetic stirrer and heater model RTC basis from IKA Labortechnik were used.

3.1.2.4 Reactor

A 100 ml glass flask connected with 3-ways valve was used as the copolymerization reactor for atmospheric pressure system and a 100 ml stainless steel autoclave was used as the copolymerization reactor for high pressure systems.

3.1.2.5 Schlenk line

Schlenk line consists of vacuum and argon lines. The vacuum line was equipped with the solvent trap and vacuum pump, respectively. The argon line was connected with the trap and the mercury bubbler that was a manometer tube and contains enough mercury to provide a seal from the atmosphere when argon line was evacuated. The schlenk line was shown in **Figure 3.4**.
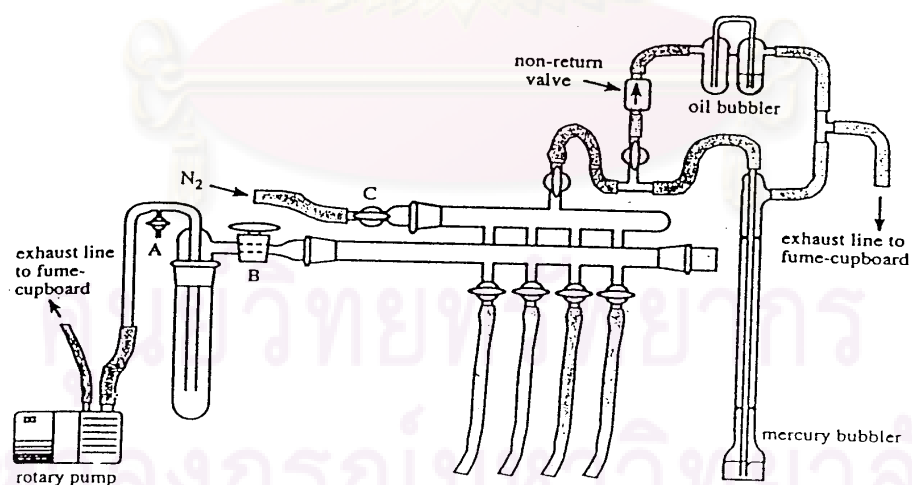
Figure 3.4 Schlenk line

3.1.2.6 Schlenk tube

A tube with a ground glass joint and side arm, which was three-way glassvalve. Sizes of Schlenk tubes were 50, 100 and 200 mL used to prepare catalyst and store materials which are sensitive to oxygen and moisture. The Schlenk tube picture was shown in **Figure 3.5**.
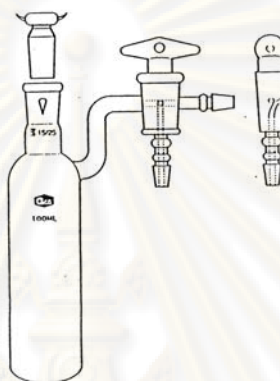
Figure 3.5 Schlenk tube

3.1.2.7 Vacuum pump

The vacuum pump model 195 from Labconco Corporation was used. A pressure of 10^{-1} to 10^{-3} mmHg was adequate for the vacuum supply to the vacuum line in the Schlenk line. The vacuum pump is shown in **Figure 3.6**.
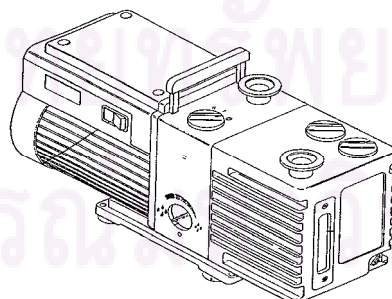
Figure 3.6 Vacuum pump.

3.1.2.8 Polymerization line
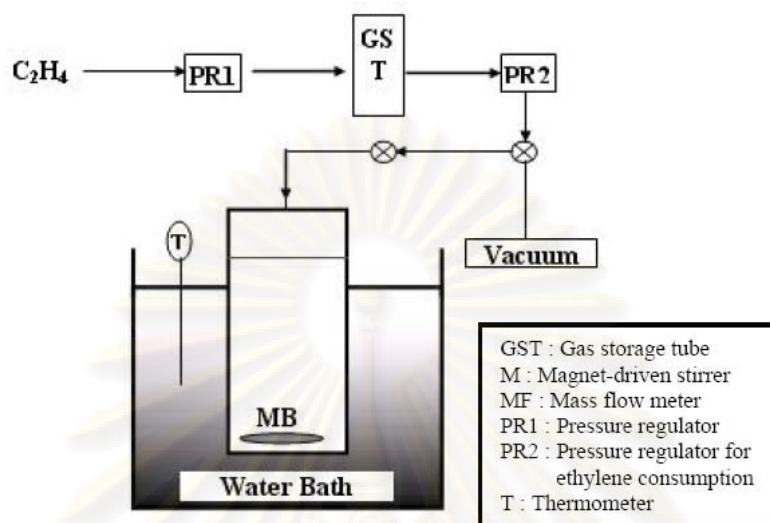
Figure 3.7 Diagram of system in slurry phase polymerization

3.2 Preparation of nano-TiO$_2$ fillers

3.2.1 Preparation of different crystallite size of nano-TiO$_2$ fillers

Nano-TiO$_2$ fillers were synthesized by the sol-gel method using titanium isopropoxide as the titania precursor. First, titania precursor was dissolved in ethanol and mixed with a different water:alkoxide molar ratio in the range of 4 to 80. And then a precursor solution was added dropwise to the aqueous solution with stirring by ultrasonic at room temperature. White precipitates of hydrous oxides were produced instantly and the mixture was stirred for at least 2 hours. The amorphous precipitates were separated from the mother liquor by centrifugation and redispersed in ethanol for five times to minimize particle agglomeration. The resulting materials were dried and calcined at 450 ^{o}C for 2 hours [Suriye et al., 2005;2007].

3.2.2 Preparation of different modification of nano-TiO$_2$ fillers

A Ga-modified TiO$_2$ fillers / Zr-modified TiO$_2$ fillers were prepared by incipient wetness impregnation method. A designed amount of gallium (III) nitrate

hydrate / zirconium (IV) *n*-propoxide was dissolved in deionized water and then impregnated into the nano-TiO_2 fillers with 1 wt% Ga and 1 wt% Zr by calculating of the required amounts of Ga/Zr loading (see **Appendix A**). The fillers was dried at 110˚C for 12 hours and calcined in air at 500˚C for 4 hours for Ga modification and calcined at 350˚C for 2 hours for Zr modification.

3.3 *In situ* impregnation and polymerization reaction

In situ impregnation and polymerization reaction were conducted upon the methods as follows. The ethylene and 1-hexene copolymerization reaction was carried out in a 100 ml semi-batch stainless steel autoclave reactor equipped with magnetic stirrer. In the glove box, the desired amount of the nanofiller was allowed to contact with 1.14 ml of MMAO for 30 minutes in reactor with magnetic stiring. Then toluene was introduced in to the reactor (to make the total volume of 30 ml). The desired amount of Et(Ind)$_2$ZrCl$_2$ (5 x 10^{-5} M.) and TMA ([Al]$_{TMA}$/[Zr]$_{cat}$ = 2500) was mixed and stirred for 5 minutes aging at room temperature, separately, then was injected into the reactor. The reactor was frozen in liquid nitrogen to stop reaction and then 0.018 mol of 1-hexene was injected into the reactor. The reactor was evacuated to remove argon. The reactor was heated up to polymerization temperature (70˚C). To start reaction, 0.018 mole of ethylene (6 psi was observed from the pressure gauge) was fed into the reactor containing the comonomer and catalyst mixtures. After all ethylene was consumed, the reaction was terminated by addition of acidic methanol and stirred for 30 minutes. After filtration, the obtained copolymer (white powder) was washed with methanol and dried at room temperature.

3.4 Characterization procedures

3.4.1 Characterization of nano-TiO$_2$ fillers

3.4.1.1 X-ray diffraction (XRD)

XRD was performed to determine the bulk crystalline phases of sample. It was conducted using a SIEMENS D-5000 X-ray diffractometer connected with a computer with Diffract ZT version 3.3 program for fully control of the XRD analyzer. The experiments were carried out by using CuKα (λ = 1.54439 Å) radiation with Ni filter in the range 2θ = 20-80° resolution 0.04.

3.4.1.2 Transmission electron microscopy (TEM)

Transmission electron microscopy: TEM was used to determine the shape and size of nano-TiO$_2$ fillers. The sample was dispersed in ethanol before using TEM (JEOL JEM-2010) for microstructural characterization.

3.4.1.3 Thermal gravimetric analysis (TGA)

Thermal gravimetric analysis: TGA was performed using a TA Instruments SDT Q-600 analyzer. The samples of 10-20 mg and a temperature ramping from 25 to 600°C at 2°C /min were used in the operation. The carrier gas was N$_2$ UHP.

3.4.1.4 Scanning electron microscopy (SEM) and energy dispersive X-ray spectroscopy (EDX)

Scanning electron microscopy and energy dispersive X-ray spectroscopy: SEM and EDX were used to investigate the sample morphologies and elemental distribution throughout the nano- TiO$_2$ fillers. The SEM of JEOL mode JSM-5800 LV

scanning microscope was employed. EDX was further performed using Link Isis series 300 program.

3.4.1.5 BET surface area

Surface area measurement was carried out by low temperature nitrogen adsorption in a Micromeritic ChemiSorb 2750 system. Calculation was performed on the basis of the BET isotherm. 0.2 grams of sample was loaded into u-shape cell made from Pyrex and heated in helium to 200˚C for 1 hours in order to eliminate trace amount of water adsorbed on surface, then cooled down to room temperature. The analysis gas consist of $30\%N_2$ in helium was introduced to Pyrex cell. Sample adsorbed nitrogen at low temperature by dipped cell into liquid nitrogen dewar until its surface was satuated with nitrogen and desorbed nitrogen at room temperature by moved away the dewar. The nitrogen that was desorbed from sample was measured by TCD detector.

3.4.2 Characterization of polymer

3.4.2.1 Scanning electron microscopy (SEM) and energy dispersive X-ray spectroscopy (EDX)

Scanning electron microscopy and energy dispersive X-ray spectroscopy: SEM and EDX were performed to study the morphologies of polymer and elemental distribution within polymer matrix. The same equipment as mentioned above was employed

3.4.2.2 Transmission electron microscopy (TEM)

Transmission electron microscopy: TEM was used to determine the dispersion of nano-TiO_2 fillers in LLDPE. The same equipment as mentioned above was employed.

3.4.2.3 Differential scanning calorimetry (DSC)

Differential scanning calorimetry: the melting temperature of ethylene/1-hexene copolymer products was determined with a Perkin-Elmer diamond DSC. The analyses were performed at the heating rate of 20°C/min in the temperature range of 50-150°C. The heating cycle was run twice. In the first scan, sample was heated and cooled to 150°C. In the second scan, sample was reheated at the same rate, but only the result of the second scan was reported because the first scan was influenced by the mechanical and thermal history of sample.

3.4.2.4 Nuclear magnetic resonance (NMR)

^{13}C NMR spectroscopy: ^{13}C NMR spectroscopy was used to determine the 1-hexene incorporation and copolymer microstructure. Chemical shifts were referenced internally to the $CDCl_3$ and calculated according to the method described by Randall. Each sample solution was prepared by dissolving 50 mg of copolymer in 1,2 dicholobenzene and $CDCl_3$. The ^{13}C NMR spectra were taken at 100°C using a BRUKER AVANCE II 400 operating at 100 MHz with an acquisition time of 1.5 s and delay time of 4 s.

CHAPTER IV

RESULTS AND DISCUSSIONS

This chapter is divided into two sections :

Section 1 : Investigation of the effect of the crystallite size of nano-TiO_2 fillers on the characteristics of LLDPE/TiO_2 nanocomposites synthesized by *in situ* polymerization of ethylene/1-hexene using a zirconocene/MMAO catalyst, which prepared by *in situ* impregnation method.

Section 2 : Investigation of the effect of the modification of nano-TiO_2 fillers on the characteristics of LLDPE/TiO_2 nanocomposites synthesized by *in situ* polymerization of ethylene/1-hexene using a zirconocene/MMAO catalyst, which prepared by *in situ* impregnation method.

4.1 Investigation of the effect of the crystallite size of nano-TiO$_2$ fillers on the characteristics of LLDPE/TiO$_2$ nanocomposites synthesized by *in situ* polymerization of ethylene/1-hexene using a zirconocene/MMAO catalyst, which prepared by *in situ* impregnation method.

In this section, nano-TiO$_2$ fillers were prepared by the sol-gel method using different water:alkoxide ratios in the range of 4 to 80 in order to obtain different crystallite sizes of TiO$_2$.

4.1.1 Characterization of fillers

4.1.1.1 BET surface areas

The most common procedure for determining surface area of a solid is based on adsorption and condensation of nitrogen at liquid nitrogen temperature. This method is also called BET (Brunauer Emmett Teller) method.

BET surface areas, water: alkoxide ratio, and average crystallite size of nano-TiO$_2$ fillers are shown in **Table 4.1**. An increase in water: alkoxide ratio in the range of 4-80 resulted in decreased crystallite size of nano-TiO$_2$ fillers and increased in BET surface area.

Table 4.1 Water: alkoxide ratio, average crystallite size, and BET surface areas of nano-TiO$_2$ fillers

Sample	Water : alkoxide ratio	Average crystallite size[a] (nm)	BET surface area (m^2/g)
TiO$_2$_10 nm	80	10	79
TiO$_2$_13 nm	16	13	58
TiO$_2$_16 nm	4	16	48

[a] Determined by XRD

4.1.1.2 X-ray Diffraction (XRD)

The XRD patterns of nano-TiO$_2$ fillers with different crystallite size are shown in **Figure 4.1**. They were collected at diffraction angle (2θ) between 20° and 80°, it was observed that all nano-TiO$_2$ fillers exhibited XRD peaks at 25°, 37°, 48°, 55°, 56°, 62°, 69°, 71°, and 75° assigning to anatase TiO$_2$.
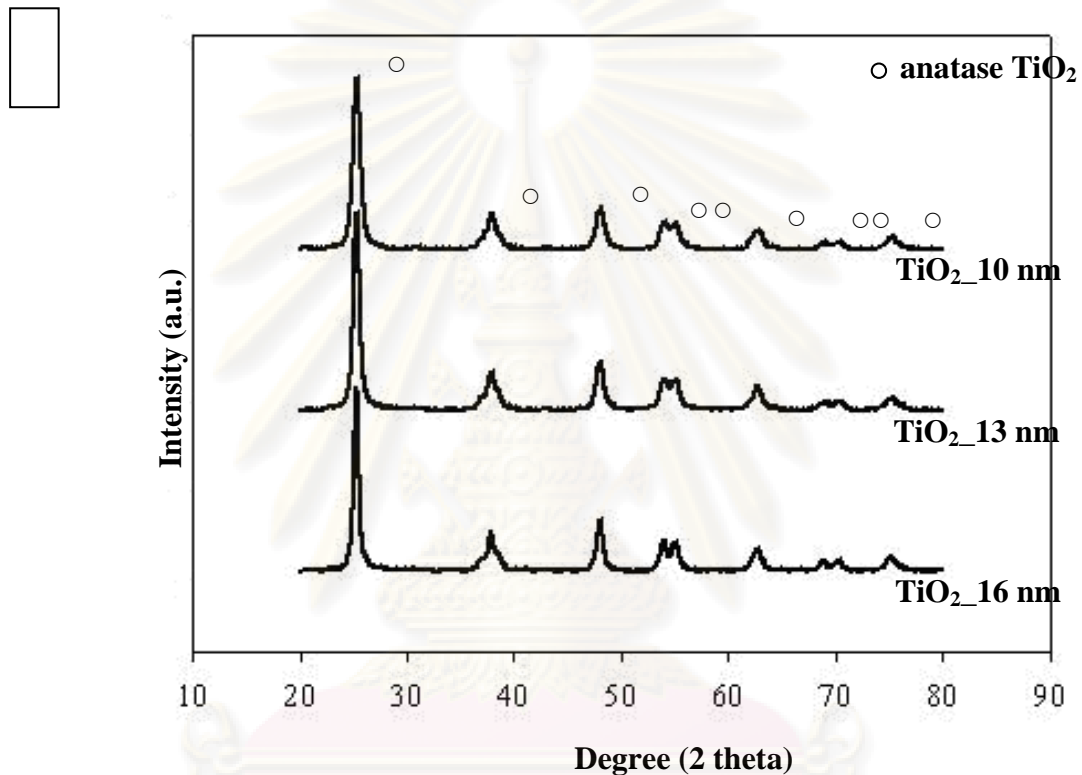
Figure 4.1 XRD patterns of nano-TiO$_2$ fillers with different crystallite sizes

4.1.1.3 Scanning electron microscopy (SEM)

Scanning electron microscopy (SEM) is a powerful tool for observing directly surface texture, morphology and particle granule size of materials. In the backscattering mode (SEM), the electron beam focused on the sample is scanned by a set of deflection coil. Backscattered electrons or secondary electrons emitted from the sample are detected.

The typical SEM micrographs of nano-TiO$_2$ fillers with different crystallite sizes are shown in **Figure 4.2**.

Figure 4.2 SEM micrographs of nano-TiO$_2$ fillers with different crystallite sizes

4.1.1.4 Transmission electron microscopy (TEM)

TEM is a useful tool for determining crystallite size and size distribution of materials. It allows determination of the micro-texture and microstructure of electron transparent samples by transmission of a focused parallel electron beam to a fluorescent screen with a resolution presently better than 0.2 nm.

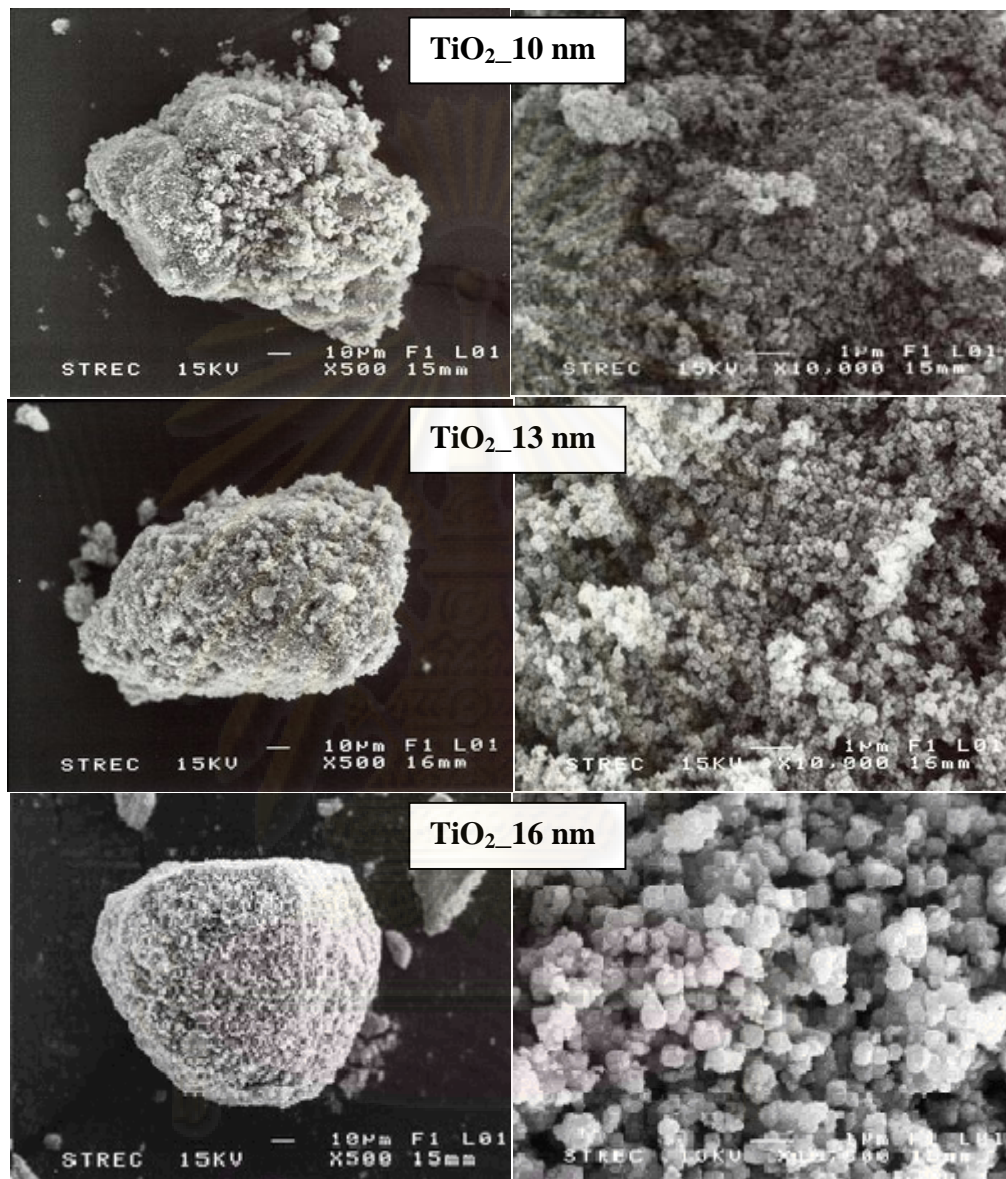The typical TEM micrographs of nano-TiO$_2$ fillers with different crystallite sizes are shown in **Figure 4.3**.
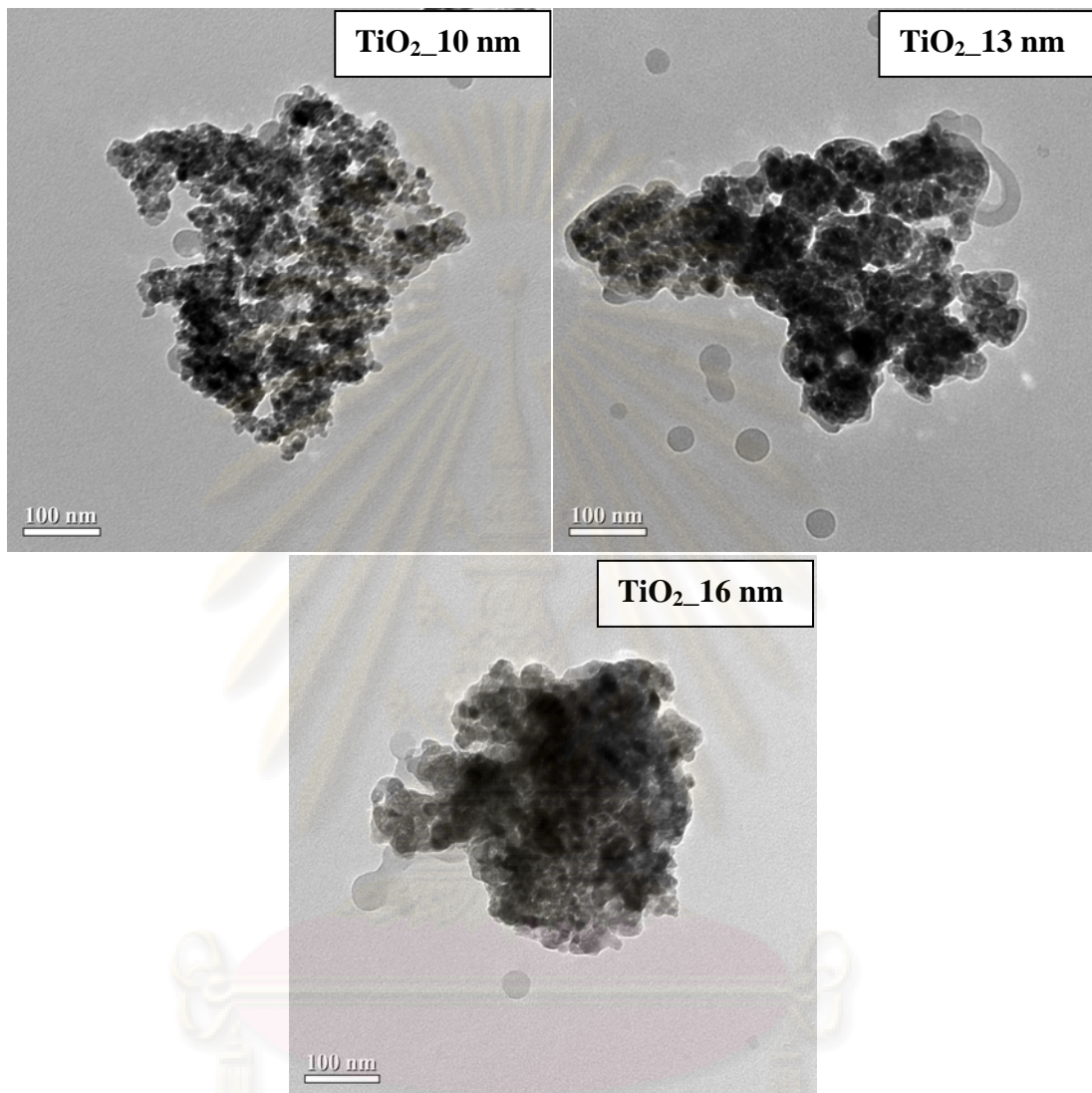
Figure 4.3 TEM micrographs of nano-TiO$_2$ fillers with different crystallite sizes

4.1.2 Effect of the crystallite size of nano-TiO$_2$ fillers on the characteristics of LLDPE/TiO$_2$ nanocomposites

Table 4.2 shows the polymerization activities of LLDPE/TiO$_2$ nanocomposites, which different crystallite sizes of nano-TiO$_2$ fillers synthesized by *in situ* impregnation method. **Table 4.3** shows the comparison of polymerization activities of LLDPE/TiO$_2$ nanocomposites synthesized by *in situ* impregnation

method and *ex situ* impregnation method. The procedure to synthesize the LLDPE/TiO$_2$ nanocomposites by *ex situ* impregnation method was also described in **Appendix B**.

Table 4.2 Polymerization activities of LLDPE/TiO$_2$ nanocomposites (*In situ* impregnation method)

Sample	Polymerization time [a] (sec)	Polymerization yield [b] (g)	Catalytic activity (kg polymer/mol Zr.h)
Homogeneous	126	1.16	22055
TiO$_2$_10 nm	103	1.30	30296
TiO$_2$_13 nm	115	1.54	32112
TiO$_2$_16 nm	102	1.44	33922

[a] A period of time used for the total 0.018 mol of ethylene to be consumed.

[b] Measurement at polymerization temperature of 70˚C, [ethylene] = 0.018 mol, [Al]$_{MMAO}$/[Zr] = 1135, [Al]$_{TMA}$ /[Zr]$_{cat}$ = 2500, in toluene with total volume = 30 mL, and [Zr]$_{cat}$ = 5 x 10^{-5} M.

Considering, activities for different nano-TiO$_2$ crystallite size of 10 nm(TiO$_2$_10 nm), 13 nm (TiO$_2$_13 nm) and 16 nm (TiO$_2$_16 nm). It was found that TiO$_2$_16 nm exhibited the highest activities among the TiO$_2$_13 nm and TiO$_2$_10 nm fillers. The higher activities can be attributed to fewer interactions between TiO$_2$ and MMAO arising from the larger particles. The smaller crystallite size may interact more with MMAO resulting in decreased activities because it is more difficult for metallocene to react with the strongly interaction MMAO on TiO$_2$ surface. Besides, the strong interaction between MMAO and TiO$_2$, it should be mentioned that the smaller crystallite size also render more steric hindrance [Chaichana et al., 2007]. On the other hand, The degree of interaction between the nanofillers and [Al]$_{MMAO}$ can be determined using the TGA measurement. To give a better understanding, Severn et al. explained that the connection of the support (nanofillers) and cocatalyst occurred via the O$_{filler}$---Al$_{cocatalyst}$ linkage [Severn et al., 2005]. In particular, the TGA can only provide useful information on the degree of interaction for the [Al]$_{MMAO}$ bound to the

support in terms of weight loss and removal temperature. As a matter of fact, too strong interaction can result in it being more difficult for the $[Al]_{MMAO}$ bound to the support to react with metallocene catalyst during activation processes, leading to low activity for polymerization. In contrast, the leaching of $[Al]_{MMAO}$ can occur due to very weak interaction resulting in low activity as well. Experimentally, the TGA measurement was performed to prove the interaction between the $[Al]_{MMAO}$ and each nanofiller. The TGA profile of $[Al]_{MMAO}$ on each nanofiller are shown in **Figure 4.4**. It was found that the weight loss of $[Al]_{MMAO}$ on each nanofiller was in the order of TiO_2_16 nm (17%) > TiO_2_13 nm (16%) > TiO_2_10 nm (13%). This indicated that the $[Al]_{MMAO}$ present on the TiO_2_10 nm nanofiller exhibited the stronger interaction than that on the TiO_2_13 nm nanofiller and TiO_2_16 nm nanofiller, respectively. So based on the TGA measurement the observed polymerization activities were affected by crystallite sizes as listed in **Table 4.2**.
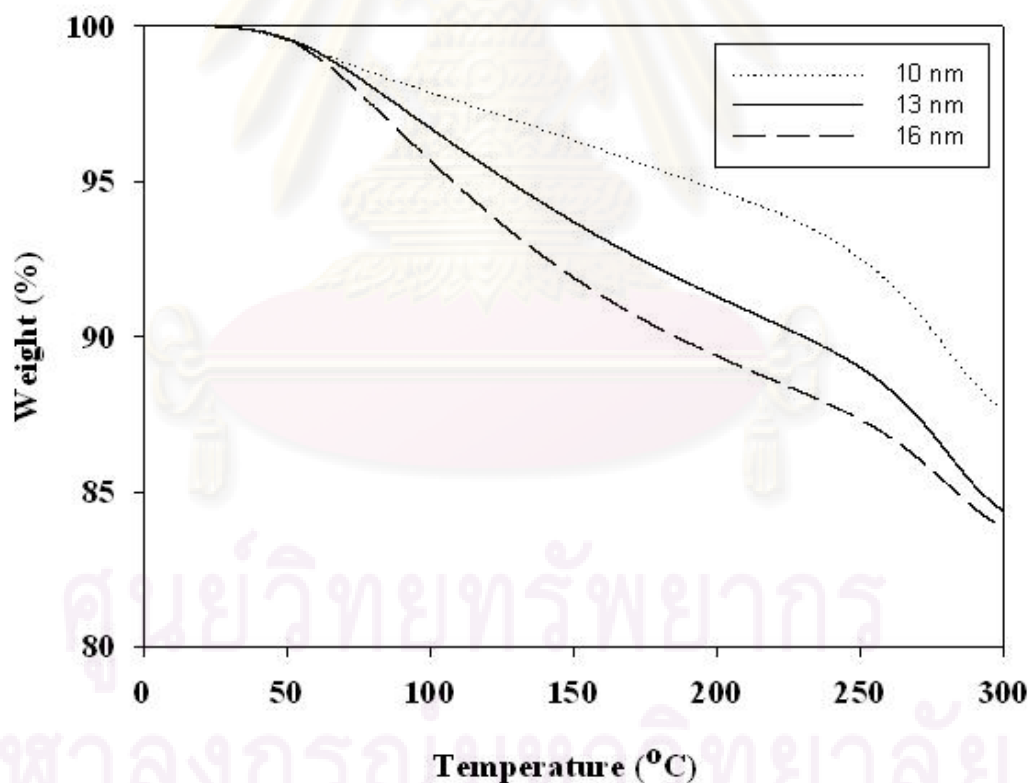

Figure 4.4 The TGA profile of $[Al]_{MMAO}$ on different crystallite size of nano-TiO_2 fillers.

Table 4.3 Comparison of polymerization activities of LLDPE/TiO$_2$ nanocomposites synthesized by *in situ* impregnation method and *ex situ* impregnation method

Sample	Polymerization time [a] (sec)	Polymerization yield [b] (g)	Catalytic activity (kg polymer/mol Zr.h)
Homogeneous	126	1.16	22055
Homogeneous*	145	0.998	16510
TiO$_2$_10 nm	103	1.30	30296
TiO$_2$_10 nm*	207	0.786	9112

[a] A period of time used for the total 0.018 mol of ethylene to be consumed.

[b] Measurement at polymerization temperature of 70˚C, [ethylene] = 0.018 mol, [Al]$_{MMAO}$/[Zr] = 1135 ,[Al]$_{TMA}$ /[Zr]$_{cat}$ = 2500, in toluene with total volume = 30 mL, and [Zr]$_{cat}$ = 5 x 10^{-5} M.

* LLDPE/TiO$_2$ nanocomposites synthesized by *ex situ* impregnation method. [More details see **Appendix B**.]

It was found that LLDPE/TiO$_2$ nanocomposites synthesized by *in situ* impregnation method exhibited higher activities about 3 times than LLDPE/TiO$_2$ nanocomposites synthesized by *ex situ* impregnation method. This can be explained as the following; (i) for the *ex situ* method, partial MMAO can reach into the pore of support and lead to loss of active species. Thus, the 1-hexene comonomer cannot adsorp on active site present in the pore, and (ii) for the *in situ* method, MMAO can be present in the bulk, which differs from the *ex situ* one that is only present inside the support. This makes, the *in situ* impregnation similar to homogeneous system, and hence enhances the polymerization activity. Moreover, by comparison of different systems for the *in situ* method, the heterogeneous gives better activity than the homogeneous one due to the following reasons; (i) the heterogeneous system exhibits higher bulk density than homogeneous system. Good bulk density can improve distribution of active site. In addition, it can reduce reactor fouling, which is resulted from the adhesion polymer to the reactor [Koltzenburg et al., 1997].

4.1.3 Characterization of LLDPE/TiO$_2$ nanocomposites

4.1.3.1 Differential scanning calorimeter (DSC)

The melting temperatures (T$_m$) of LLDPE/TiO$_2$ nanocomposites evaluated by the differential scanning calorimeter (DSC) are shown in **Table 4.4**.

Table 4.4 Thermal properties of LLDPE/TiO$_2$ nanocomposites obtained from DSC measurement

Sample	T$_m$ (°C)	Crystallinity (%)
Homogeneous	n.o.	n.o.
TiO$_2$_10 nm	n.o.	n.o.
TiO$_2$_13 nm	n.o.	n.o.
TiO$_2$_16 nm	n.o.	n.o.

n.o. refers to can not be observed from the measurement

From the characterization of LLDPE/TiO$_2$ nanocomposites in **Table 4.4**, it revealed that no melting temperature was found indicating non-crystalline polymer produced in this specified polymerization system. The non-crystalline polymers were attributed to the high degree of 1-hexene insertion, which can be confirmed by ^{13}C NMR.

4.1.3.2 Nuclear magnetic resonance (NMR)

The quantitative analysis of triad distribution for all copolymers was conducted on the basis assignment of the ^{13}C NMR spectra of ethylene/1-hexene copolymer (EH) and calculated according to the method of Randal et al. [1989]. The characteristics of ^{13}C NMR spectra (as shown in **appendix D**) for all copolymers were similar indicating the copolymer of ethylene/1-hexene. The triad distribution of all polymers is shown in **Table 4.5**. Ethylene incorporation in all systems gave

copolymers with similar triad distribution. No triblock of HHH in the copolymers was found. Only the random copolymers can be produced in all systems.

Table 4.5 Triad distribution of LLDPE/TiO$_2$ nanocomposites obtained from ^{13}C NMR analysis

Sample	Triad distribution of copolymer						1-hexene insertion (mol%)
	HHH	EHH	EHE	EEE	HEH	HEE	
Homogeneous	0.000	0.349	0.116	0.287	0.059	0.190	46.5
TiO$_2$_10 nm	0.000	0.377	0.086	0.359	0.028	0.150	46.3
TiO$_2$_13 nm	0.000	0.221	0.109	0.398	0.089	0.182	33.0
TiO$_2$_16 nm	0.000	0.144	0.131	0.438	0.086	0.200	27.6

E refers to ethylene monomer and H refers to 1-hexene comonomer

4.2 Investigation of the effect of the modification of nano-TiO₂ fillers on the characteristics of LLDPE/TiO₂ nanocomposites synthesized by *in situ* polymerization of ethylene/1-hexene using a zirconocene/MMAO catalyst, which prepared by *in situ* impregnation method

In this section, modification of nano-TiO₂ fillers were prepared by the incipient wetness impregnation method with Ga and Zr to obtain Ga-modified TiO₂ fillers and Zr-modified TiO₂ fillers.

4.2.1 Characterization of fillers

4.2.1.1 BET surface areas

BET surface areas of different modifications of nano-TiO₂ fillers are shown in **Table 4.6**. When compared the BET surface areas of unmodified TiO₂ and modified-TiO₂ fillers with Zr and Ga , it was found that BET surface areas of the Zr-modified TiO₂ fillers and Ga-modified TiO₂ fillers were slightly increased.

Table 4.6 BET surface areas of different modification of nano-TiO₂ fillers

Sample	BET surface area (m^2/g)
Unmodified TiO₂	88
Zr-modified TiO₂	99
Ga-modified TiO₂	120

4.2.1.2 X-ray Diffraction (XRD)

XRD patterns of nano-TiO₂ fillers with different modification are shown in **Figure 4.5**. They were collected at diffraction angle (2θ) between 20° and 80°, it was observed that all nano-TiO₂ fillers exhibited XRD peaks at 25°, 37°, 48°, 55°, 56°, 62°, 69°, 71°, and 75° assigning to anatase TiO₂. They showed that after

modification with 1 wt% of Ga and Zr, the nano-TiO_2 fillers still exhibited the similar XRD patterns as seen for the unmodified one. This indicated that Ga and Zr were highly dispersed in nano-TiO_2 fillers which were not observed by XRD.
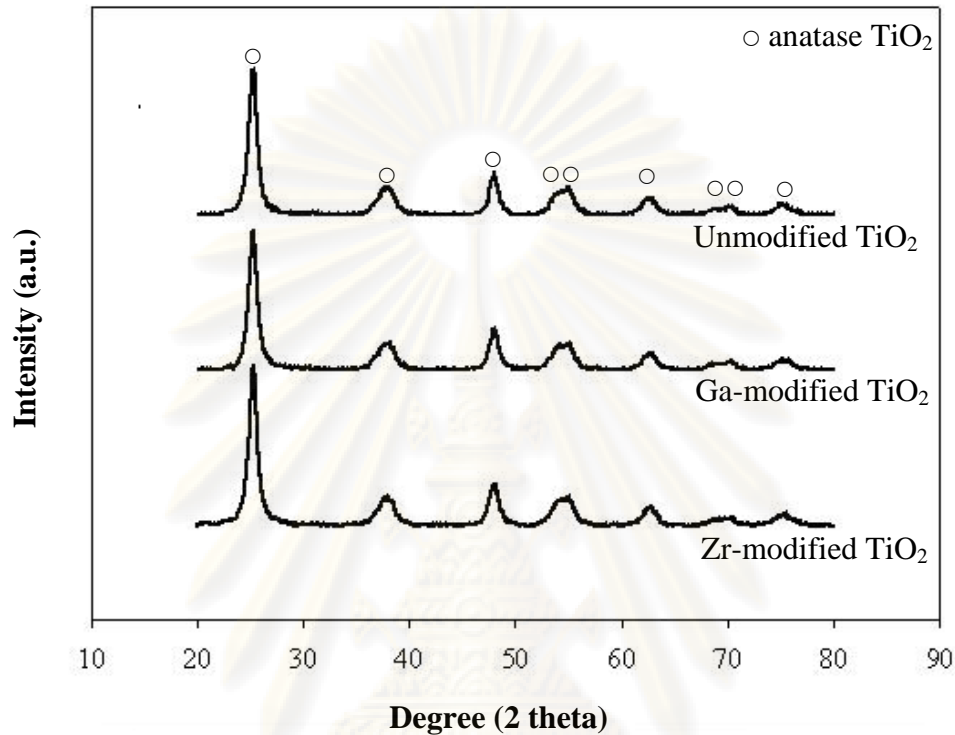

Figure 4.5 XRD patterns of nano-TiO_2 fillers with different modifications

4.2.1.3 Scanning electron microscopy (SEM)

Scanning electron microscopy (SEM) is a powerful tool for observing directly surface texture, morphology and particle granule size of materials. In the backscattering mode (SEM), the electron beam focused on the sample is scanned by a set of deflection coil. Backscattered electrons or secondary electrons emitted from the sample are detected.

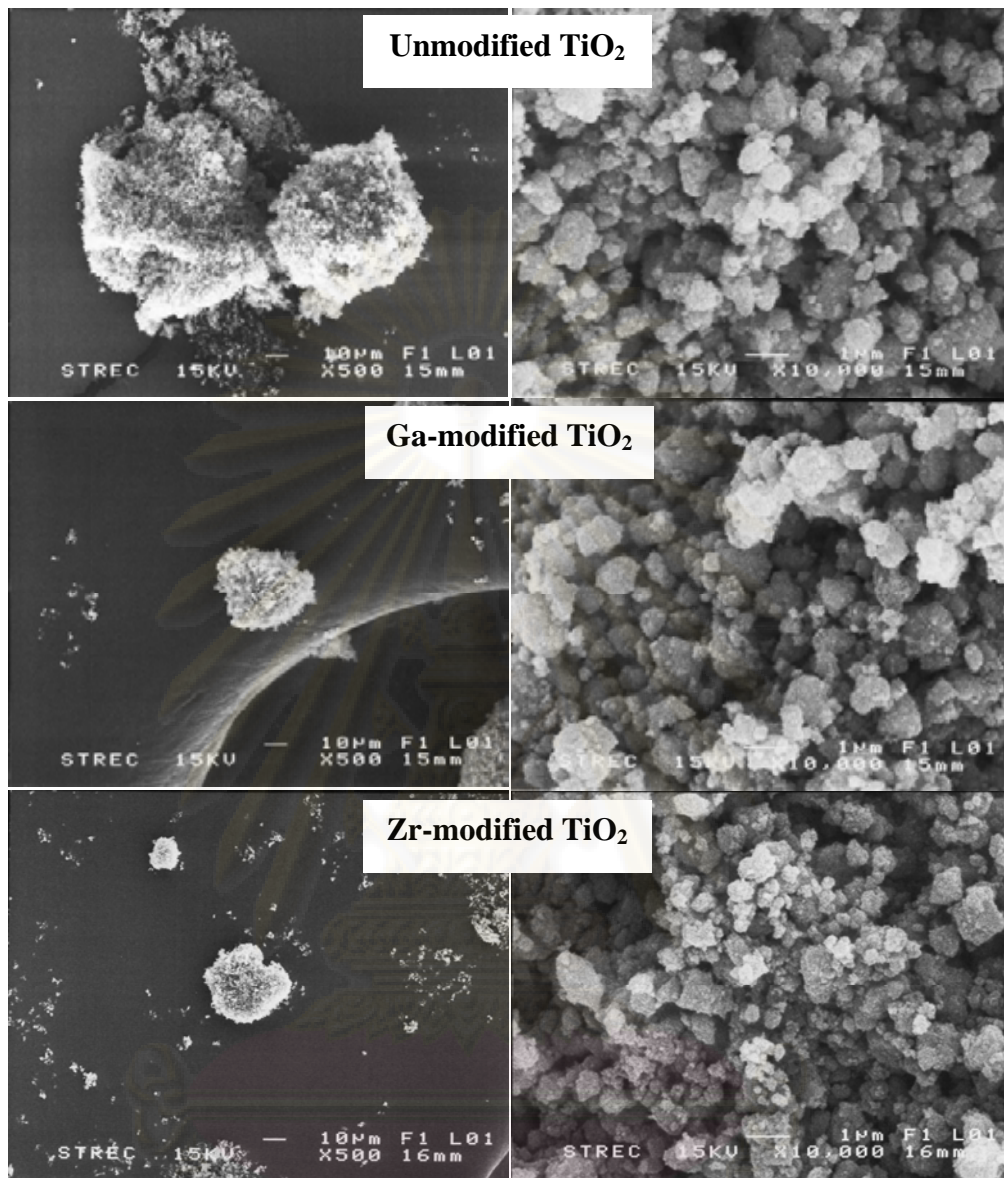The typical SEM micrographs of nano-TiO_2 fillers with different modification are shown in **Figure 4.6**.

Figure 4.6 SEM micrographs of nano-TiO$_2$ fillers with different modifications

4.2.1.4 Transmission electron microscopy (TEM)

TEM is a useful tool for determining crystallite size and size distribution of materials. It allows determination of the micro-texture and microstructure of electron transparent samples by transmission of a focused parallel electron beam to a fluorescent screen with a resolution presently better than 0.2 nm.

The typical TEM micrographs of nano-TiO$_2$ fillers with different modification are shown in **Figure 4.7**.
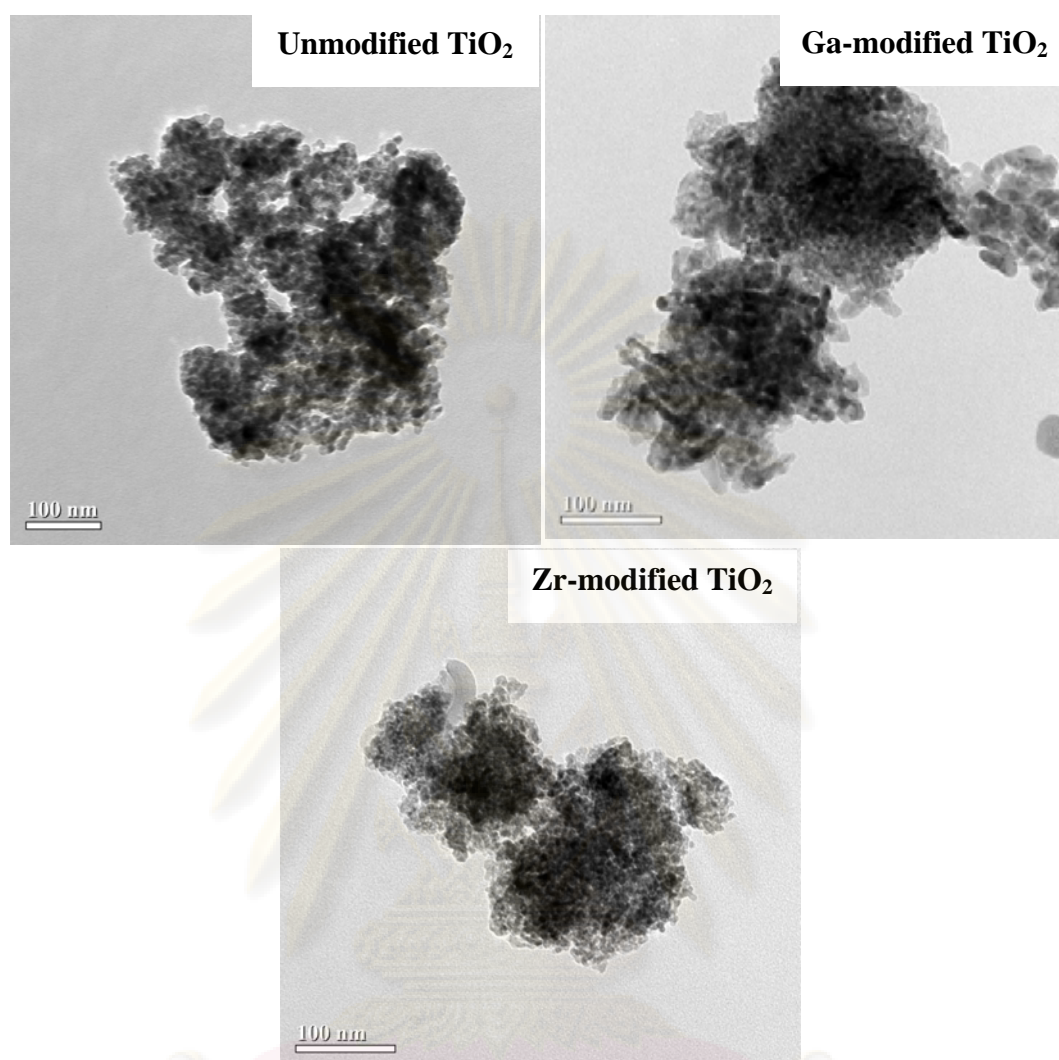
Figure 4.7 TEM micrographs of nano-TiO$_2$ fillers with different modifications

4.2.2 Effect of the modification of nano-TiO$_2$ fillers on the characteristics of LLDPE/TiO$_2$ nanocomposites

Table 4.7 shows the polymerization activities of LLDPE/TiO$_2$ nanocomposites which different modification of nano-TiO$_2$ fillers synthesized by *in situ* impregnation method. **Table 4.8** shows the comparison of polymerization activities of LLDPE/TiO$_2$ nanocomposites synthesized by *in situ* impregnation method and *ex situ* impregnation method. The procedure to synthesize the LLDPE/TiO$_2$ nanocomposites by *ex situ* impregnation method was also described in **Appendix B**.

Table 4.7 Polymerization activities of LLDPE/TiO$_2$ nanocomposites (*In situ impregnation method*)

Sample	Polymerization time [a] (sec)	Polymerization yield [b] (g)	Catalytic activity (kg polymer/mol Zr.h)
Homogeneous	126	1.16	22055
Unmodified TiO$_2$	110	1.58	34573
Zr-modified TiO$_2$	123	1.72	33473
Ga-modified TiO$_2$	128	1.48	27711

[a] A period of time used for the total 0.018 mol of ethylene to be consumed.

[b] Measurement at polymerization temperature of 70°C, [ethylene] = 0.018 mol, $[Al]_{MMAO}/[Zr] = 1135$,$[Al]_{TMA}/[Zr]_{cat} = 2500$, in toluene with total volume = 30 mL, and $[Zr]_{cat} = 5 \times 10^{-5}$ M.

It was found that unmodified TiO$_2$ exhibited the highest activities among the Zr-modified TiO$_2$ and Ga-modified TiO$_2$ fillers. The degree of interaction between the nanofillers and $[Al]_{MMAO}$ can be determined using the TGA measurement. To give a better understanding, Severn et al. explained that the connection of the support (nanofillers) and cocatalyst occurred via the O_{filler}---$Al_{cocatalyst}$ linkage [Severn et al., 2005]. In particular, the TGA can only provide useful information on the degree of interaction for the $[Al]_{MMAO}$ bound to the support in terms of weight loss and removal temperature. As a matter of fact, too strong interaction can result in it being more difficult for the $[Al]_{MMAO}$ bound to the support to react with metallocene catalyst during activation processes, leading to low activity for polymerization. In contrast, the leaching of $[Al]_{MMAO}$ can occur due to very weak interaction resulting in low activity as well. Experimentally, the TGA measurement was performed to prove the interaction between the $[Al]_{MMAO}$ and each nanofiller. The TGA profile of $[Al]_{MMAO}$ on each nanofiller are shown in **Figure 4.8**. It was found that the weight loss of $[Al]_{MMAO}$ on each nanofiller was in the order of unmodified TiO$_2$ (11%) > Zr-modified TiO$_2$ (9%) > Ga-modified TiO$_2$ (8%). This indicated that the $[Al]_{MMAO}$ present on the Ga-modified TiO$_2$ nanofiller exhibited the stronger interaction than that on the Zr-modified TiO$_2$ nanofiller and unmodified TiO$_2$ nanofiller, respectively. So

based on the TGA measurement the observed polymerization activities were decreased by Zr and Ga modification, as listed in **Table 4.7**.
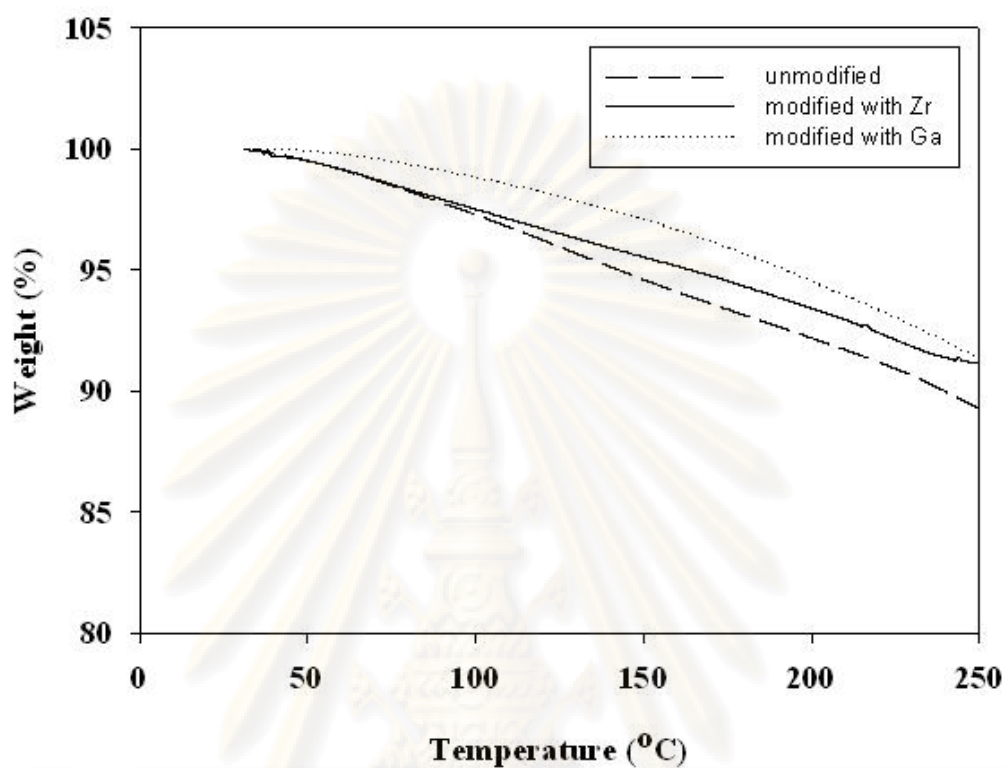

Figure 4.8 The TGA profile of $[Al]_{MMAO}$ on different modification of nano-TiO_2 fillers

Table 4.8 Comparison of polymerization activities of LLDPE/TiO$_2$ nanocomposites synthesized by *in situ* impregnation method and *ex situ* impregnation method

Sample	Polymerization time [a] (sec)	Polymerization yield [b] (g)	Catalytic activity (kg polymer/mol Zr.h)
Homogeneous	126	1.16	22055
Homogeneous*	145	0.998	16510
Unmodified TiO$_2$	110	1.58	34573
Unmodified TiO$_2$*	480	0.5036	2518

[a] A period of time used for the total 0.018 mol of ethylene to be consumed.

[b] Measurement at polymerization temperature of 70˚C, [ethylene] = 0.018 mol, [Al]$_{MMAO}$/[Zr] = 1135, [Al]$_{TMA}$ /[Zr]$_{cat}$ = 2500, in toluene with total volume = 30 mL, and [Zr]$_{cat}$ = 5 x 10^{-5} M.

* LLDPE/TiO$_2$ nanocomposites synthesized by *ex situ* impregnation method. [More details see **Appendix B**.]

The same as the **Table 4.3**, it was found that LLDPE/TiO$_2$ nanocomposites synthesized by *in situ* impregnation method exhibited higher activities than LLDPE/TiO$_2$ nanocomposites synthesized by *ex situ* impregnation method. This can be explained as the following; (i) for the *ex situ* method, partial MMAO can reach into the pore of support and lead to loss of active species. Thus, the 1-hexene comonomer cannot adsorp on active site present in the pore, and (ii) for the *in situ* method, MMAO can be present in the bulk, which differs from the *ex situ* one that is only present inside the support. This makes, the *in situ* impregnation similar to homogeneous system, and hence enhances the polymerization activity. Moreover, by comparison of different systems for the in situ method, the heterogeneous gives better activity than the homogeneous one due to the following reasons; (i) the heterogeneous system exhibits higher bulk density than homogeneous system. Good bulk density can improve distribution of active site. In addition, it can reduce reactor fouling, which is resulted from the adhesion polymer to the reactor [Koltzenburg et al., 1997].

4.2.3 Characterization of LLDPE/TiO$_2$ nanocomposites

4.2.3.1 Differential scanning calorimeter (DSC)

The melting temperatures (T$_m$) of LLDPE/TiO$_2$ nanocomposites evaluated by the differential scanning calorimeter (DSC) are shown in **Table 4.9**.

Table 4.9 Thermal properties of LLDPE/TiO$_2$ nanocomposites obtained from DSC measurement

Sample	T$_m$ (°C)	Crystallinity (%)
Homogeneous	n.o.	n.o.
Unmodified TiO$_2$	n.o.	n.o.
Zr-modified TiO$_2$	n.o.	n.o.
Ga-modified TiO$_2$	n.o.	n.o.

n.o. refers to can not be observed from the measurement

From the characterization of LLDPE/TiO$_2$ nanocomposites in **Table 4.9**, it revealed that no melting temperature was found indicating non-crystalline polymer produced in this specified polymerization system. The non-crystalline polymers were attributed to the high degree of 1-hexene insertion, which can be confirmed by ^{13}C NMR.

4.2.3.2 Nuclear magnetic resonance (NMR)

The quantitative analysis of triad distribution for all copolymers was conducted on the basis assignment of the ^{13}C NMR spectra of ethylene/1-hexene copolymer (EH) and calculated according to the method of Randal et al. [1989]. The characteristics of ^{13}C NMR spectra (as shown in **appendix D**) for all copolymers were similar indicating the copolymer of ethylene/1-hexene. The triad distribution of all polymers is shown in **Table 4.10**. Ethylene incorporation in all systems gave

copolymers with similar triad distribution. No triblock of HHH in the copolymers was found. Only the random copolymers can be produced in all systems.

Table 4.10 Triad distribution of LLDPE/TiO$_2$ nanocomposites obtained from ^{13}C NMR analysis

Sample	Triad distribution of copolymer						1-hexene insertion (mol%)
	HHH	EHH	EHE	EEE	HEH	HEE	
Homogeneous	0.000	0.349	0.116	0.287	0.059	0.190	46.5
Unmodified TiO$_2$	0.000	0.296	0.112	0.330	0.067	0.194	40.9
Zr-modified TiO$_2$	0.000	0.338	0.107	0.336	0.055	0.164	44.5
Ga-modified TiO$_2$	0.000	0.258	0.105	0.335	0.081	0.220	36.4

E refers to ethylene monomer and H refers to 1-hexene comonomer

CHAPTER V

CONCLUSIONS AND RECOMMENTDATIONS

5.1 Conclusions

5.1.1 Investigation of the effect of the crystallite size of nano-TiO_2 fillers on the characteristics of LLDPE/TiO_2 nanocomposites synthesized by *in situ* polymerization of ethylene/1-hexene using a zirconocene/MMAO catalyst, which prepared by *in situ* impregnation method.

The LLDPE/TiO_2 nanocomposites were produced via *in situ* polymerization of ethylene/1-hexene with zirconocene/MMAO catalyst using TiO_2 nanofillers having different crystallite size. The polymerization activities obtained from TiO_2 having the crystallite size 16 nm exhibited the highest activities among the TiO_2 having the crystallite size 13 nm and 10 nm, respectively. The highest activity obtained can be attributed to the TiO_2 having the crystallite size 16 nm exhibited the weakest interaction based on TGA measurement that can result in it being more easy for the $[Al]_{MMAO}$ bound to the nanofiller to react with metallocene catalyst during activation processes interaction .

5.1.2 Investigation of the effect of the modification of nano-TiO_2 fillers on the characteristics of LLDPE/TiO_2 nanocomposites synthesized by *in situ* polymerization of ethylene/1-hexene using a zirconocene/MMAO catalyst, which prepared by *in situ* impregnation method.

The LLDPE/TiO_2 nanocomposites were produced via *in situ* polymerization of ethylene/1-hexene with zirconocene/MMAO catalyst using TiO_2 nanofillers having different modification. The polymerization activities obtained from unmodified TiO_2 exhibited the highest activities among the Zr,Ga modified TiO_2. This was due to the unmodified TiO_2 had weakest interaction that can result in it being more easy for the

[Al]$_{MMAO}$ bound to the nanofiller to react with metallocene catalyst during activation processes interaction resulting in highest activity.

5.2 Recommendations

      5.2.1 Additional water:alkoxide molar ratio which related to crystallite sizes of TiO$_2$ synthesized by sol-gel method should be prepared in order to confirm the effect of TiO$_2$ crystallite size on the characteristics of LLDPE/TiO$_2$ nanocomposites.

      5.2.2 Investigation of other modification of nano- TiO$_2$ fillers should be further studied.

      5.2.3 Investigation of other nanofillers should be further studied.

      5.2.4 Reduce amount of comonomer.

REFERENCES

Albano, C., Sanchez, G., and Ismayel, A. Influence of a copolymer on the mechanical properties of a blend of PP and recycled and non-recycled HDPE. **Polymer Bulletin** 41 (1998): 91-98.

Alt, H. The heterogenization of homogeneous metallocene catalysts for olefin polymerization. **Journal of the Chemical Society, Dalton Transactions** (1999): 1703-1709.

Alt, H.G., and Köppl, A. Effect of the nature of metallocene complexes of group IV metals on their performance in catalytic ethylene and propylene polymerization. **Chemical Reviews** 100 (2000): 1205-1221.

Andersen, A., Cordes, H.G., Herwig, J., Kaminsky, K., Merck, A., Mottweiler, R., Pein, J., Sinn, H., and Vollmer, H.J. Halogen-free soluble ziegler catalysts for the polymerization of ethylene. control of molecular weight by choice of temperature. **Angewandte Chemie International Edition in English** 15 (1976): 630-632.

Bunchongturakarn, S., Jongsomjit, B., and Praserthdam, P. Impact of bimodal pore MCM-41-supported zirconocene/dMMAO catalyst on copolymerization of ethylene/1-octene. **Catalysis Communications** 9 (2008): 789-795.

Chaichana, E., Jongsomjit, B., and Praserthdam, P. Effect of nano-SiO_2 particle size on the formation of LLDPE/SiO_2 nanocomposite synthesized via the in situ polymerization with metallocene catalyst. **Chemical Engineering Science** 62 (2007): 899-905.

Chan, C.-M., Wu, J., Li, J.-X., and Cheung, Y.-K. Polypropylene/calcium carbonate nanocomposites. **Polymer** 43 (2002): 2981-2992.

Chau, J. L. H., Lin, Y-M., Li, A-K., Su, W-F., Chang, K-S., Hsu, S. L-C., and Li, T-L. Transparent high refractive index nanocomposite thin films. **Materials letters** 61 (2007): 2908-2910.

Chen, E.Y.X. and Marks, T.J. Cocatalysts for metal-catalyzed olefin polymerization: Activators, activation processes, and structure-activity relationships. **Chemical Reviews** 100 (2000): 1391-1434.

Chen, J., Zhou, Y., Nan, Q., Sun, Y., Ye, X., and Wang, Z. Synthesis, characterization and infrared emissivity study of polyurethane/TiO$_2$ nanocomposites. **Applied Surface Science** 253 (2007): 9154-9158.

Cheng, W., Wang, Z., Ren, C., Chen, H., and Tang, T. Preparation of silica/polyacrylamide/polyethylene nanocomposite via in situ polymerization. **Materials Letters** 61 (2007): 3193-3196.

Chien, J.C.W. Supported metallocene polymerization catalysis. **Topics in Cat.** 7 (1999): 23-36.

Chu, K. J., Soares, J. B. P., and Penlidis, A. Variation of molecular weight distribution (MWD) and short chain branching distribution (SCBD) of ethylene/1-hexene copolymers produced with different in-situ supported metallocene catalysts. **Macromolecular Chemistry and Physics** 201 (2000): 340-348.

Coates, G. W. Precise control of polyolefin stereo chemistry using single-site metal catalysts. **Chemical Reviews** 100 (2000): 1223-1252.

Danjaji, I. D., Nawang, R., Ishiaku, U. S., Ismail, H., and Mohd Ishak, Z. A. M. Degradation studies and moisture uptake of sago-starch-filled linear low-density polyethylene composites. **Polymer Testing** 21 (2002): 75-81.

Ewen, J. A., Jones, R. L., Razavi, A., and Ferrara, J. P. Syndiospecific propylene polymerizations with group 4 metallocenes. **Journal of the American Chemical Society** 110 (1988): 6255-6256.

Gambarotta, S. Coord. Vanadium-based Ziegler-Natta: Challenges, promises, problems **Chem. Rev.** 273 (2003): 229-243.

Giannetti, E., Nicolett, G.M., and Mazzocchi, R. Homogeneous Ziegler-Natta catalyst. II. Ethylene polymerization by IVB transition metal complexes/methyl aluminoxane catalyst systems. **Journal of polymer science Part A-1: Polymer chemistry** 23 (1985): 2117-2134.

Gupta, V.K., Satish, S., and Bhardwaj, I.S. Metallocene complexes of group 4 elements in the polymerization of monoolefins. **Macromolecular Science - Reviews in Macromolecular Chemistry and Physics** C34 (1994): 439-514.

Ioku, A., Hasan, T., Shiono, T., and Ikeda, T. Effects of cocatalysts on propene polymerization with [t-BuNSiMe$_2$(CSMe$_4$)]TiMe$_2$. **Macromolecular Chemistry and Physics** 203 (2002): 748-755.

Jiamwijitkul, S., Jongsomjit, B., and Praserthdam, P. Effect of Boron-modified MCM-41-supported dMMAO/zirconocene catalyst on copolymerization of ethylene/1-octene for LLDPE synthesis. **Iranian Polymer Journal** 16 (2007): 549-559.

Jongsomjit, B., Ngamposri, S., and Praserthdam, P. Catalytic activity during copolymerization of ethylene and 1-hexene via mixed TiO$_2$/SiO$_2$ -supported MAO with rac-Et[Ind] $_2$ ZrCl$_2$ metallocene catalyst. **Molecules** 10 (2005): 672-678.

Jongsomjit, B., Panpranot, J., and Praserthdam, P. Effect of nanoscale SiO$_2$ and ZrO$_2$ as the fillers on the microstructure of LLDPE nanocomposites synthesized via in situ polymerization with zirconocene. **Materials Letters** 61 (2007): 1376-1379.

Jordan, J., Jacob, K. I., Tannenbaum, R., Sharaf, M. A., and Jasiuk, I. Experimental trends in polymer nanocomposites--a review. **Materials Science and Engineering A** 393 (2005): 1-11.

Kaminsky, W. The discovery of metallocene catalysts and their present state of the art. **Journal Polymer Science Part A: Polymer Chemistry** 42 (2004): 3911-3921.

Kaminsky, W., and Laban, A. Metallocene catalysis. **Applied Catalysis A: General** 222 (2001): 47-61.

Kashiwa, N.J. The discovery and progress of $MgCl_2$-supported $TiCl_4$ catalysts. **Pol. Sci. Part A: Polym. Chem.** 42 (2004): 1-8.

Kim, J. D., and Soares, J. B. P. Copolymerization of ethylene and 1-hexene with supported metallocene catalysts: Effect of support treatment. **Macromolecular Rapid Communications** 20 (1999): 347-350.

Kissin, Y.V.J. Multicenter nature of titanium-based Ziegler-Natta catalysts: Comparison of ethylene and propylene polymerization reactions. **Pol. Sci.: Polym. Chem.** 41 (2003): 1745-1758.

Koide, Y., Bott,S. G., and Barron, A.R. Alumoxanes as cocatalysts in the palladium-catalyzed copolymerization of carbon monoxide and ethylene: Genesis of a structure-activity relationship. **Organometallics** 15 (1996): 2213-2226.

Kontou, E., and Niaouakis, M. Thermo-mechanical properties of $LLDPE/SiO_2$ nanocomposites. **Polymer** 47 (2006): 1267-1280.

Kristen, M.O. Supported metallocene catalysts with MAO and boron activators. **Topic in Catalysis** 7 (1999): 89-95.

Kuo, M. C., Tsai, C. M., Huang, J. C., and Chen, M. PEEK composites reinforced by nano-sized SiO_2 and Al_2O_3 particulates. **Materials Chemistry and Physics** 90 (2005): 185-195.

Li, K.-T., Dai, C.-L., and Kuo, C.-W. Ethylene polymerization over a nano-sized silica supported Cp_2ZrCl_2/MAO catalyst. **Catalysis Communications** 8 (2007): 1209-1213.

Liu, G., Li, Y-F., Yan, F-Y., Zhao, Z-X., Zhou, L-C., and Xue, Q-J. Effect of nanoscale SiO_2 and TiO_2 as the fillers on the mechanical properties and aging behavior of linear low-density polyethylene/low-density polyethylene blends." **Journal of polymers and the environment** 13 (2005): 339-348.

Milione, S., Cavallo, G., Tedesco, C., Grassi, A.J. Synthesis of α-diimine V(III) complexes and their role as ethylene polymerisation catalysts **Chem. Soc., Dalton Trans.** 8 (2002): 1839-1846.

Ma, D., Akpalu, Y. A., Li, Y., Siegel, R. W., and Schadler, L. S. Effect of titania nanoparticles on the morphology of low density polyethylene. **Journal of polymer science: Part B: Polymer Physics** 43 (2005): 488-497.

Mashima, K., Nakayama, Y., and Nakamura, A. Recent trends in the polymerization of α-olefins catalyzed by organometallic complexes of early transition metals. **Advances Polymer Science** 133 (1997): 1-51.

Mason, M.R., Smith, J.M., Bott, S.G., and Barron, A.R. Hydrolysis of tri67 tert-butylaluminum: The first structural characterization of alkylalumoxanes $[(R_2Al)_2O]n$ and $(RAlO)_n$. **Journal of the American Chemical Society** 115 (1993): 4971-4984.

Naga, N. and Imanishi, Y. Recent developments in olefin polymerizations with transition metal catalysts. **Progress in Polymer Science** 26 (2001): 1147-1198.

Naga, N., and Imanishi, Y. Structure of cyclopentene unit in the copolymer with propylene obtained by stereospecific zirconocene catalysts. **Polymer** 43 (2002): 2133-2139.

Nakayama, N., and Hayashi, T. Preparation and characterization of TiO_2 and polymer nanocomposite films with high refractive index. **Journal of applied polymer science** 105 (2007): 3662-3672.

Nawang, R., Danjaji, I. D., Ishiaku, U. S., Ismail, H., and Mohd Ishak, Z. A. Mechanical properties of sago starch-filled linear low density polyethylene (LLDPE) composites. **Polymer Testing** 20 (2001): 167-172.

Newburg,N.R. Bis - (Cyclopentadienyl - Titaniumdichloride - alkylaluminum complexes as catalysts for the polymerization of ethylene. **Journal of the American Chemical Society** 79 (1957): 5072-5073.

Pietikainen, P., and Seppala, J. V. Low molecular weight ethylene/propylene copolymers. Effect of process parameters on copolymerization with homogeneous Cp_2ZrCl_2 catalyst. **Macromolecules** 27 (1994): 1325-1328.

Quijada, R., Galland, G. B., and Mauler, R. S. The influence of the comonomer in the copolymerization of ethylene with α-olefins using $C_2H_4[Ind]_2ZrCl_2/$ methylaluminoxane as catalyst system. **Macromolecular Chemistry and Physics** 197 (1996): 3091-3098.

Richards, C.T. Plastic Rubber Composites. **Processing and Applications** 27 (1998): 3-7.

Rossi, G. B., Beaucage, G., Dang, T. D., and Vaia, R. A. Bottom-up synthesis of polymer nanocomposites and molecular composites: ionic exchange with PMMA latex. **Nano Letters** 2 (2002): 319-323.
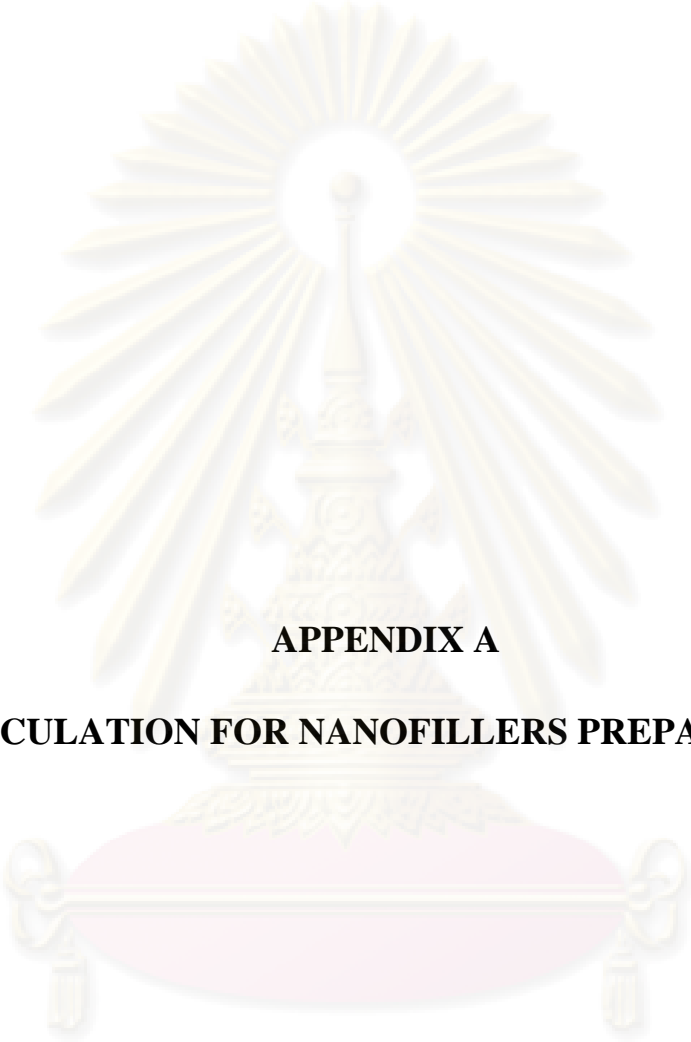
Sacchi, M.C., Zucchi, D., Tritto, I., and Locatelli, P. Silica-supported metallocenes: stereochemical comparison between homogeneous and heterogeneous catalysis. **Macromol. Rapid Commun** 16 (1995): 581-590.

Sarwar, M.I., Zulfiqar, S., and Ahmad, Z. Preparation and properties of polyamide–titania nanocomposites. **Sol-Gel Science and Technology** 44 (2007): 41-46.

Shan, C. L. P., Chu, K. J., Soares, J. B. P., and Penlidis, A. Using alkylaluminum activators to tailor short chain branching distributions of ethylene/1-hexene copolymers produced with in-situ supported metallocene catalysts. **Macromolecular Chemistry and Physics** 201 (2000): 2195-2202.

Shan, C. L. P., Soares, J. B. P., and Penlidis, A. Ethylene/1-octene copolymerization studies with in situ supported metallocene catalysts: Effect of polymerization parameters on the catalyst activity and polymer microstructure. **Journal Polymer Science Part A: Polymer Chemistry** 40 (2002): 4426-4451.

Shi, L., Qin, Y., Cheng, W., Chen, H., and Tang, T. Effect of swelling response of the support particles on ethylene polymerization. **Polymer** 48 (2007): 2481-2488.

Shiono, T., Yoshida, S., Hagihara, H., and Ikeda, T. Additive effects of trialkylaluminum on propene polymerization with (t-BuNSiMe(2)Flu) TiMe$_2$-based catalysts. **Applied Catalysis A: General** 200 (2000): 145-152.

Sinn, H., Kaminsky, W. Ziegler-Natta catalyst. **Advances in Organometallic Chemistry** 18 (1980): 99-149.

Sinn, H. Proposals for structure and effect of methylalumoxane bases on mass balances and phase-separation experiments. **Macromolecular Symposia** 97 (1995): 27-52.

Smedberg, A., Hjertbert, T., Gustafsson, B.J. Characterization of an unsaturated low-density polyethylene. **Pol. Sci. Part A: Pol.Chem.** 41 (2003): 2974-2984.

Soga, K., and Kaminaka, M. Polymerization of propene with the heterogeneous catalyst system. **Macromolecular Chemistry Rapid Communications** 13 (1992): 221-224.

Tritto, I., Mealares, C., Sacchi, M.C., and Locatelli, P. Methylaluminoxane: NMR analysis, cryoscopic measurements and cocatalytic ability in ethylene polymerization. **Macromolecular Chemistry and Physics** 198 (1997): 3963-3977.

Verbeek, C. J. R. Effect of preparation variables on the mechanical properties of compression-moulded phlogopite/LLDPE composites. **Materials Letters** 56 (2002a): 226-231.

Verbeek, C. J. R. Highly filled polyethylene/phlogopite composites. **Materials Letters** 52 (2002b): 453-457.

Wang, Z., Li, G., and Zhang, X. Z. Dispersion behavior of TiO_2 nanoparticles in LLDPE/LDPE/TiO_2 nanocomposites. **Macromolecular Chemistry and Physics** 206 (2005): 258-262.

Ystenes, M., Eilertsen, J.L., Liu, J.K., Ott, M., Rytter, E., Stovneng, J.A. Experimental and theoretical investigations of the structure of methylaluminoxane (MAO) cocatalysts for olefin polymerization. **Journal of Polymer Science Part A: Polymer Chemistry** 38 (2000): 3106-3127.

Zan, L., Tian, L., Liu, Z., and Peng, Z. A new polystyrene-TiO_2 nanocomposite film and its photocatalytic degradation. **Applied Catalysis A: General** 264 (2003): 237-242.

APPENDICES

APPENDIX A

CALCULATION FOR NANOFILLERS PREPARATION

Calculation for the preparation of TiO$_2$ by sol-gel (base precipitation) method

Preparation of TiO$_2$ by sol-gel (base precipitation) method are shown as follows:

    Reagent: -   Titanium ethoxide, Molecular weight = 284.22

The preparation by using water:alkoxide molar ratio	=	X
	=	10 g
	=	10/284.22 mole
The amount of water used	=	10/284.22×18(X)
The volume of water used	=	10/284.22×18(X)
The volume of ethanol used in the first solution with ethanol=		50 ml
The volume of ethanol used in the second solution with titanium ethoxide = 50 ml		

Calulation for the preparation of Ga-modified TiO$_2$ by incipient wetness impregnation method

Preparation of Ga-modified TiO$_2$ nanofillers with 1%wt Ga by incipient wetness impregnation method are shown as follows:

    Reagent: -   Gallium (III) nitrate hydrate (Ga(NO$_3$)$_3$)

                    Molecular weight   =   255.7 g/mol

                    Gallium (Ga), Atomic weight = 69.7 g/mol

          -     nano-TiO$_2$ fillers

Based on 100 g of catalyst used, the composition of the catalyst will be as follows:

        Gallium   =   1 g

        TiO$_2$ =   100 – 1   =   99 g

For 1 g of filler (TiO_2)

$$\text{required} \quad = \quad 1 \times \frac{1}{99} = \quad 0.0101 \text{ g}$$

Gallium 0.0101 g was prepared from Gallium (III) nitrate hydrate

$$\text{Gallium (III) nitrate hydrate required} \quad = \quad \frac{0.0101}{69.7} \times 255.7$$

$$= \quad 0.037 \text{ g}$$

Calulation for the preparation of Zr-modified TiO_2 by incipient wetness impregnation method

Preparation of Zr-modified TiO_2 nanofillers with 1%wt Zr by incipient wetness impregnation method are shown as follows:

Reagent :- Zirconium (IV) *n*-propoxide 70wt% solution in

1-propanol ($Zr(OC_3H_7)_4$)

Molecular weight = 327.88 g/mol

Zirconium (Zr), Atomic weight = 91.224 g/mol

- nano-TiO_2 fillers

Based on 100 g of catalyst used, the composition of the catalyst will be as follows:

Zirconium = 1 g

TiO_2 = 100 – 1 = 99 g

For 1 g of filler (TiO_2)

$$\text{required} \quad = \quad 1 \times \frac{1}{99} = \quad 0.0101 \text{ g}$$

Zirconium 0.0101 g was prepared from ($Zr(OC_3H_7)_4$)

$$(Zr(OC_3H_7)_4) \text{ required} \quad = \quad \frac{0.0101}{91.224} \times 327.88$$

$$= \quad 0.036 \text{ g}$$

$Zr(OC_3H_7)_4$ 0.036 g was prepared from $Zr(OC_3H_7)_4$ 70 wt% solution in 1-proponol

As a consequence, $Zr(OC_3H_7)_4$ 70 wt% solution in 1-proponol required

$$= \frac{\text{percent of solution} \times Zr(OC_3H_7)_4 \text{ required}}{\text{percent of } Zr(OC_3H_7)_4 \text{ in solution}}$$

$$= (100/70) \times 0.036$$

$$= 0.051 \text{ g}$$
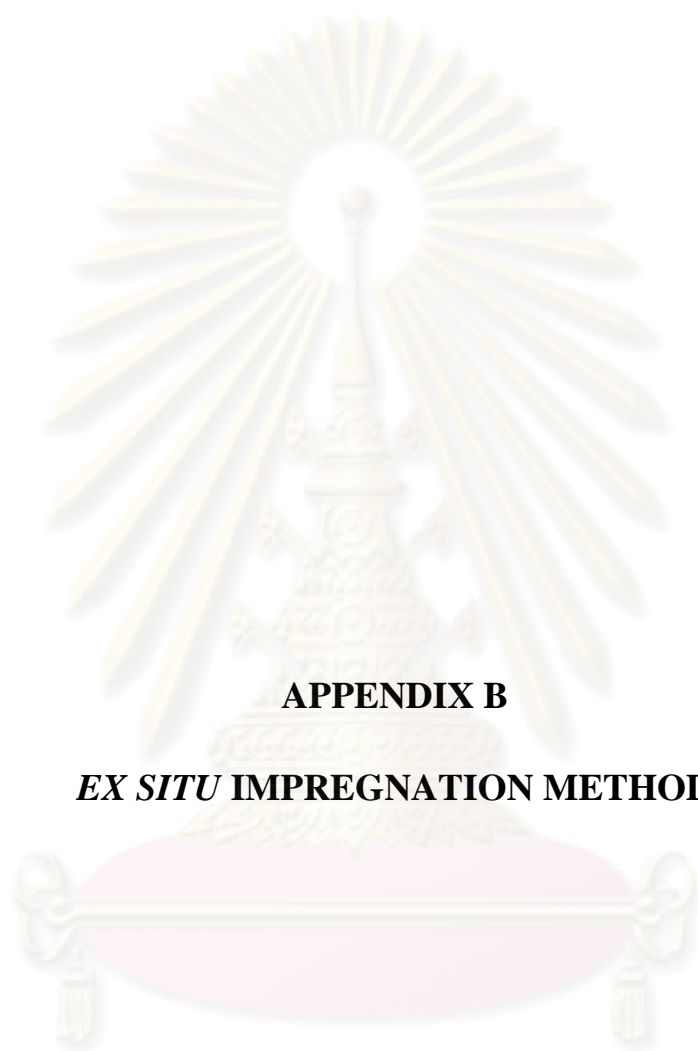
APPENDIX B

EX SITU **IMPREGNATION METHOD**

Preparation of dried MMAO (dMMAO)

60 ml of MMAO solution in toluene was evacuated at room temperature and washed with toluene (40 ml) for 2 times to remove the impurity. Then continued to wash with heptane (60 ml) for 7 times to remove TMA and TIBA in MMAO to obtained dMMAO as white solid.

Preparation of dMMAO impregnated on TiO$_2$ nanofillers (dMMAO/TiO$_2$)

Nanomaterials was be heated under vacuum at 400 °C for 6 hours. After that dMMAO was impregnated onto the nanomaterials, the method was described as follows. 1 g of the nanomaterials was reacted with the desired amount of dMMAO in 20 ml of toluene at room temperature and it was stirred for 30 min. The solvent was removed from the mixture. The white powder obtained was dried under vacuum, washed with hexane 10 ml for 3 times to ensure the removal of impurities. Then, the solid part was dried under vacuum at room temperature to obtained white powder of the nanomaterials/dMMAO (dMMAO/TiO$_2$).

Polymerization reaction

Polymerization reaction was conducted upon the methods as follows. The ethylene and 1-hexene copolymerization reaction was carried out in a 100 ml semi-batch stainless steel autoclave reactor equipped with magnetic stirrer. In the glove box, the desired amount of the dMMAO/TiO$_2$ along with toluene (to make the total volume of 30 ml) were put into the reactor. The desired amount of Et(Ind)$_2$ZrCl$_2$ (5 x 10-5 M.) and TMA ([Al]$_{TMA}$/[Zr]$_{cat}$ = 2500) was mixed and stirred for 5 minutes aging at room temperature, separately, then was injected into the reactor. The reactor was frozen in liquid nitrogen to stop reaction and then 0.018 mol of 1-hexene was injected into the reactor. The reactor was evacuated to remove argon. The reactor was heated up to polymerization temperature (70°C). To start reaction, 0.018 mole of ethylene (6 psi was observed from the pressure gauge) was fed into the reactor

containing the comonomer and catalyst mixtures. After all ethylene was consumed, the reaction was terminated by addition of acidic methanol   and stirred for 30 minutes. After filtration, the obtained copolymer (white powder) was washed with methanol and dried at room temperature.

This chapter is divided into two sections :

Section 1 : Investigation of the effect of the crystallite size of nano-TiO$_2$ fillers on the characteristics of LLDPE/TiO$_2$ nanocomposites synthesized by *in situ* polymerization of ethylene/1-hexene using a zirconocene/dMMAO catalyst, which prepared by *ex situ* impregnation method.

Section 2 : Investigation of the effect of the modification of nano-TiO$_2$ fillers on the characteristics of LLDPE/TiO$_2$ nanocomposites synthesized by *in situ* polymerization of ethylene/1-hexene using a zirconocene/dMMAO catalyst, which prepared by *ex situ* impregnation method.

B.1 <u>Investigation of the effect of the crystallite size of nano-TiO$_2$ fillers on the characteristics of LLDPE/TiO$_2$ nanocomposites synthesized by *in situ* polymerization of ethylene/1-hexene using a zirconocene/dMMAO catalyst, which prepared by *ex situ* impregnation method.</u>

<u>Characterization of dMMAO/ TiO$_2$</u>

- X-Ray Diffraction (XRD)

XRD patterns of TiO$_2$ and dMMAO/ TiO$_2$ with different crystallite sizes are shown in **Figure B-1**. They were collected at diffraction angle (2θ) between 20° and 80°, it was observed that all nano-TiO$_2$ fillers exhibited XRD peaks at 25°, 37°, 48°, 55°, 56°, 62°, 69°, 71°, and 75° assigning to anatase TiO$_2$. It was found that after impregnation with dMMAO the XRD patterns for three samples exhibited the

similar patterns. No peaks of dMMAO were detected. This was suggested that the dMMAO was in the highly dispersed form on the nano-TiO_2 fillers.
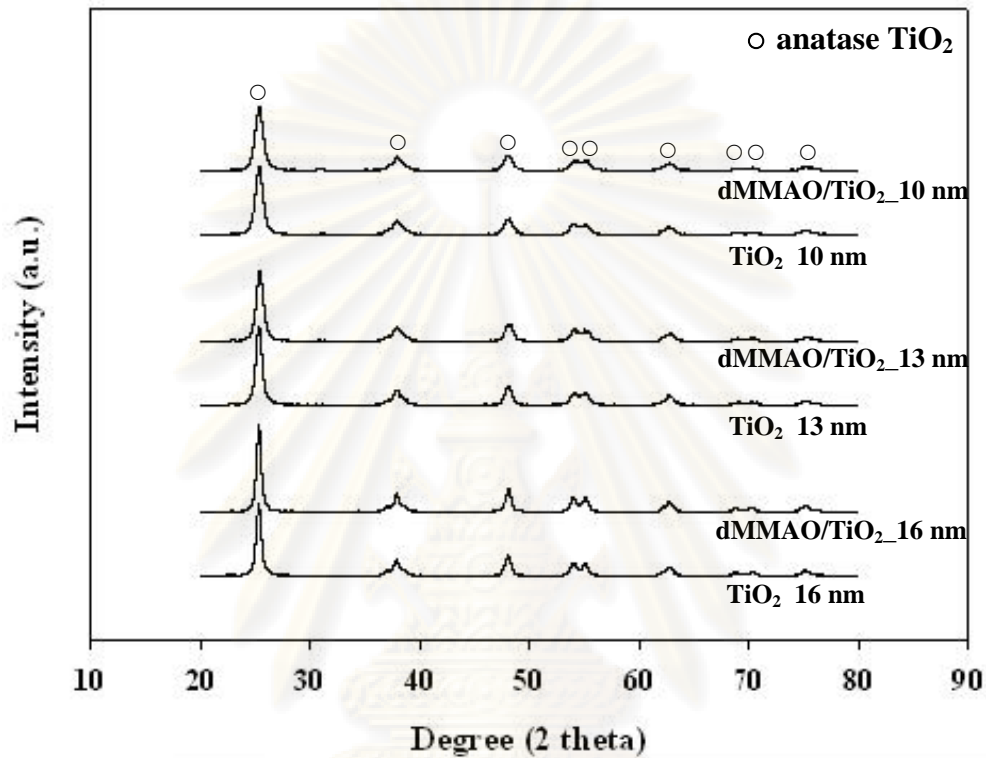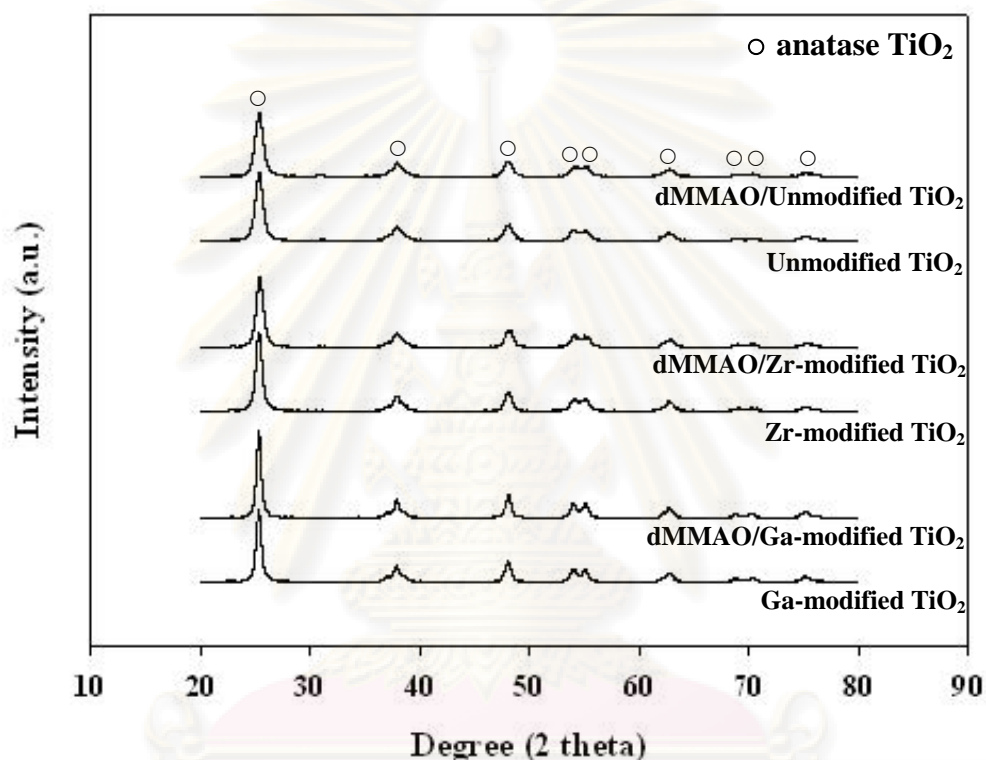

Figure B-1 XRD patterns of TiO_2 and dMMAO/ TiO_2 with different crystallite sizes

- **Scanning electron microscope (SEM) and energy dispersive X-ray spectroscopy (EDX)**

The SEM micrographs and EDX mapping for the dMMAO/TiO_2 are shown in **Figure B-2**. It can be observed that the dMMAO was well distributed all over the TiO_2 granules as seen by the EDX mapping.
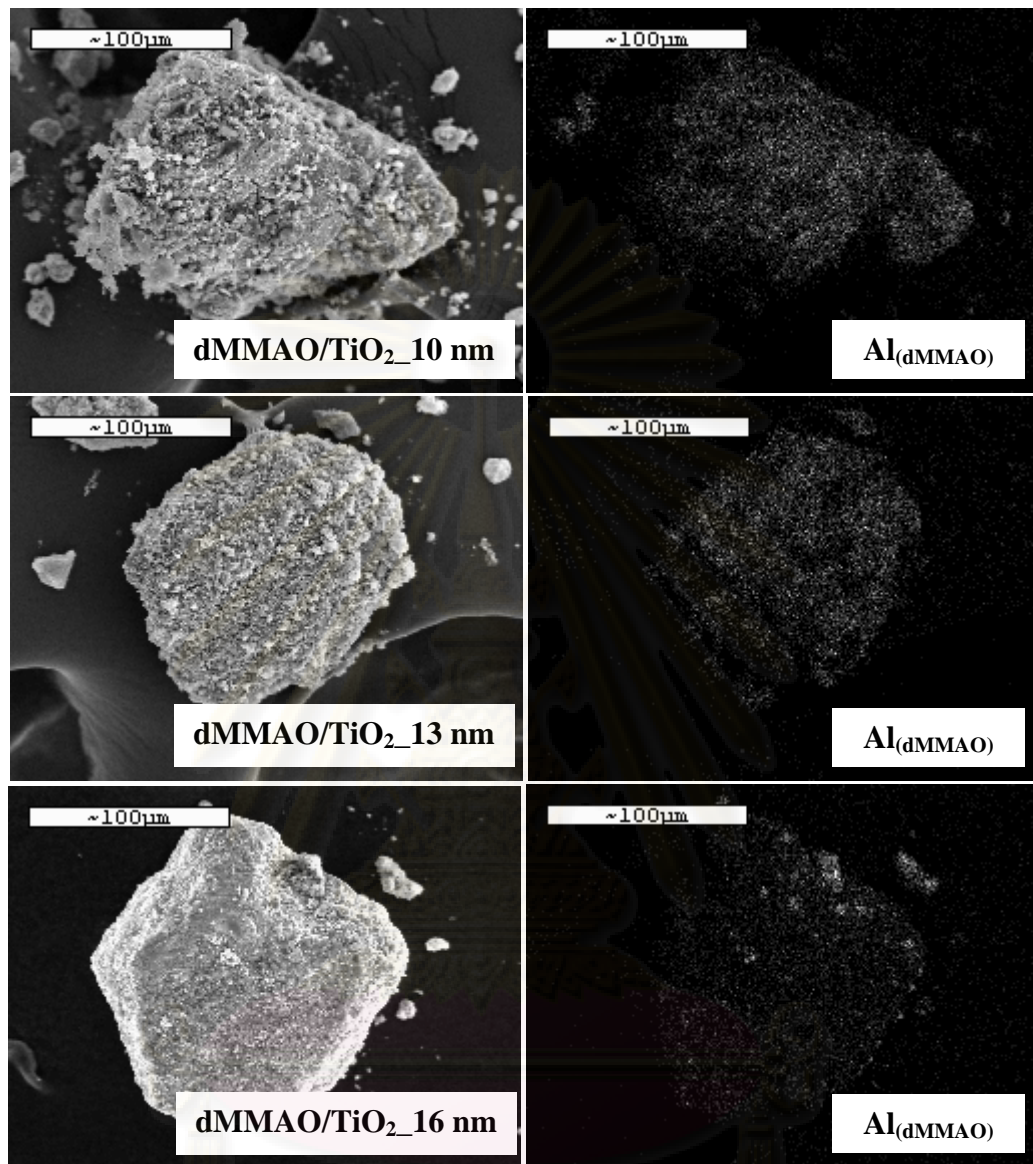
Figure B-2 SEM micrographs and EDX mapping for different dMMAO/TiO$_2$ nanofillers

-   Transmission electron microscopy (TEM)

The TEM micrographs of nano-TiO$_2$ fillers with different crystallite sizes before and after impregnation with dMMAO are also shown in **Figure B-3**. It indicated that the crystal sizes for all nano-TiO$_2$ fillers samples became larger after impregnation with dMMAO due to the deposition of dMMAO on the nano-TiO$_2$ fillers.
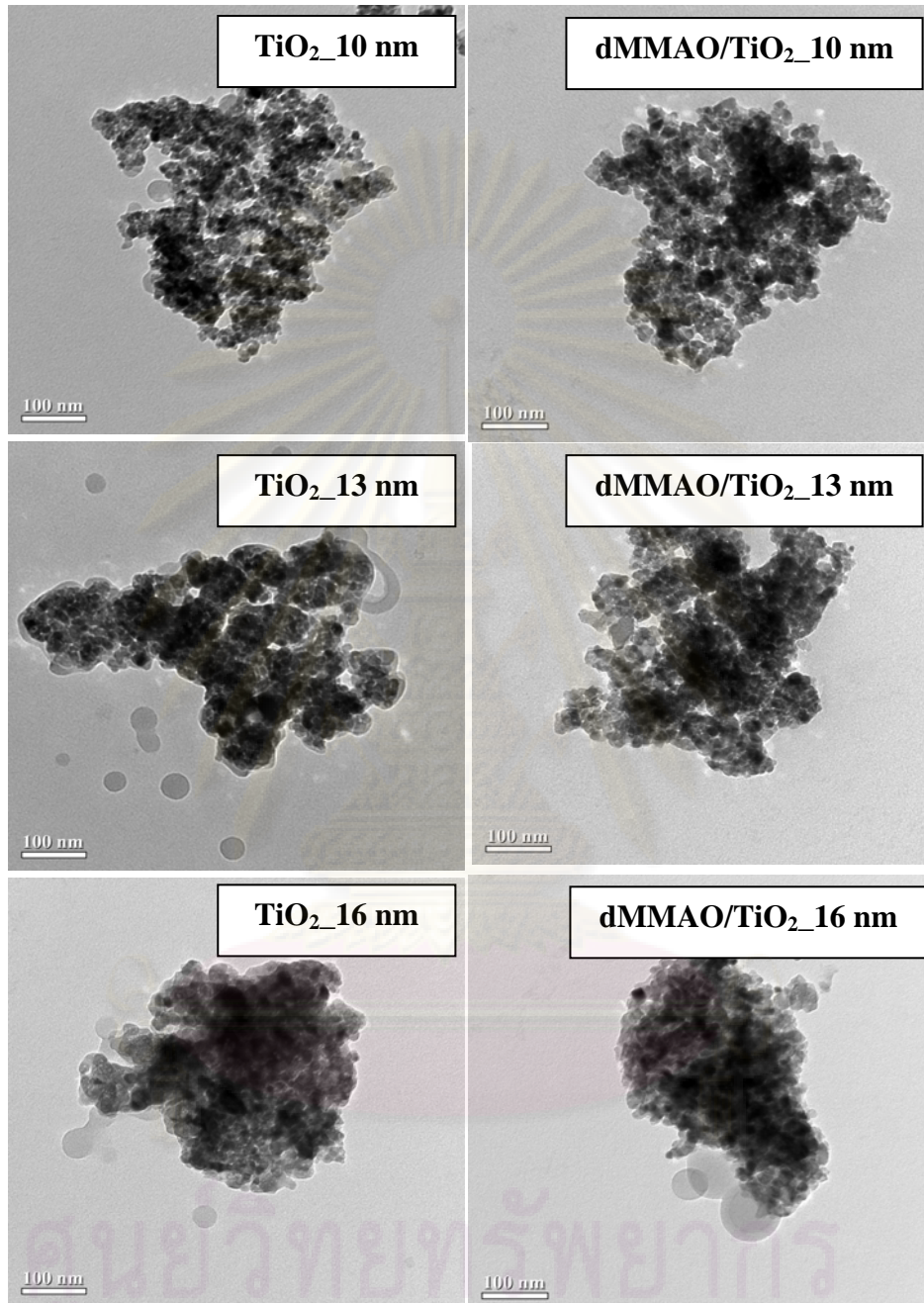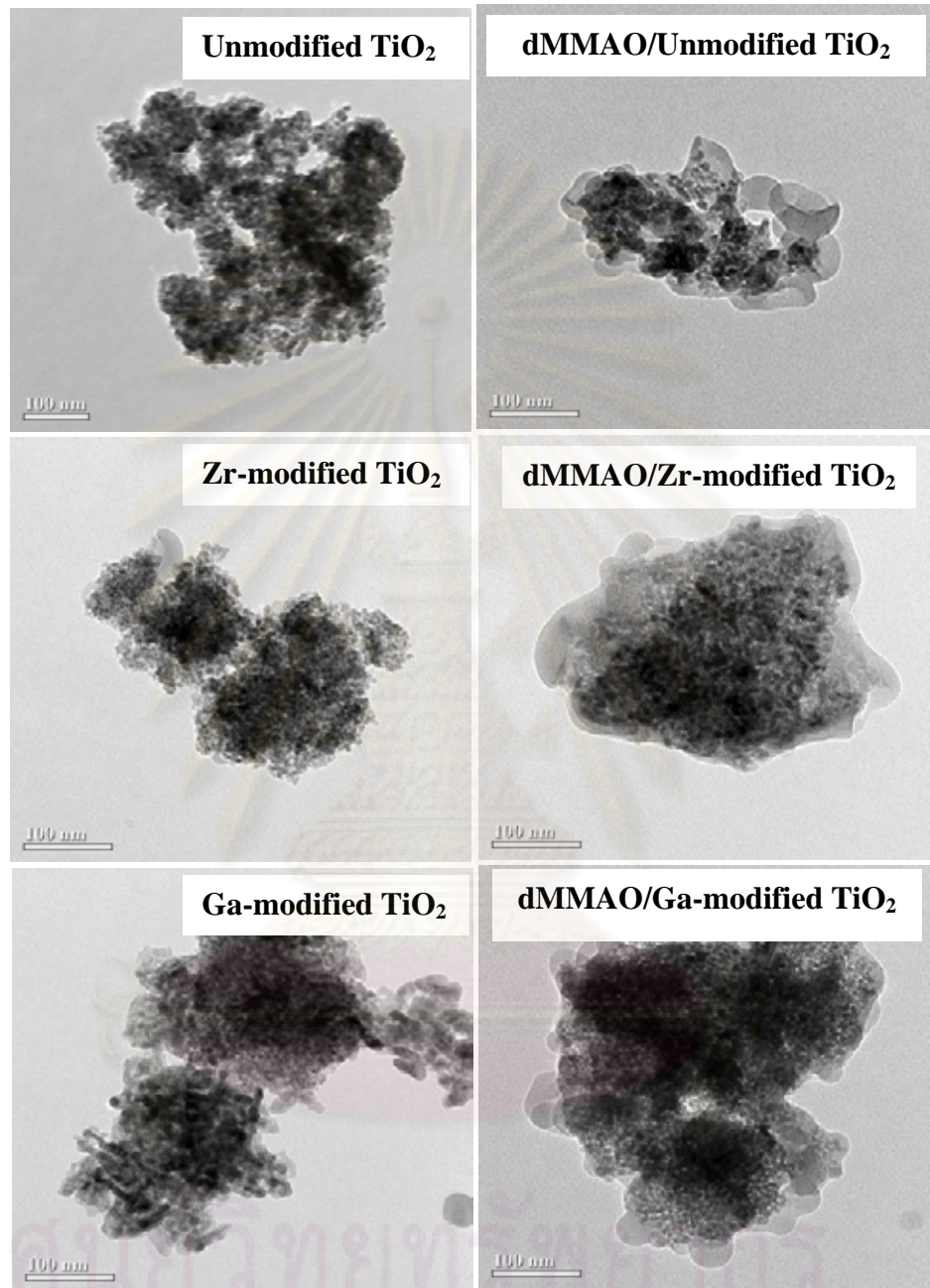
Figure B-3 TEM micrographs of nano-TiO$_2$ fillers with different crystallite sizes before and after impregnation with dMMAO

Effect of the crystallite size of nano-TiO$_2$ fillers on the characteristics of LLDPE/TiO$_2$ nanocomposites

Table B-1 Polymerization activities of LLDPE/TiO$_2$ nanocomposites (*Ex situ* impregnation method)

Sample	Polymerization time [a] (sec)	Polymerization yield [b] (g)	Catalytic activity (kg polymer/mol Zr.h)
Homogeneous	145	0.998	16510
TiO$_2$_10 nm	207	0.786	9112
TiO$_2$_13 nm	n.o.	n.o.	n.o.
TiO$_2$_16 nm	n.o.	n.o.	n.o.

n.o. refers to can not be observed from the experiment

[a] A period of time used for the total 0.018 mol of ethylene to be consumed.

[b] Measurement at polymerization temperature of 70˚C, [ethylene] = 0.018 mol, [Al]$_{MMAO}$/[Zr] = 1135, [Al]$_{TMA}$ /[Zr]$_{cat}$ = 2500, in toluene with total volume = 30 mL, and [Zr]$_{cat}$ = 5 x 10^{-5} M.

B.2 Investigation of the effect of the modification of nano-TiO$_2$ fillers on the characteristics of LLDPE/TiO$_2$ nanocomposites synthesized by *in situ* polymerization of ethylene/1-hexene using a zirconocene/dMMAO catalyst, which prepared by *ex situ* impregnation method

Characterization of dMMAO/ TiO$_2$

- X-Ray Diffraction (XRD)

XRD patterns of TiO$_2$ and dMMAO/ TiO$_2$ with different modifications are shown in **Figure B-2**. They were collected at diffraction angle (2θ) between 20° and 80°, it was observed that all nano-TiO$_2$ fillers exhibited XRD peaks at 25°, 37°,

48°, 55°, 56°, 62°, 69°, 71°, and 75° assigning to anatase TiO_2. It was found that after impregnation with dMMAO the XRD patterns for three samples exhibited the similar patterns. No peaks of dMMAO were detected. This was suggested that the dMMAO was in the highly dispersed form on the nano-TiO_2 fillers.

Figure B-4. XRD patterns of TiO_2 and dMMAO/ TiO_2 with different modifications

- **Transmission electron microscopy (TEM)**

The TEM micrographs of nano-TiO_2 fillers with different modification before and after impregnation with dMMAO are also shown in **Figure B-5**. It indicated that the crystal sizes for all nano-TiO_2 fillers samples became larger after impregnation with dMMAO due to the deposition of dMMAO on the nano-TiO_2 fillers.

Figure B-5 TEM micrographs of nano-TiO$_2$ fillers with different modification before and after impregnation with dMMAO

Effect of the modification of nano-TiO$_2$ fillers on the characteristics of LLDPE/TiO$_2$ nanocomposites

Table B-2 Polymerization activities of LLDPE/TiO$_2$ nanocomposites (*Ex situ* impregnation method)

Sample	Polymerization time [a] (sec)	Polymerization yield [b] (g)	Catalytic activity (kg polymer/mol Zr.h)
Homogeneous	145	0.998	16510
Unmodified TiO$_2$	480	0.5036	2518
Zr-modified TiO$_2$	n.o.	n.o.	n.o.
Ga-modified TiO$_2$	n.o.	n.o.	n.o.

n.o. refers to can not be observed from the experiment

[a] A period of time used for the total 0.018 mol of ethylene to be consumed.

[b] Measurement at polymerization temperature of 70˚C, [ethylene] = 0.018 mol, $[Al]_{MMAO}/[Zr] = 1135$, $[Al]_{TMA}/[Zr]_{cat} = 2500$, in toluene with total volume = 30 mL, and $[Zr]_{cat} = 5 \times 10^{-5}$ M.
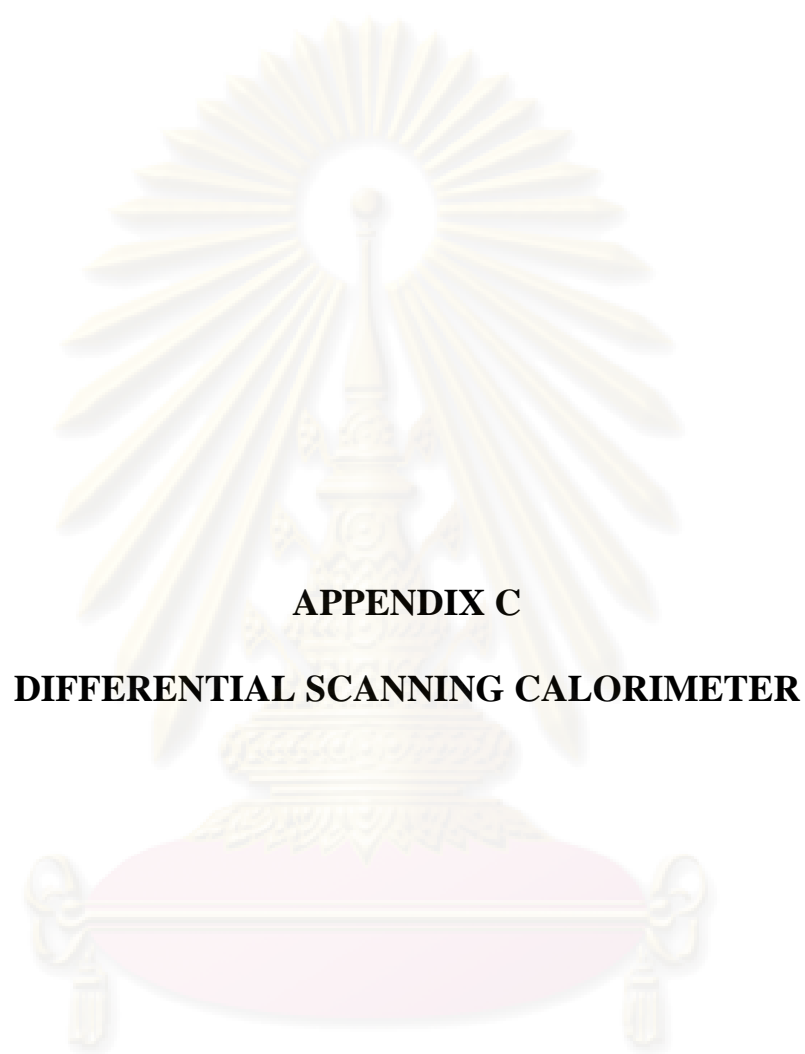
APPENDIX C

DIFFERENTIAL SCANNING CALORIMETER
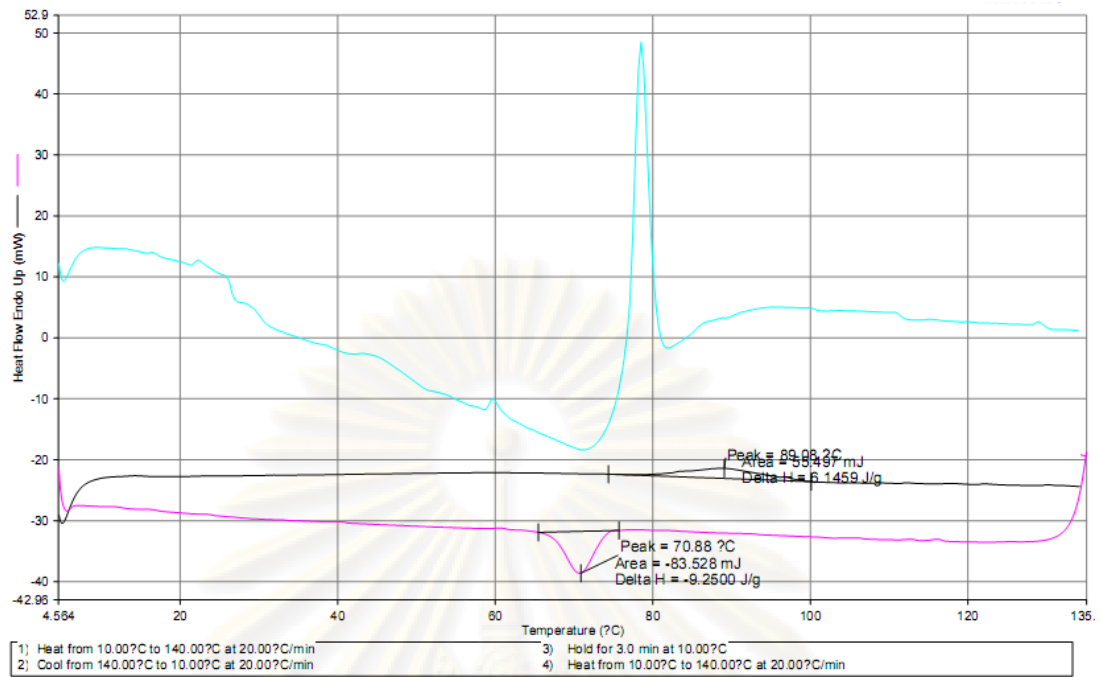
Figure C-1. DSC curve of LLDPE/TiO$_2$ nanocomposites (Homogeneous by *ex situ* impregnation)
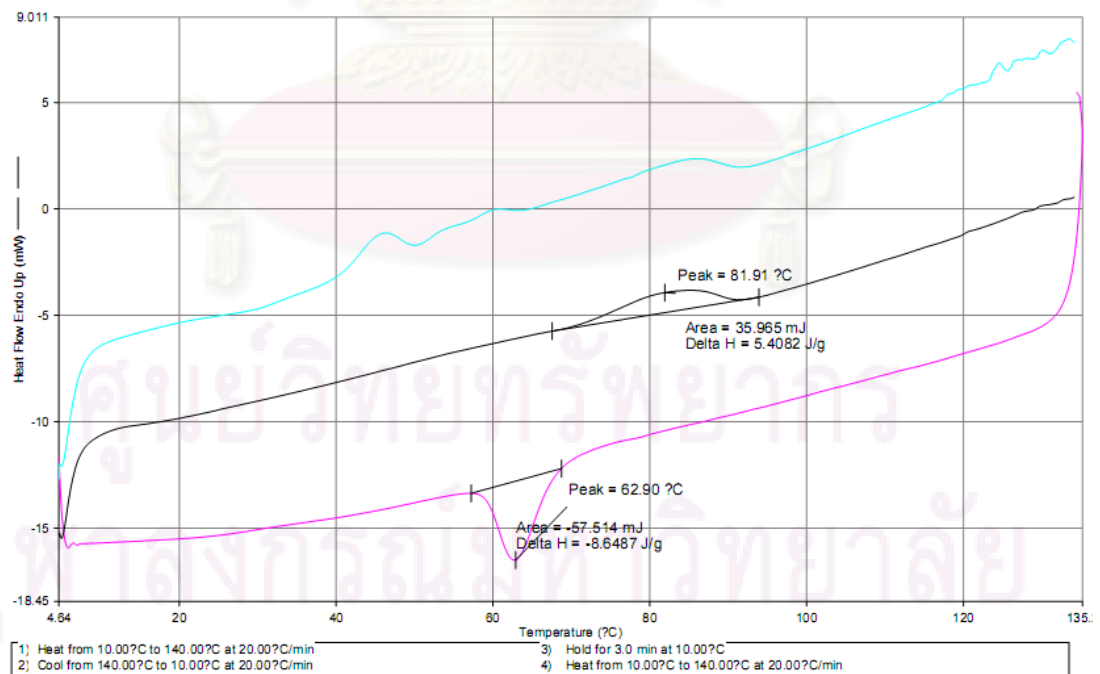
Figure C-2. DSC curve of LLDPE/TiO$_2$ nanocomposites (TiO$_2$_10 nm by *ex situ* impregnation
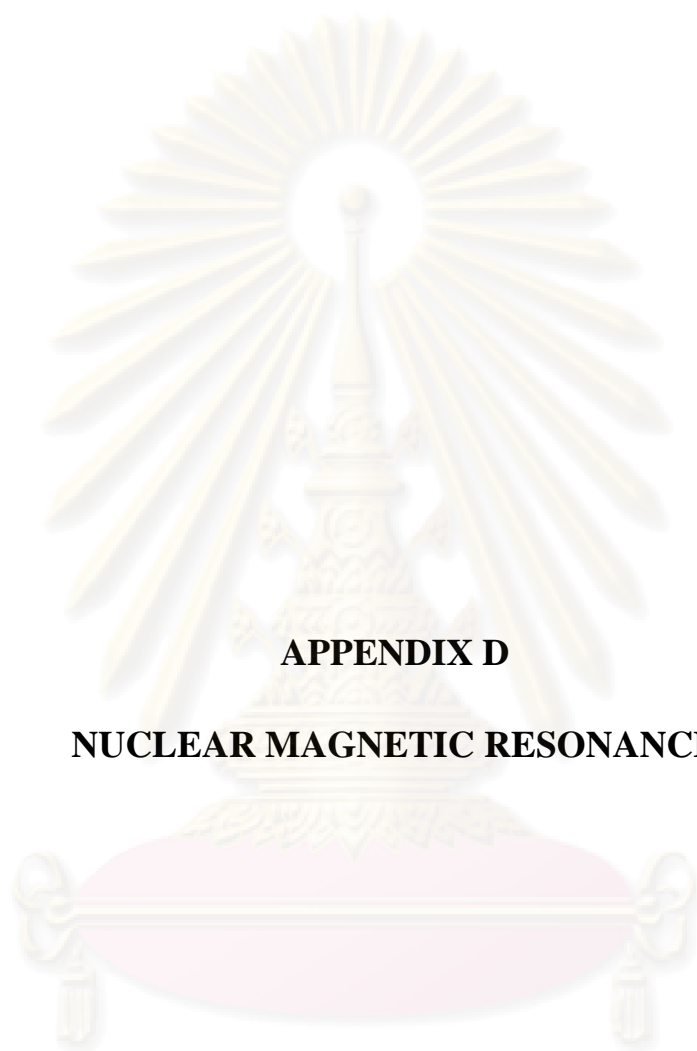
APPENDIX D

NUCLEAR MAGNETIC RESONANCE
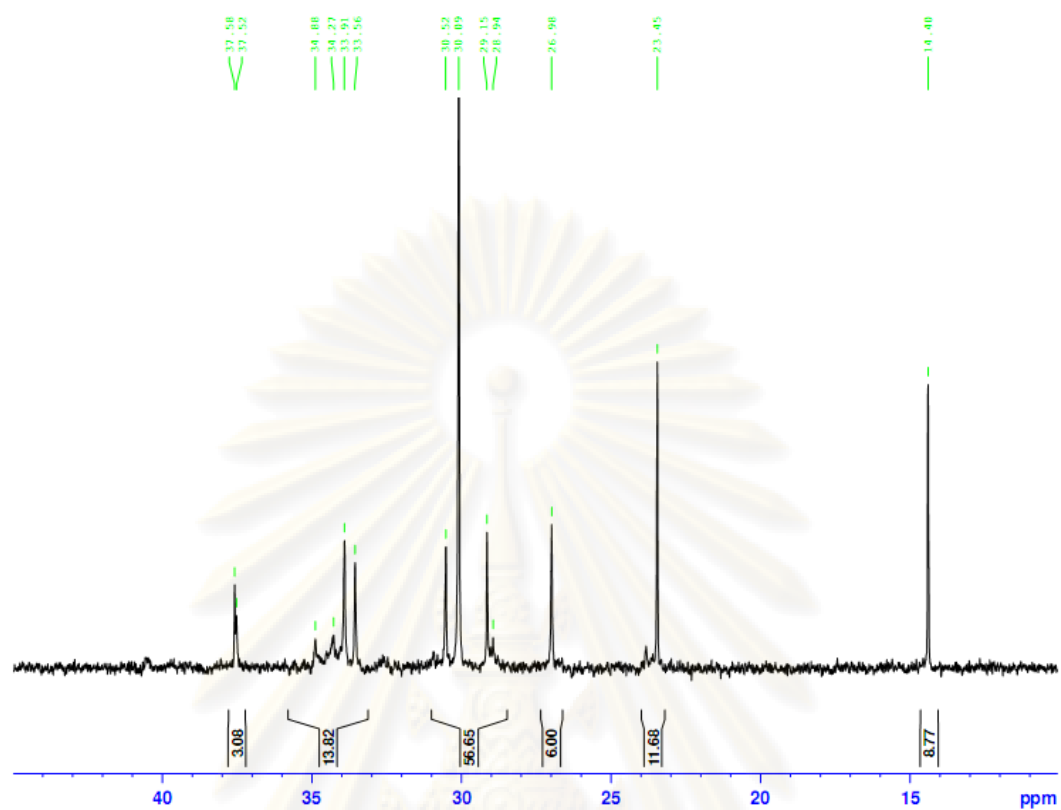
Figure D-1 ^{13}C NMR spectrum of ethylene/1-hexene copolymer
(Homogenous by *ex situ* impregnation)
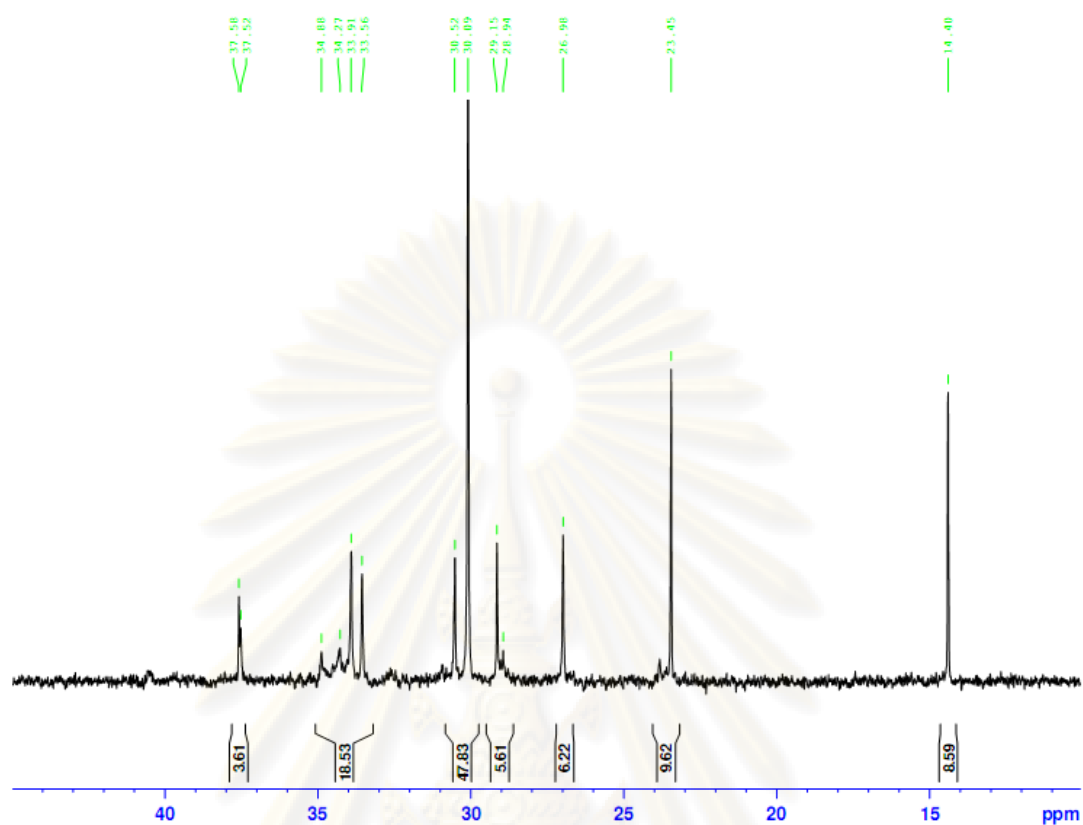
Figure D-2 ^{13}C NMR spectrum of ethylene/1-hexene copolymer (TiO$_2$_10 nm by *ex situ* impregnation)
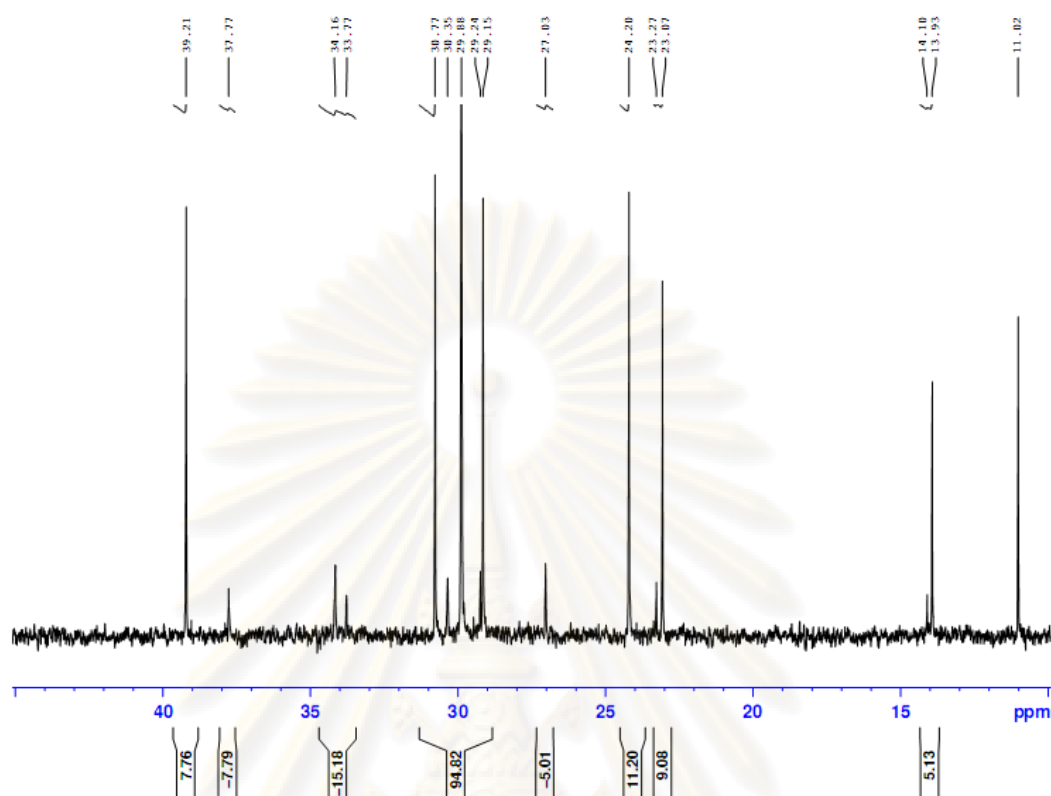
Figure D-3 ¹³C NMR spectrum of ethylene/1-hexene copolymer (Unmodified TiO₂ by *ex situ* impregnation)
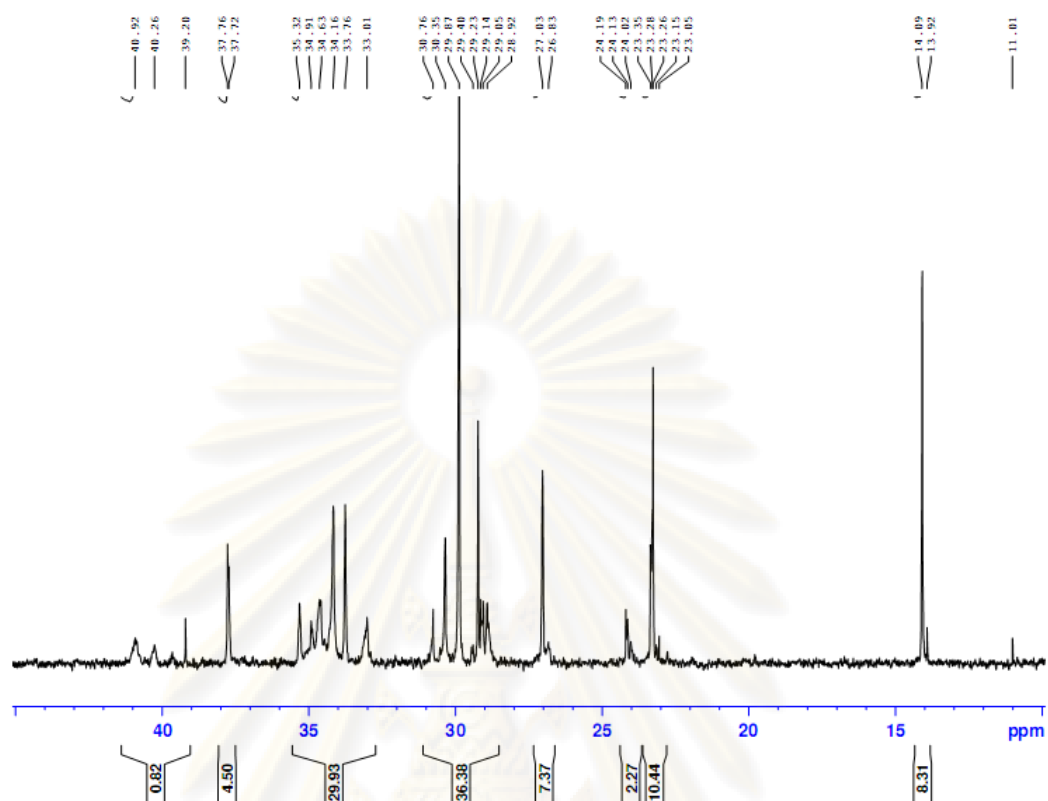
Figure D-4 ^{13}C NMR spectrum of ethylene/1-hexene copolymer (Homogeneous by *in situ* impregnation)
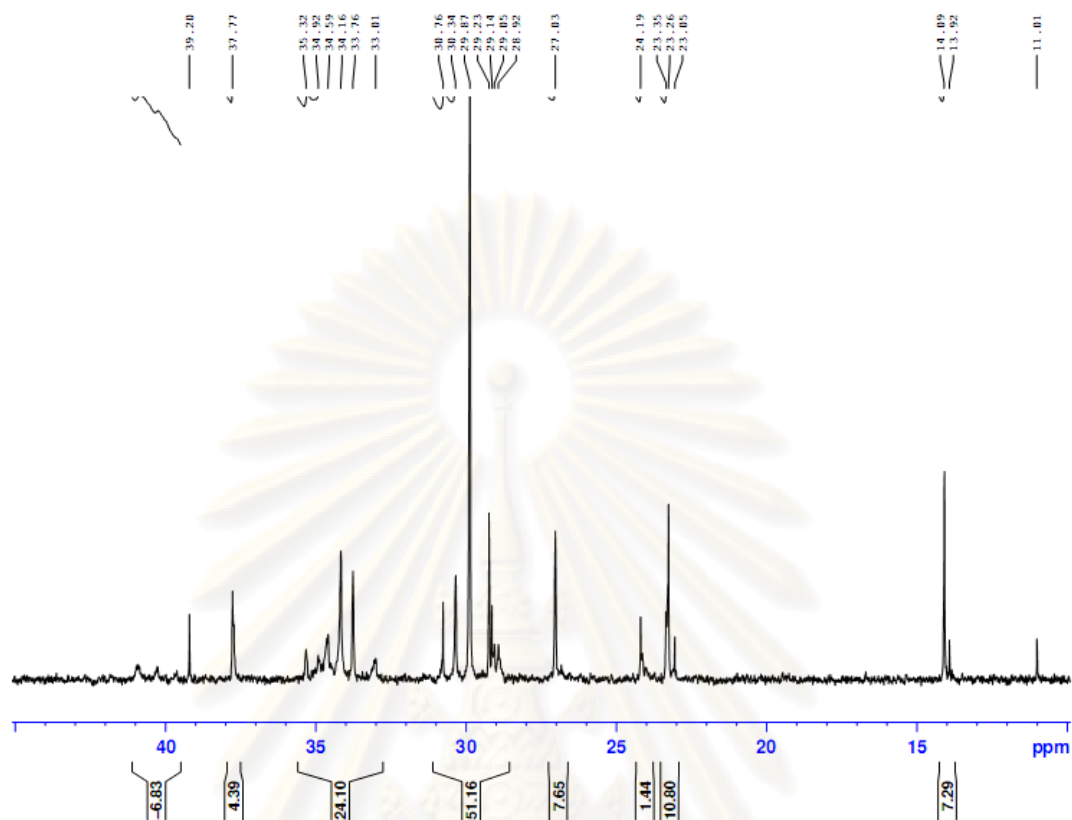
Figure D-5 ^{13}C NMR spectrum of ethylene/1-hexene copolymer (TiO$_2$_10 nm by *in situ* impregnation)
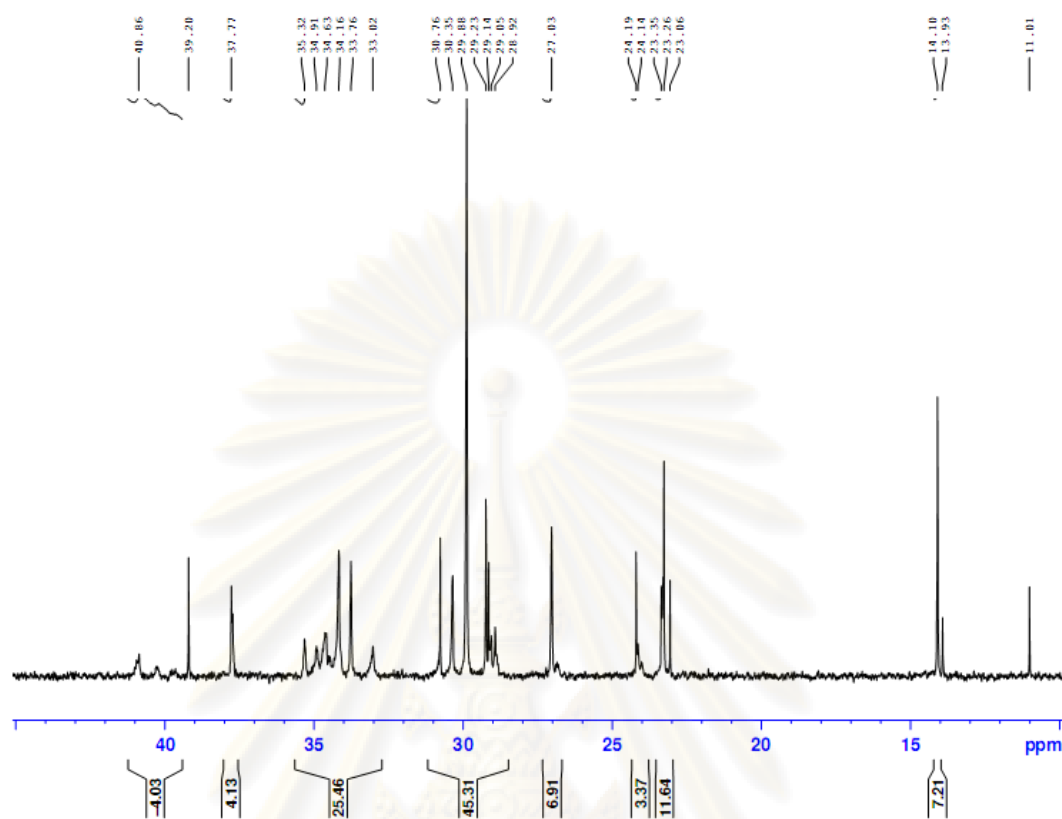
Figure D-6 ^{13}C NMR spectrum of ethylene/1-hexene copolymer (TiO$_2$_13 nm by *in situ* impregnation)
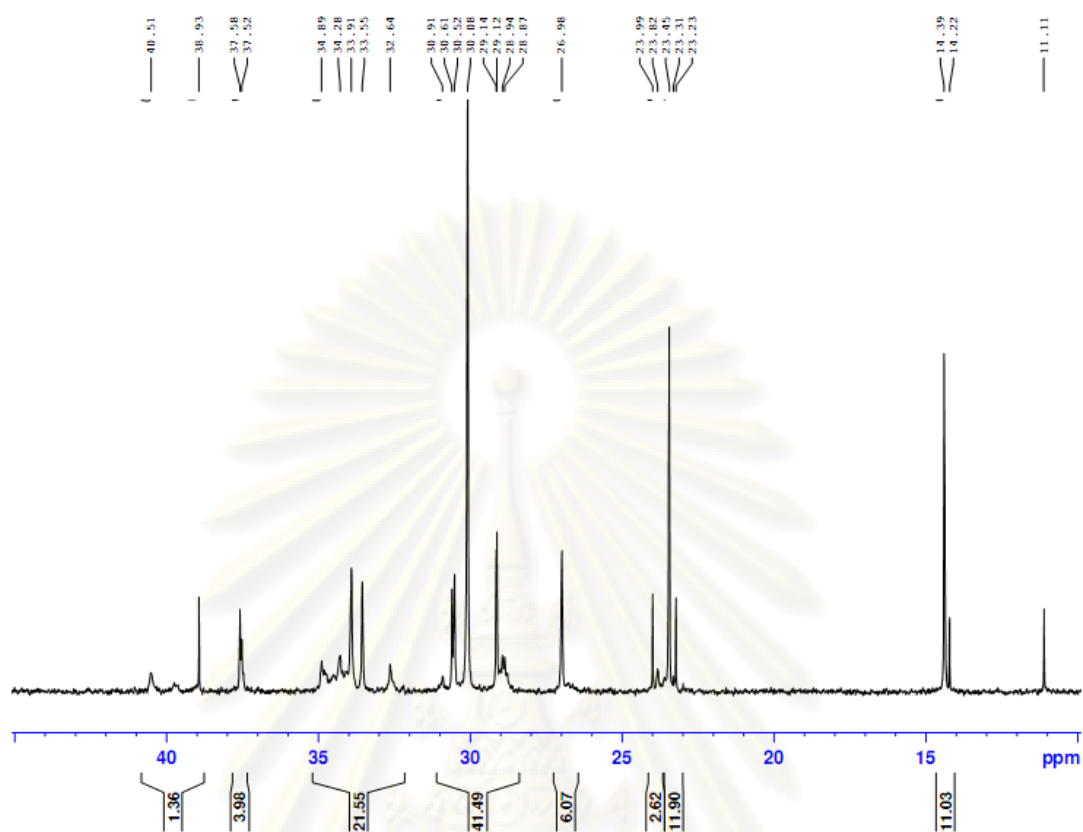
Figure D-7 ^{13}C NMR spectrum of ethylene/1-hexene copolymer (TiO$_2$_16 nm by *in situ* impregnation)
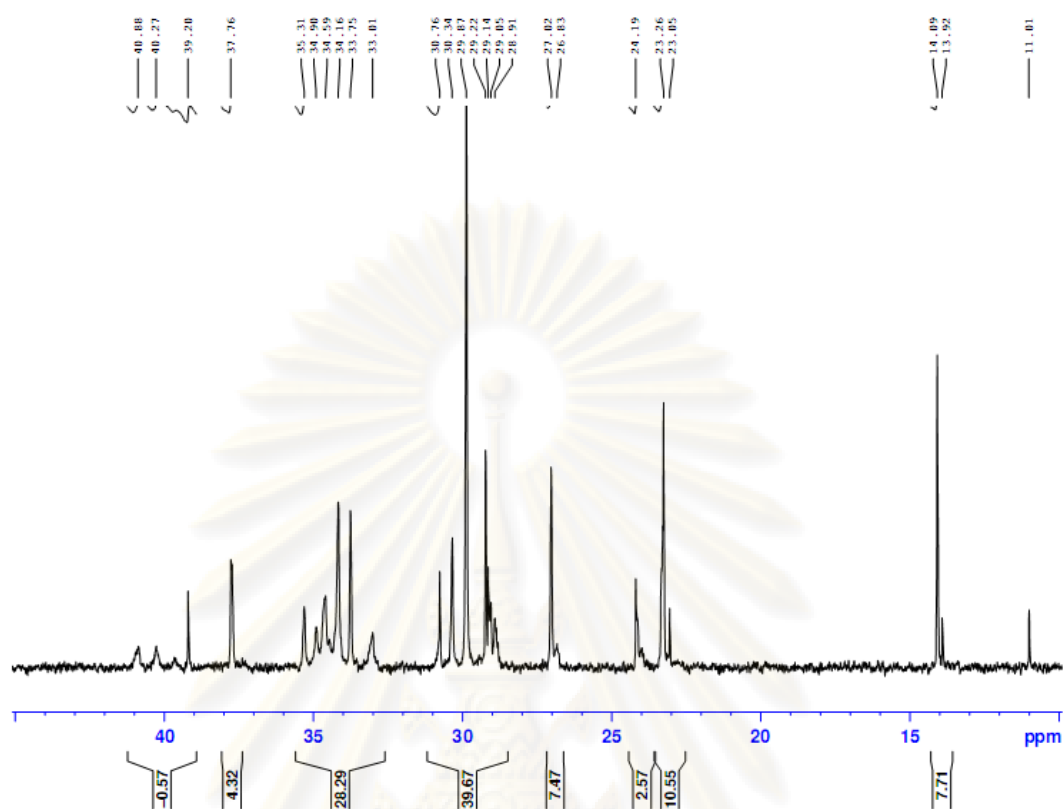
Figure D-8 ^{13}C NMR spectrum of ethylene/1-hexene copolymer (Unmodified TiO$_2$ by *in situ* impregnation)
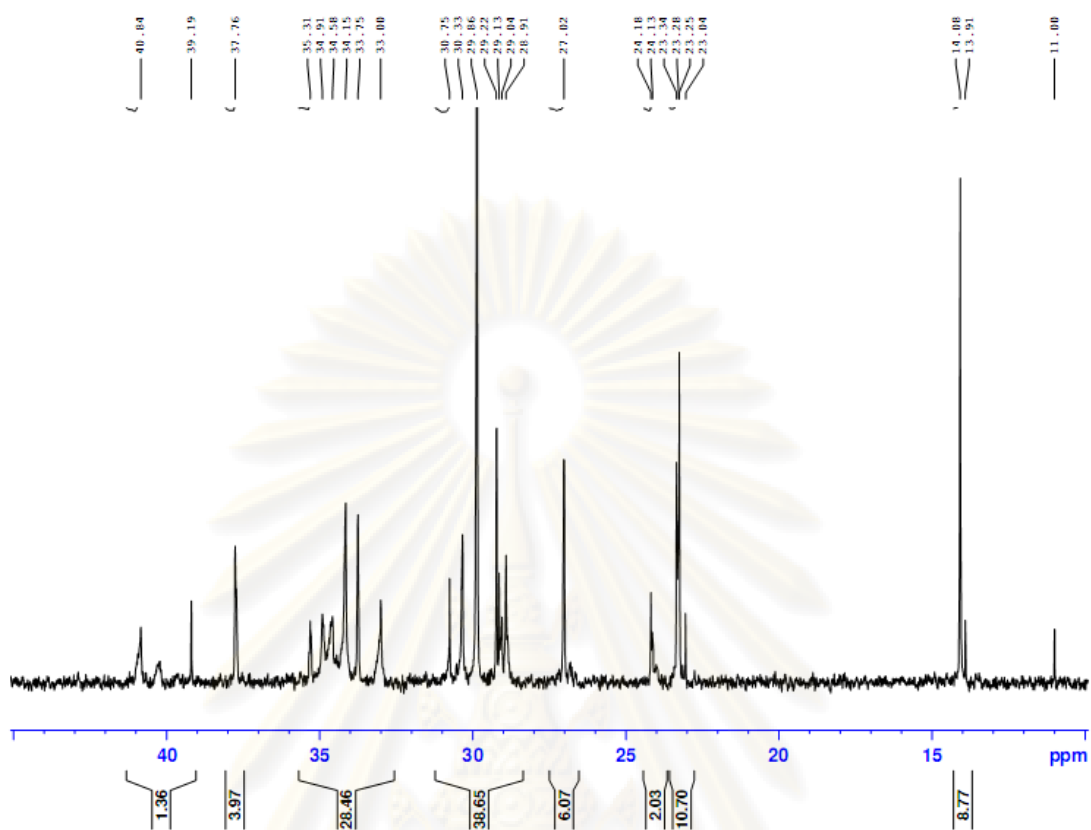
Figure D-9 ¹³C NMR spectrum of ethylene/1-hexene copolymer (Zr-modified TiO₂ by *in situ* impregnation)
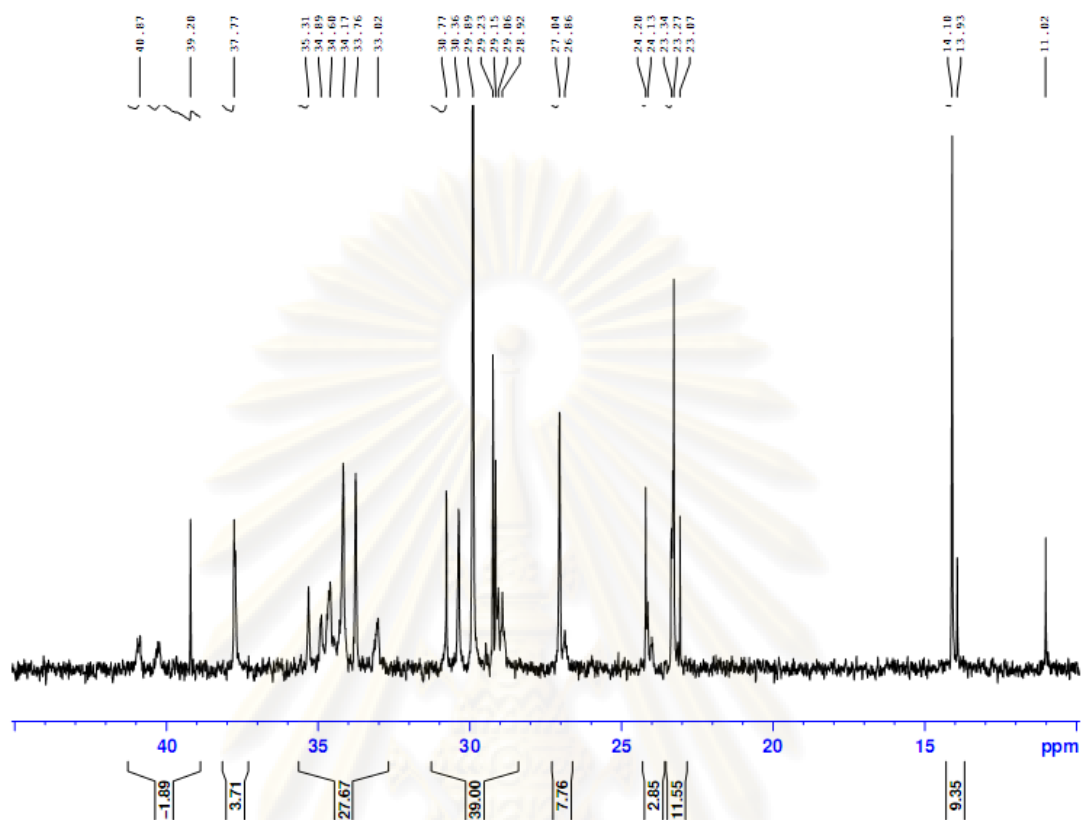
Figure D-10 ^{13}C NMR spectrum of ethylene/1-hexene copolymer (Ga-modified TiO$_2$ by *in situ* impregnation)
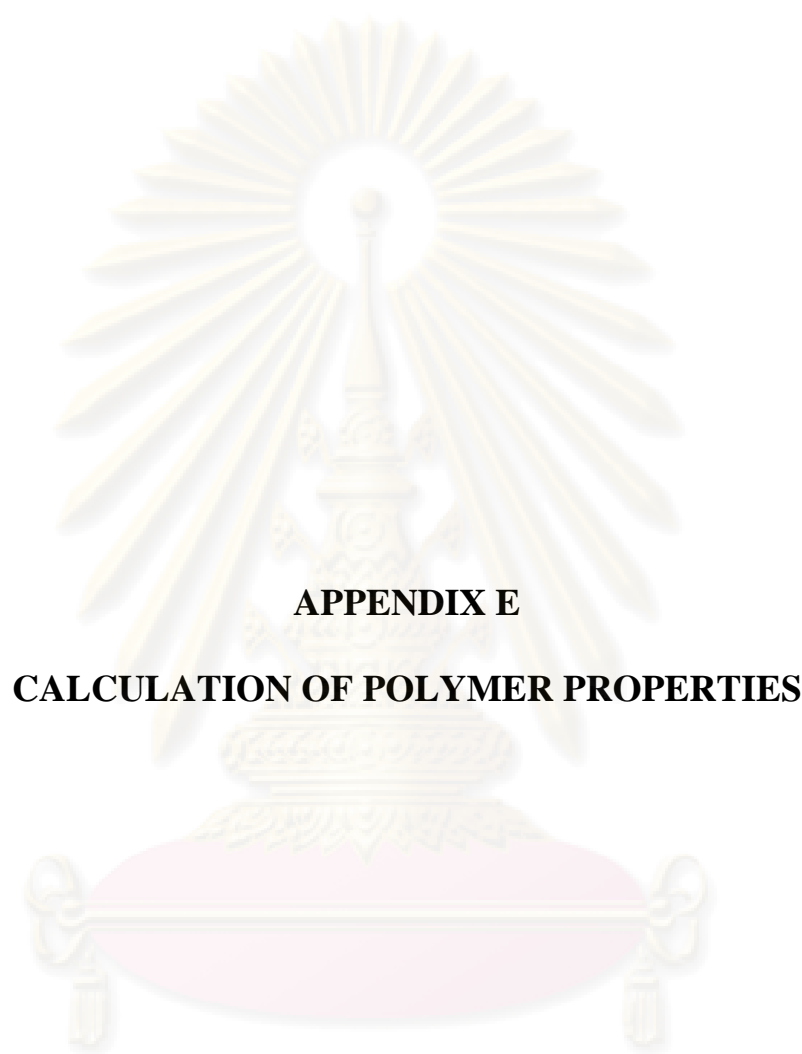
APPENDIX E

CALCULATION OF POLYMER PROPERTIES

Calculation of polymer microstructure

Polymer microstructure and also triad distribution of monomer can be calculated according to the Prof. James C. Randall. The detail of calculation was be interpreted as follow

Ethylene/1-hexene copolymer

The integral area of ^{13}C-NMR spectrum in the specify rage are listed.

T_A	=	39.5 - 42	ppm
T_B	=	38.1	ppm
T_C	=	33 - 36	ppm
T_D	=	28.5 - 31	ppm
T_E	=	26.5 - 27.5	ppm
T_F	=	24 - 25	ppm
T_G	=	23.4	ppm
T_H	=	14.1	ppm

Triad distribution was calculated as the followed formular

k[HHH]	=	$2T_A - T_C + T_G + 2T_F + T_E$
k[EHH]	=	$2T_C - 2T_G - 4T_F - 2T_E - 2T_A$
k[EHE]	=	T_B
k[EEE]	=	$0.5T_D - 0.5T_G - 0.25T_E$
k[HEE]	=	T_F
k[HEH]	=	T_E

Calculation of crystallinity for ethylene/1-olefin copolymer

The crystallinities of copolymers were determined by differential scanning calorimeter. % crystallinity of copolymers is calculated from equation.

$$\% Crystallinity = \frac{\Delta H_m}{\Delta H_m^o} \times 100$$

Where ΔH_m = the heat of fusion of sample (J/g)

ΔH_m^o = the heat of fusion of perfectly crystalline polyethylene

= 286 J/g
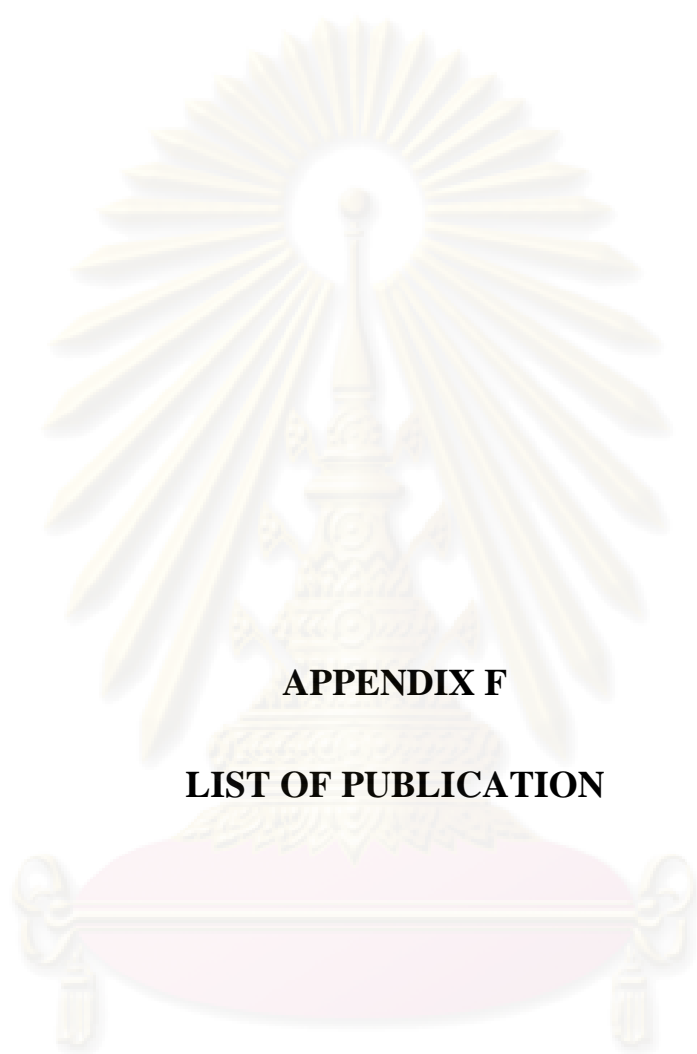
APPENDIX F

LIST OF PUBLICATION

1. Pathomsap, S. and Jongsomjit, B. "Characteristics of LLDPE/TiO$_2$ nanocomposites synthesized by *in situ* polymerization using metallocene catalyst " (The Proceeding of 18th Thailand Chemical Engineering and Applied Chemistry Conference, TIChe 2008, Pattaya, Thailand.)

VITA

Miss Somsakun Pathomsap was born on October 29, 1984 in Chonburi, Thailand. She finished high school from Triamudomsuksa school, Bangkok and she received the Bachelor's Degree of Chemical Engineering from the Department of Chemical Engineering, Faculty of Engineering, King Mongkut's University of Technology North Bangkok in March 2007 (Second Class Honours). She continued her Master's Degree study at Chulalongkorn University in June, 2007.